Water pollution is a global problem which requires ongoing evaluation of water treatment technologies. Traditional water treatment is not enough effective to eliminate pollutants having environmental, ecotoxicological and human health risk. Such contaminants are e.g. pharmaceuticals, widely used by humans and thus present in surface and drinking waters. Consequently, additional techniques, such as Advanced Oxidation Processes (AOPs), are needed to be integrated in the traditional processes. Beside highly reactive hydroxyl radical, several reactive species form during the application of AOPs. However, only a few data are given concerning the reactions of these species. This work presents their role and importance, investigated during the vacuum ultraviolet photolysis of four selected drugs. Thus, suggestions could be put forward concerning the effects of different parameters on the radical set and on the role of various reactive species on the transformation of the studied drugs. These results could contribute to improve the efficiency of AOPs and therefore may be useful for both newcomers and professionals working in the field of water cleaning or interested in reaction mechanisms.

Eszter Arany, PhD: Chemist MSc in 2010 and Teacher of Chemistry MSc in 2012 at the University of Szeged. PhD in Environmental Chemistry in 2015 at the University of Szeged. Research interest in Advanced Oxidation Processes and Environmental Chemistry. Junior research fellow in the Institute of Material Sciences at the University of Szeged, Hungary.

978-3-659-45798-2

Reactive species against selected drugs

Arany (Ed.), Alapi, Schrantz

Eszter Arany (Ed.)
Tünde Alapi
Krisztina Schrantz

Reactive species against selected nonsteroidal anti-inflammatory drugs

Radical scavengers, radical transfers, reaction mechanisms

LAP LAMBERT Academic Publishing

Eszter Arany (Ed.)
Tünde Alapi
Krisztina Schrantz

Reactive species against selected nonsteroidal anti-inflammatory drugs

Eszter Arany (Ed.)
Tünde Alapi
Krisztina Schrantz

Reactive species against selected nonsteroidal anti-inflammatory drugs

Radical scavengers, radical transfers, reaction mechanisms

LAP LAMBERT Academic Publishing

Impressum / Imprint
Bibliografische Information der Deutschen Nationalbibliothek: Die Deutsche Nationalbibliothek verzeichnet diese Publikation in der Deutschen Nationalbibliografie; detaillierte bibliografische Daten sind im Internet über http://dnb.d-nb.de abrufbar.

Bibliographic information published by the Deutsche Nationalbibliothek: The Deutsche Nationalbibliothek lists this publication in the Deutsche Nationalbibliografie; detailed bibliographic data are available in the Internet at http://dnb.d-nb.de.

Coverbild / Cover image: www.ingimage.com

Verlag / Publisher:
LAP LAMBERT Academic Publishing
ist ein Imprint der / is a trademark of
OmniScriptum GmbH & Co. KG
Heinrich-Böcking-Str. 6-8, 66121 Saarbrücken, Deutschland / Germany
Email: info@lap-publishing.com

Herstellung: siehe letzte Seite /
Printed at: see last page
ISBN: 978-3-659-45798-2

ZugI. / Approved by: Szeged, University of Szeged, Diss., 2014

Table of contents

Abbreviations

1,2-DHB: 1,2-dihydroxybenzene

1,4-DHB: 1,4-dihydroxybenzene

A_{DICL}: an aromatic by-product of the VUV photolysis of DICL, presumably its monohydroxylated derivative

A_{IBU}: an aromatic by-product of the VUV photolysis of IBU, presumably its monohydroxylated derivative

A_{KETO}: an aromatic by-product of the VUV photolysis of KETO, presumably 3-ethylbenzophenone

A_{NAP}: an aromatic by-product of the VUV photolysis of NAP, presumably 2-methoxy-6-vinylnaphthalene

AOP: advanced oxidation process

B_{DICL}: an aromatic by-product of the VUV photolysis of DICL, presumably 1-(8-chlorocarbazolyl)acetic acid

B_{IBU}: an aromatic by-product of the VUV photolysis of IBU, presumably its dihydroxylated derivative

B_{KETO}: an aromatic by-product of the VUV photolysis of KETO, presumably 3-(1-hydroperoxyethyl)benzophenone

B_{NAP}: an aromatic by-product of the VUV photolysis of NAP, presumably 1-(6-methoxynaphthalene-2-yl)ethylhydroperoxide

C_{DICL}: an aromatic by-product of the VUV photolysis of DICL, presumably 1-(8-hydroxycarbazolyl)acetic acid

C_{IBU}: an aromatic by-product of the VUV photolysis of IBU, presumably 1-isobutyl-4-isopropylbenzene

C_{KETO}: an aromatic by-product of the VUV photolysis of KETO, presumably 3-(1-hydroxyethyl)benzophenone

C_{NAP}: an aromatic by-product of the VUV photolysis of NAP, presumably 1-(2-methoxynaphthalene-6-yl)ethanone

D_{IBU}: an aromatic by-product of the VUV photolysis of IBU, presumably 2-[4-(2-hydroxypropyl)phenyl]propanoic acid or hydroxy(4-isobutylphenyl)acetic acid

DICL: diclofenac

D_{KETO}: an aromatic by-product of the VUV photolysis of KETO, presumably 3-hydroperoxybenzophenone

ε: the molar absorption coefficient of the contaminant molecule at the emission wavelength of the light source

IBU: ibuprofen

k': apparent reaction rate constant

$k^0_{obs.}$: the initial VUV-induced degradation rate of methanol

$k_{recomb.}$: the reaction rate constant of the recombination reaction of $HO_2^{\bullet}/O_2^{\bullet-}$

KETO: ketoprofen

NAP: naproxen

NSAID: nonsteroidal anti-inflammatory drug

$[HO^{\bullet}]_{SS}$: the steady-state concentration of hydroxyl radicals

PB: phosphate buffer

pH_{max}: pH where the solubility of the NSAIDs was the highest

PhOH: phenol

$R^{\bullet}$ or $RH\text{-}R^{\bullet}$: carbon-centered radical

$[radicals]_{SS}$: the steady-state concentration of reactive radicals

RH: organic compound

$RO^{\bullet}$: oxyl radical

$ROO^{\bullet}$, $RH\text{-}ROO^{\bullet}$ or $(RHOH)\text{-}O_2^{\bullet}$: peroxyl radical

ROOOOR: tetroxide

ROS: reactive oxygen species

SD: standard deviation

1. Preface

Since the traditional wastewater treatment techniques are based on biological methods, and there are several pollutants (*e.g.* nonsteroidal anti-inflammatory drugs) which can not be eliminated completely by the used microorganisms, the decontamination of these waters is of upmost interest nowadays. The application of advanced oxidation processes (AOPs) as additive methods during the treatment of wastewaters may solve this problem.

AOPs are based on the generation of reactive radicals, which can induce the transformation of the contaminants. Although there is plenty of information about the reactions of the most reactive radical, the hydroxyl radical ($HO^{\bullet}$), only a few data are given concerning the less reactive radicals, which might also contribute to the degradation of the pollutant molecules if their concentration is increased.

Vacuum ultraviolet (VUV) photolysis is a suitable method, among the AOPs, to study the effects of different parameters (*e.g.* the presence of dissolved O_2 or other radical transfer molecules) on the radical set and on the degradation of organic contaminants, since the generated radical set is known, using this technique. These results could contribute to improve the efficiency of AOPs.

2. Literature background

2.1. The investigated nonsteroidal anti-inflammatory drugs

Nonsteroidal anti-inflammatory drugs (NSAIDs) are used for multiple indications in both human and veterinary medicine, *e.g.* to treat inflammation and pain, to relieve fever, and sometimes they are also used for long-term treatment of rheumatic diseases. They act by inhibiting the prostaglandin synthesis by blocking, either reversibly or irreversibly, one or both of the two isoforms of the cyclooxygenase enzyme (COX-1 and COX-2). Most of their side effects (gastric ulceration, renal and liver damages) can be related to their nonspecific inhibition of the prostaglandin synthesis [1]. Since prostaglandins are also produced in non-mammalian vertebrates like fish, amphibians and birds, in invertebrates such as corals, sponges, coelenterates, molluscs, crustaceans, insects, as well as in marine algae and higher plants [2, 3], NSAIDs released in the environment can cause adverse effects also in the ecosystem, especially when they are present as a mixture [2, 4-11].

Table I. The IUPAC name, the chemical structure and the acidic dissociation constant of the investigated compounds.

comp.	IUPAC name	structure	pK_a	ref.
IBU	(*RS*)-2-(4-(2-methylpropyl)phenyl)propanoic acid	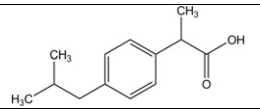	4.4	[12-14]
KETO	(*RS*)-2-(3-benzoylphenyl)propanoic acid	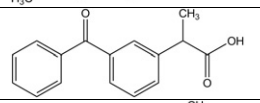	4.1	[14]
NAP	(*RS*)-2-(6-methoxynaphthalen-2-yl)propanoic acid	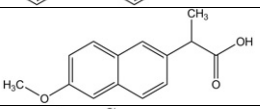	4.2	[15, 16]
DICL	2-(2-(2,6-dichlorophenylamino)phenyl) acetic acid	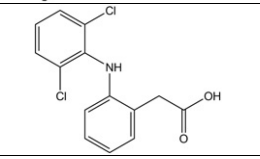	4.2	[14, 17]

Four arylcarboxylic acids were selected among NSAIDs: ibuprofen (IBU), containing only one phenyl group, ketoprofen (KETO), a benzophenone derivative, naproxen (NAP), a naphthalene derivative and the Cl-containing diclofenac (DICL) (Table I). As it can be seen from Table I and Fig. 1, these pharmaceuticals are week acids.

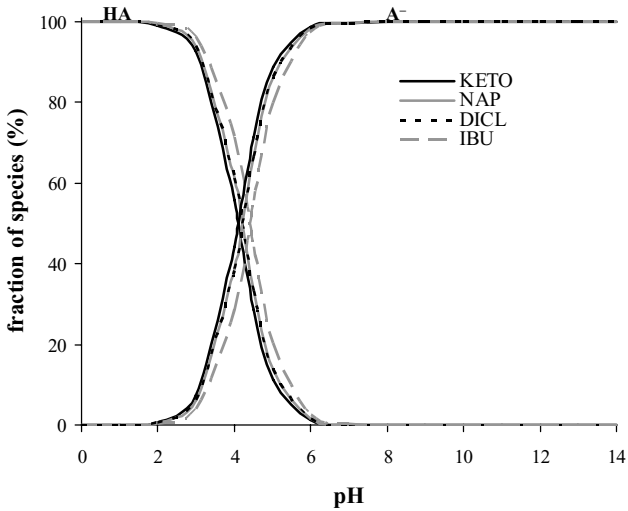

Fig.1. pH dependence of the undissociated and dissociated forms of the investigated NSAIDs.

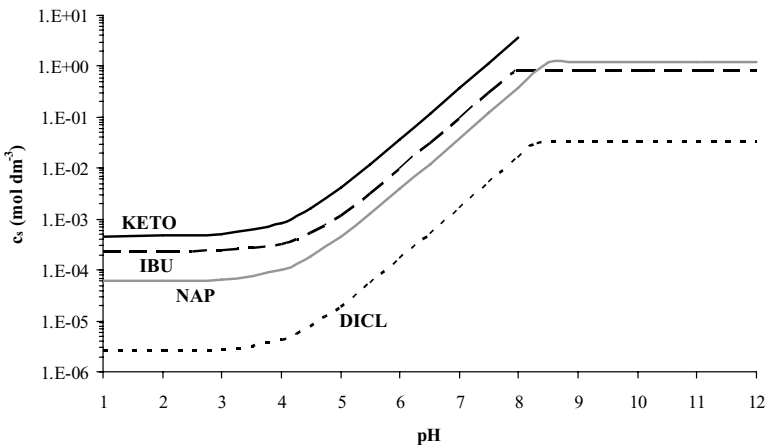

Fig. 2. pH-dependence of the solubility of the studied NSAIDs.

Since the solubility of the undissociated ($[HA]_s$) and dissociated ($[A^-]_s$) forms of the studied NSAIDs differs with at least three orders of magnitude (Table II), the solubility of these drugs (c_s) is significantly pH-dependent (Fig. 2). (Unfortunately no information was found in the literature concerning the $[A^-]_s$ value of KETO.)

Table II. The solubility of the undissociated and dissociated forms of the used compounds in water at 25°C.

comp.	$[HA]_s$ ($\times 10^{-4}$ mol dm^{-3})	$[A^-]_s$ (mol dm^{-3})	ref.
IBU	2.40	0.80	determined from [18]
KETO	4.60	n.d.*	determined from [18]
NAP	0.69	0.85	[19]
DICL	0.03	0.03	determined from [18]

*not determined

The c_s values were calculated according to *Chowhan* [19], using the parameters of Tables I and II. At low pH values the solubility of the undissociated species is the limiting factor (Eq. I) and the c_s values may be calculated according to Eq. IV (derived from Eqs. I–III). Since the $[A^-]_s$ values are with orders of magnitude higher than the $[HA]_s$ values (Table II), Eq. IV was used also in case of intermediate pH values, when the pH of the solution was lower than pH_{max} (the pH where the solubility of the NSAIDs was the highest), in accordance with the work of *Chowhan* [19].

$$c_s^{pH<pH_{max}} = [HA]_s + [A^-] \quad \text{(I)}$$

$$c_s^{pH<pH_{max}} = [HA]_s + \frac{K_a [HA]_s}{[H_3O^+]} \quad \text{(II)}$$

$$c_s^{pH<pH_{max}} = [HA]_s \times \left(1 + \frac{K_a}{[H_3O^+]}\right) \quad \text{(III)}$$

$$c_s^{pH<pH_{max}} = [HA]_s \times \left(1 + 10^{(pH-pK_a)}\right) \quad \text{(IV)}$$

While at higher pH values the solubility of the ionized species is the liming factor (Eq. V). Therefore, in this case Eq. VI was used.

$$c_s^{\mathrm{pH}\rangle \mathrm{pH}_{\max}} = [\mathrm{HA}] + [\mathrm{A}^-]_s \quad \text{(V)}$$

$$c_s^{\mathrm{pH}\rangle \mathrm{pH}_{\max}} = [\mathrm{A}^-]_s \times \left(1 + 10^{(\mathrm{p}K_a - \mathrm{pH})}\right) \quad \text{(VI)}$$

These pharmaceuticals are among the most often prescribed drugs, their annual consumption varying usually between several hundreds and several thousands mg person^{-1} year^{-1} (Fig. 3). However, in 2005 17890 mg person^{-1} year^{-1} IBU was consumed in Finland. It has to be also mentioned that the annual consumption of these NSAIDs increases in the course of time [20].

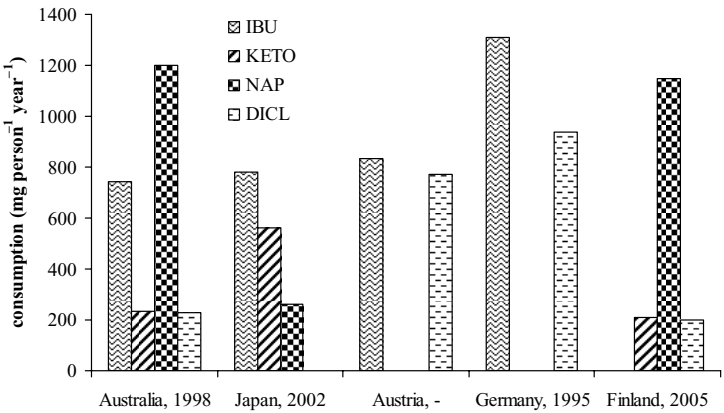

Fig. 3. The annual consumption of the studied NSAIDs in different countries [20].

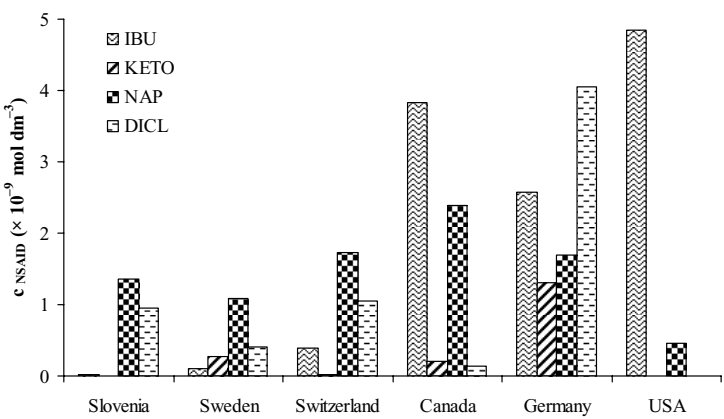

Fig. 4. The maximal detected concentrations of the investigated compounds in surface waters in different countries [20].

After administration, the investigated compounds are only partly metabolized and 5–33% of IBU, 80% of KETO, 70% of NAP and 3–30% of DICL is excreted in form of the parent compound or its conjugates. Additionally, although IBU is usually eliminated in 86–99% in wastewater treatment plants, in some cases its elimination efficiency is only 38–64% and the elimination efficiency of the other three NSAIDs is also lower (45–77% in the case of KETO, 46–93% in the case of NAP and 17–69% in the case of DICL). These compounds occur therefore in surface waters (Fig. 4). Additionally, IBU was detected in ~15×10^{-9} mol dm^{-3} in a UK river, in 1.0×10^{-9} mol dm^{-3} in a German groundwater and in 6.5×10^{-9} mol dm^{-3} in a USA drinking water sample. KETO and DICL were also detected in 0.1×10^{-9} mol dm^{-3} and 2.0×10^{-9} mol dm^{-3}, respectively in a German groundwater sample [20].

These results make reasonable the elaboration of new water treatment technologies, which could enhance the elimination of these pharmaceutically active compounds from waters. The addition of AOPs to the traditional water treatment techniques seems to be a promising alternative. For the determination of the efficiency of these methods as well as for the suggestions of the possible reaction mechanisms, the comparison of the treatment technologies with a simple-structured, well-known organic compound may be useful. In this work phenol (PhOH) was chosen for these purposes.

2.2. Advanced oxidation processes

2.2.1. General characterization of the AOPs

AOPs are based on the generation of reactive radicals ($HO^{\bullet}$, hydrogen atom/hydrated electron ($H^{\bullet}/e_{aq}^{-}$), hydroperoxyl radical/superoxide radical ion ($HO_2^{\bullet}/O_2^{\bullet-}$) *etc.*), reacting with the organic contaminants to induce the degradation of pollutant molecules. Among the formed radicals, the $HO^{\bullet}$ is the most reactive and less selective one. The second order rate constants (k) of its reactions with the studied compounds are listed in Table III. These values were measured by either pulse radiolysis or competitive techniques. Generally the directly measured values

(determined by pulse radiolysis: 8.4 × 10^9 mol^{-1} dm^3 s^{-1} in the case of PhOH [21], (6.0–6.1) × 10^9 mol^{-1} dm^3 s^{-1} in the case of IBU [22, 23], (4.6–5.5) × 10^9 mol^{-1} dm^3 s^{-1} in the case of KETO [23, 24], (3.5–7.5) × 10^9 mol^{-1} dm^3 s^{-1} in the case of NAP [22, 23] and (8.1–9.6) × 10^9 mol^{-1} dm^3 s^{-1} in the case of DICL [22, 23, 25]) are considered to be the most reliable.

Table III. The second order rate constants of the reactions of $HO^•$, e_{aq}^- and $H^•$ with the investigated compounds.

comp.	***k* (× 10^9 mol^{-1} dm^3 s^{-1})**					
	$HO^•$	**ref.**	**e_{aq}^-**	**ref.**	**$H^•$**	**ref.**
PhOH	6.6–18.0	[21, 26, 27]	0.03	[28]	1.2–2.1	[29-31]
IBU	6.0–18.0	[12, 16, 17, 22, 23, 32, 33]	8.5–8.9	[23, 34]	4.0	[34]
KETO	4.6–10.0	[23, 24, 33, 35-37]	20.0–26.1	[23, 24]	n.d.	–
NAP	3.5–22.0	[15, 16, 22, 23, 33, 36, 37]	4.9	[23]	n.d.	–
DICL	6.0–24.0	[17, 22, 23, 25, 33, 36]	1.5–1.7	[23, 25]	n.d.	–

The major AOPs are the followings [5]:

- radiolysis
  - electron beam irradiation
  - γ-radiation
- photochemical processes
  - visible (Vis) light initiated photolysis
  - ultraviolet (UV) light initiated photolysis
  - VUV light initiated photolysis
  - UV/VUV light initiated photolysis
  - the combination of UV photolysis with H_2O_2
  - sonolysis
  - microwave irradiation
- ozone based processes

- simple ozonation
- the combination of ozonation with UV photolysis
- the combination of ozonation with H_2O_2
- the combination of ozonation with both UV photolysis and H_2O_2

➢ homogeneous photocatalytic processes
- Fenton reaction
- photo-Fenton reaction
- electro-photo-Fenton reaction

➢ heterogeneous photocatalytic processes
- Vis/TiO_2
- UV/TiO_2
- UV/TiO_2/O_3

➢ electrochemical processes

➢ super critical water oxidation

➢ non-thermal plasma techniques

Radiolysis, photochemical processes, ozone based processes, homogeneous photocatalytic and heterogeneous photocatalytic processes are the most significant AOPs. It has to be mentioned that, there are no strict borders between the listed categories since these processes may be combined in much more different ways [5].

2.2.2. UV photolysis of the investigated compounds

UV photolysis is the most widely used photochemical process among AOPs. The efficiency of direct photolysis is determined by the quantum yield of the process (Φ) and the overlap between the absorption spectrum of the target molecule (Fig. 5) and the emission spectrum of the light source [38]. In case of a monochromatic lamp this latter factor is expressed by the value of the molar absorption coefficient of the contaminant at the emission wavelength of the light source (ε). The reported Φ values (Table IV) are usually < 1, suggesting that only a part of the excited molecules

degrade. Besides this, it is likely that other deactivation processes without degradation (like the emission of the incident radiation, the transformation of the photon energy to thermal energy, or fluorescence) also take place in the systems [39, 40]. The big difference between the reported values may be attributed to the differences in the photon flux and emission wavelength of the used light sources or to the differences in the reaction conditions (like the pH and the concentration of dissolved O_2).

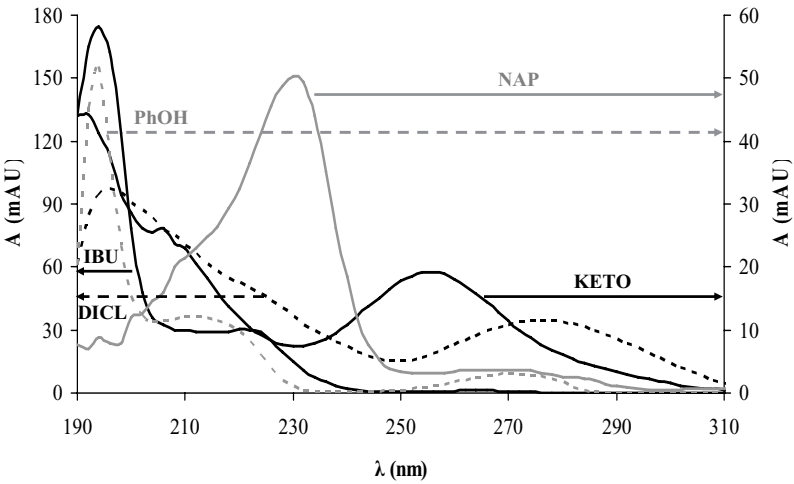

Fig. 5. UV absorbance of the investigated compounds.

Table IV. The quantum yield values of the photolysis of the investigated NSAIDs.

comp.	Φ	λ (nm)	ref.
PhOH	0.02–0.12	254	[41, 42]
IBU	0.04–0.19	254	[43, 44]
	0.33	300–400	[12]
KETO	0.17–0.26	254	[37, 43, 45]
	0.38	200–300	[37]
	0.75	313 or 333	[46]
NAP	0.0093–0.061	254	[15, 37, 39, 47]
	0.0556	200–300	[37]
	0.001 and 0.012	310–390	[40]
DICL	0.27	254	[48-52]
	0.41	238–334	[52]
	0.22	365	[50]
	0.0313	305, 313 and 366	[53]
	0.0375–0.24	sunlight	[16, 48, 49, 51, 53]

Although UV irradiation is often used for water disinfection, the total mineralization of contaminant molecules is not feasible by performing solely UV photolysis with the UV doses typically used during water disinfection (50–400 J m^{-2}). Under the mentioned conditions, IBU may be removed in ~10%, NAP in 29% and DICL in 21–34% [52, 54, 55]. The only exception is KETO which is reported to be eliminated in > 90% using a UV dose of 380 J m^{-2} [56]. The reason of the high efficiency of KETO elimination might be that usually low-pressure mercury lamps (emitting photons with an intensity maximum at 254 nm) are used in water disinfection techniques, and the value of $\varepsilon_{\mathrm{KETO,\ 254\ nm}}$ is relatively high (14104–15450 mol^{-1} dm^3 cm^{-1} [43, 45, 56]).

Although VUV photolysis is a photochemical process too, its mechanism differs a lot from that of UV photolysis. The reason is that in the first case the incident photons are mainly absorbed by the solvent molecules and the transformation of the contaminant starts with the reaction of the radicals formed from the solvent, while in the latter case the irradiation excites the solute molecules which results in their further transformation. The mechanism of VUV photolysis shows similarities with radiolysis, since similar radicals form during both methods.

2.2.3. Radiolysis

Radiolysis is one of the AOPs, where the generated radical set is known. Furthermore, in this case the distribution of the reactive intermediates may be considered homogeneous. This method is suitable therefore for performing some mechanistic investigations concerning the role of different radicals during the radiolysis of the studied compounds.

During irradiation of water with ionizing radiation $HO^{\bullet}$, e_{aq}^{-} and $H^{\bullet}$ form as reactive radical intermediates (1). In dilute aqueous solution they may react with solute molecules with *G* values (the yields of the radicals) of 0.28, 0.28 and 0.062 μmol J^{-1}, respectively [57, 58].

$$H_2O + \gamma \rightarrow HO^{\bullet}, e_{aq}^{-}, H^{\bullet} \quad (1)$$

Radiolytic experiments have revealed that although in the case of PhOH, IBU and KETO $HO^{\bullet}$ is more effective than e_{aq}^{-} in decomposing the NSAIDs [24, 34, 59], these reactive intermediates are similarly effective in degrading DICL, and the contribution of e_{aq}^{-} is lower only from the point of view of DICL mineralization [25, 60]. The reactions of $HO^{\bullet}$ with IBU, KETO and DICL lead to hydroxycyclohexadienyl-type radical intermediates, which in their further reactions yield hydroxylated derivatives of these compounds [24, 25, 34, 60]. Although in case of IBU e_{aq}^{-} attacks the carboxyl group [34], in case of KETO it is scavenged by the carbonyl oxygen and the electron adduct protonates to ketyl radical [24]. In case of DICL, the reaction with e_{aq}^{-} results in the dechlorination of the molecule [25, 60]. Unfortunately, no information was found in the literature concerning the radiolysis of NAP.

2.2.4. Vacuum ultraviolet photolysis

VUV photolysis is the other method among the AOPs where the generated radical set is known, and suggestions may therefore be put forward concerning the effects of different parameters on the radical set and on the degradation of organic contaminants. These results could contribute to the optimization of other AOPs.

Because of the low concentration of the contaminants (usually $< 10^{-2}$ mol dm^{-3}) relative to concentration of water (practically 55.56 mol dm^{-3}) in aqueous solutions, the VUV photons (100 nm $< \lambda <$ 200 nm) are mainly absorbed by the solvent molecules. The relatively high energy of the VUV light (6.20 eV $< Q_{\lambda} <$ 12.40 eV) excites H_2O molecules and results in the homolysis of H_2O (2). By the way, in a minor extent, also the ionisation of H_2O (3) may occur [61]. *E.g.* the 172 ± 14 nm radiation emitted by the widely used xenon excimer lamps (Xe excilamps) is practically absorbed completely within a 0.04-mm-thick H_2O layer, due to the high molar absorption coefficient of H_2O at this wavelength ($\varepsilon_{H_2O}^{172\ nm}$ = 10 mol^{-1} dm^{3} cm^{-1}) [62]. In this case bond homolysis is realized with a quantum yield of: $\Phi_{HO^{\bullet}}^{172\ nm}$

= 0.42 ± 0.04 [62] and e_{aq}^- (the conjugate base pair of $H^\bullet$ (4)) are produced with a Φ value of lower than 0.05 [63].

$$H_2O + h\nu_{\lambda < 190\,nm} \rightleftharpoons H_2O^* \underset{k_{-2}}{\overset{k_2}{\rightleftharpoons}} H^\bullet + HO^\bullet \quad (2)$$

$$H_2O + h\nu_{\lambda < 190\,nm} \rightleftharpoons H_2O^* \rightleftharpoons H^+ + HO^\bullet + e_{aq}^- \quad (3)$$

$$H^\bullet + H_2O \rightleftharpoons e_{aq}^- + H_3O^+ \qquad pK_a = 9.6\ [58]\ (4)$$

The deactivation of electronically excited H_2O molecules (H_2O^*) is also promoted by the surrounding water molecules, which can form a solvent cage [64-66]. The cage hinders the separation of the primary radicals, which therefore recombine very effectively, with the formation of H_2O ($k_{-2} = 7\times10^9$ mol^{-1} dm^3 s^{-1} in the bulk) [67]. These processes explain why $\Phi_{H_2O}^{172\,nm}$ is much lower than 1.

VUV photolysis was found to be an effective method in the decomposition of PhOH from diluted aqueous solution [64]. The presence of VUV light along the UV photons increased significantly the transformation rates of PhOH [42], IBU [43] and NAP [39] as well as the mineralization rates of IBU and KETO [68]. These results made reasonable the investigation of the simple VUV photolysis of the NSAIDs and the role of the generated radicals, which were not studied earlier.

2.3. The effects of radical transfers on the radical set formed during the VUV photolysis of aqueous solutions

2.3.1. The effects of dissolved O_2

Due to their short lifetime, the role of different radicals can be investigated only with indirect methods. One of these is the addition of radical transfer materials to the treated solutions. In this case, the target molecules and the radical transfers compete for the primary radicals of VUV photolysis ($HO^\bullet$ and $H^\bullet/e_{aq}^-$). Since the concentration of the reactive intermediates available for the contaminants is therefore reduced, it will decrease the transformation rates of the pollutant molecules. The degree of inhibition will depend on the concentration of the investigated compounds

and the radical transfers, on the ratio of their reaction rate constants with the primary radicals and on the *k* values of the studied organic compounds and the radicals formed in the reactions of the transfer molecules and the primary radicals. If the *k* values of the pollutants and the radical transfers with the primary radicals are in the same order of magnitude and the concentration of the transfer molecules is high enough, almost all of the primary radicals react with the radical transfers. In this case the transformation of the target compounds may be initiated by the radicals formed in the reactions of the transfer molecules and the primary radicals.

A widely used radical transfer is dissolved O_2, which hinders the recombination reactions of $H^\bullet/e_{aq}^-$ and $HO^\bullet$, and converts reductive $H^\bullet/e_{aq}^-$ to oxidative $HO_2^\bullet/O_2^{\bullet-}$ (5–7). The concentration of reactive oxygen species (ROS: $HO^\bullet$, $HO_2^\bullet/O_2^{\bullet-}$, peroxyl radicals *etc.*) is therefore very likely to be increased in the presence of O_2.

$$H^\bullet + O_2 \rightarrow HO_2^\bullet \qquad k_5 = 2.1 \times 10^{10}\ \mathrm{mol^{-1}\ dm^3\ s^{-1}}\ [29] \quad (5)$$

$$e_{aq}^- + O_2 \rightarrow O_2^{\bullet-} \qquad k_6 = 1.9 \times 10^{10}\ \mathrm{mol^{-1}\ dm^3\ s^{-1}}\ [29] \quad (6)$$

$$HO_2^\bullet \rightleftharpoons H^+ + O_2^{\bullet-} \qquad pK_a = 4.8\ [69] \quad (7)$$

If an organic contaminant reacts with $HO^\bullet$ either by H-abstraction (8, 9) or electrophilic addition (10), carbon-centered radicals form ($R^\bullet$, $RH\text{-}R^\bullet$ or $(RHOH)^\bullet$) [70]. Although the disproportionation reaction of these carbon-centered radicals (11, 12) leads on the one hand to a transformation product of the pollutant, on the other hand the contaminant molecule is regenerated. Similarly, the parent molecules might be regenerated also during the dismutation of carbon-centered radicals formed in the reactions of the pollutants with $H^\bullet$. The dissolved O_2 might affect the degradation efficiency also by scavenging the carbon-centered radicals (13 – 15) to furnish in peroxyl radicals ($ROO^\bullet$, $RH\text{-}ROO^\bullet$ or $(RHOH)\text{-}O_2^\bullet$). Since O_2 addition (13 – 15) competes with the disproportionation of these radicals (11, 12), the regeneration of the pollutant molecules is hindered in the presence of dissolved O_2.

$$RH + HO^\bullet \rightarrow R^\bullet + H_2O \quad (8)$$

$$RH\text{-}RH + HO^\bullet \rightarrow RH\text{-}R^\bullet + H_2O \quad (9)$$

$$RH + HO^{\bullet} \rightarrow (RHOH)^{\bullet} \quad (10)$$

$$RH\text{-}R^{\bullet} + RH\text{-}R^{\bullet} \rightarrow R{=}R + RH\text{-}RH \quad (11)$$

$$(RHOH)^{\bullet} + (RHOH)^{\bullet} \rightarrow ROH + RH + H_2O \quad (12)$$

$$R^{\bullet} + O_2 \rightleftharpoons ROO^{\bullet} \quad (13)$$

$$RH\text{-}R^{\bullet} + O_2 \rightleftharpoons RH\text{-}ROO^{\bullet} \quad (14)$$

$$(RHOH)^{\bullet} + O_2 \rightleftharpoons (RHOH)\text{-}O_2^{\bullet} \quad (15)$$

2.3.2. The effects of formate ions

Formate ion is also a well known $HO^{\bullet}$ transfer because it reacts with reactive $HO^{\bullet}$ with high rate constant and forms negligibly reactive carboxyl radical/carbon dioxide radical anion ($^{\bullet}COOH/CO_2^{\bullet-}$) (16–18):

$$HCOOH + HO^{\bullet} \rightarrow {}^{\bullet}COOH + H_2O \qquad k_{16} = 1.3 \times 10^8\ mol^{-1}\ dm^3\ s^{-1}\ [71]\ (16)$$

$$HCOO^- + HO^{\bullet} \rightarrow CO_2^{\bullet-} + H_2O \qquad k_{17} = 3.2 \times 10^9\ mol^{-1}\ dm^3\ s^{-1}\ [71]\ (17)$$

$$^{\bullet}COOH \rightleftharpoons H^+ + CO_2^{\bullet-} \qquad pK_a = 1.4\ [72]\ (18)$$

In the presence of O_2, $^{\bullet}COOH/CO_2^{\bullet-}$ transform to $HO_2^{\bullet}/O_2^{\bullet-}$ (19, 20):

$$^{\bullet}COOH + O_2 \rightarrow HO_2^{\bullet} + CO_2 \qquad k_{19} = 3 \times 10^9\ mol^{-1}\ dm^3\ s^{-1}\ [72]\ (19)$$

$$CO_2^{\bullet-} + O_2 \rightarrow O_2^{\bullet-} + CO_2 \qquad k_{20} = 4.2 \times 10^9\ mol^{-1}\ dm^3\ s^{-1}\ [73]\ (20)$$

Summarizing, in the presence of both O_2 and formate ions, all of the primary reactive species of VUV photolysis ($HO^{\bullet}$ and $H^{\bullet}/e_{aq}^-$) transform to $HO_2^{\bullet}/O_2^{\bullet-}$, therefore the effect of these species ($HO_2^{\bullet}/O_2^{\bullet-}$) may be investigated using these reaction conditions.

2.3.3. The effects of radical scavengers

If the reactivity of a radical (formed in the reaction of the transfer molecules and the primary radicals) is low enough, so that its contribution to the transformation of the contaminant might be neglected, the radical transfer is called radical scavenger. Two widely used radical scavengers are methanol (CH_3OH) and *tert*-butanol ($C(CH_3)_3OH$). They react with $HO^\bullet$ with pretty high rate constants ($k_{21} = 9.7 \times 10^8$ mol^{-1} dm^3 s^{-1} and $k_{22} = 6.0 \times 10^8$ mol^{-1} dm^3 s^{-1} [29]):

$$CH_3OH + HO^\bullet \rightarrow {}^\bullet CH_2OH + H_2O \quad (21)$$

$$C(CH_3)_3OH + HO^\bullet \rightarrow {}^\bullet CH_2C(CH_3)_2OH + H_2O \quad (22)$$

In the presence of dissolved O_2, the carbon centered radicals formed in (21 and 22) are converted to peroxyl radicals (the k_{23} being 4.2×10^9 mol^{-1} dm^3 s^{-1} [74], while the k_{24} being 1.4×10^9 mol^{-1} dm^3 s^{-1} [75]):

$${}^\bullet CH_2OH + O_2 \rightarrow {}^\bullet OOCH_2OH \quad (23)$$

$${}^\bullet CH_2C(CH_3)_2OH + O_2 \rightarrow {}^\bullet OOCH_2C(CH_3)_2OH \quad (24)$$

$H^\bullet/e_{aq}^-$ react also with these radical scavengers (25–28), but there is a difference of 4–6 orders of magnitude between their reaction rate constants with the scavenger molecules and with dissolved O_2 (k_5, k_6, k_{25}–k_{28}). Therefore, in the presence of both O_2 and radical scavengers, $HO_2^\bullet/O_2^{\bullet-}$, ${}^\bullet OOCH_2OH$ and ${}^\bullet OOCH_2C(CH_3)_2OH$ will be present in the solution among the reactive intermediates.

$$CH_3OH + H^\bullet \rightarrow {}^\bullet CH_2OH + H_2 \qquad k_{25} = 2.6 \times 10^6\ mol^{-1}\ dm^3\ s^{-1}\ [29] \quad (25)$$

$$CH_3OH + e_{aq}^- \rightarrow H^\bullet + CH_3O^- \qquad k_{26} < 1 \times 10^4\ mol^{-1}\ dm^3\ s^{-1}\ [29] \quad (26)$$

$$C(CH_3)_3OH + H^\bullet \rightarrow {}^\bullet CH_2C(CH_3)_2OH + H_2 \qquad k_{27} = 1.7 \times 10^5\ mol^{-1}\ dm^3\ s^{-1}\ [31] \quad (27)$$

$$C(CH_3)_3OH + e_{aq}^- \rightarrow \text{products} \qquad k_{28} < 4 \times 10^5\ mol^{-1}\ dm^3\ s^{-1}\ [76] \quad (28)$$

2.4. The reaction mechanism of the VUV decomposition of phenol

The detailed review of the reaction mechanism and possible transformation ways of the VUV initiated decomposition of PhOH (Fig. 6), a simple structured aromatic compound might help us to understand the VUV initiated transformation of the NSAIDs, containing aromatic rings too.

In the absence of dissolved O_2 the transformation of PhOH is initiated by its reaction with either $HO^{\bullet}$ or $H^{\bullet}$ to yield dihydroxycyclohexadienyl ($DHCD^{\bullet}$) and hydroxycyclohexadienyl ($HCD^{\bullet}$) radicals. The reaction of PhOH with e_{aq}^{-} is of minor relevance because of the low quantum yield of e_{aq}^{-} production during the VUV photolysis of water and because of the *k* value of this reaction is with 2–3 orders of magnitude lower than that of PhOH with $HO^{\bullet}$ (Table III).

In O_2-free solutions the formed $DHCD^{\bullet}$ may dimerize to yield a bicyclohexadiene or dismutate to result in dihydroxybenzene and regenerate PhOH. Another possibility of the transformation of $DHCD^{\bullet}$ is its dehydration reaction, which yields an instable radical cation [70]. The deprotonation of this radical cation leads to a resonance-stabilized phenoxyl radical [77, 78]. Phenoxyl radicals either dimerize to yield a bicyclohexadienone or react with $HO^{\bullet}$ to produce fragmentation products [70]. However the transformation of $DHCD^{\bullet}$ through phenoxyl radicals is of lower significance.

Similar to the transformation of $DHCD^{\bullet}$, the disproportionation of $HCD^{\bullet}$ might also regenerate PhOH, along with a cyclohexadiene. On the other hand, the recombination of $HCD^{\bullet}$-s yields a bicyclohexadiene [70].

In oxygenated solutions, O_2 addition competes with the dismutation reaction of $DHCD^{\bullet}$. Because of the usually significantly higher concentration of dissolved O_2 (c_{O_2}) than that of $DHCD^{\bullet}$, these radicals mainly transform to the respective peroxyl radicals. The further transformation of these latter species involves $HO_2^{\bullet}$ elimination to result in dihydroxybenzene.

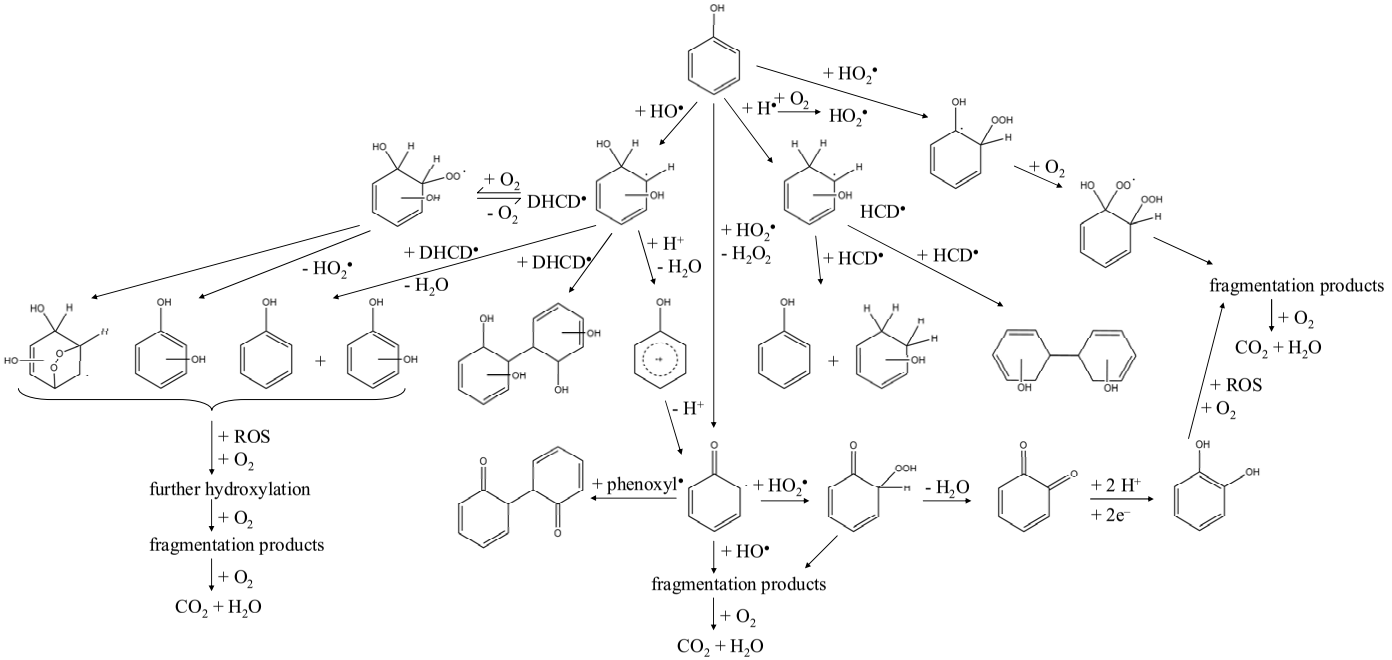

Fig. 6. The reaction mechanism of the VUV decomposition of PhOH.

On the other hand, the intramolecular reactions of these peroxyl radicals mainly yield ring-opening products. Due to the further reactions of the ring-opening products with the ROS present in the solution, finally the mineralization of PhOH is reached in VUV irradiated, O_2-saturated solutions. [70].

In the absence of dissolved O_2 the transformation of PhOH is initiated by its reaction with either $HO^{\bullet}$ or $H^{\bullet}$ to yield dihydroxycyclohexadienyl ($DHCD^{\bullet}$) and hydroxycyclohexadienyl ($HCD^{\bullet}$) radicals. The reaction of PhOH with e_{aq}^{-} is of minor relevance because of the low quantum yield of e_{aq}^{-} production during the VUV photolysis of water and because of the *k* value of this reaction is with 2–3 orders of magnitude lower than that of PhOH with $HO^{\bullet}$ (Table III).

In O_2-free solutions the formed $DHCD^{\bullet}$ may dimerize to yield a bicyclohexadiene or dismutate to result in dihydroxybenzene and regenerate PhOH. Another possibility of the transformation of $DHCD^{\bullet}$ is its dehydration reaction, which yields an instable radical cation [70]. The deprotonation of this radical cation leads to a resonance-stabilized phenoxyl radical [77, 78]. Phenoxyl radicals either dimerize to yield a bicyclohexadienone or react with $HO^{\bullet}$ to produce fragmentation products [70]. However the transformation of $DHCD^{\bullet}$ through phenoxyl radicals is of lower significance.

Similar to the transformation of $DHCD^{\bullet}$, the disproportionation of $HCD^{\bullet}$ might also regenerate PhOH, along with a cyclohexadiene. On the other hand, the recombination of $HCD^{\bullet}$-s yields a bicyclohexadiene [70].

In oxygenated solutions, O_2 addition competes with the dismutation reaction of $DHCD^{\bullet}$. Because of the usually significantly higher concentration of dissolved O_2 (c_{O_2}) than that of $DHCD^{\bullet}$, these radicals mainly transform to the respective peroxyl radicals. The further transformation of these latter species involves $HO_2^{\bullet}$ elimination to result in dihydroxybenzene. On the other hand, the intramolecular reactions of these peroxyl radicals mainly yield ring-opening products. Due to the further reactions of the ring-opening products with the ROS present in the solution, finally

the mineralization of PhOH is reached in VUV irradiated, O_2-saturated solutions. [70].

Although the transformation of PhOH in VUV irradiated solutions is mainly initiated by its reaction with $HO^{\bullet}$, the possible role and importance of the other ROS formed has to be regarded as well. In O_2 saturated solutions, O_2 and PhOH molecules compete for $H^{\bullet}/e_{aq}^{-}$. If the concentration of PhOH is lower than that of c_{O_2}, $HO_2^{\bullet}/O_2^{\bullet-}$ react with the solute molecules instead of $H^{\bullet}/e_{aq}^{-}$ (because of the similar k values of the reactions of O_2 and PhOH with $H^{\bullet}/e_{aq}^{-}$). On the other hand, $HO_2^{\bullet}$ elimination reactions are typical during the transformation of peroxyl radicals (see the next Section). Thus, $HO_2^{\bullet}/O_2^{\bullet-}$ are the most important ROS after $HO^{\bullet}$.

The k value of the reaction of PhOH with $HO_2^{\bullet}$ (although with 6–7 orders of magnitude lower than that of with $HO^{\bullet}$) is with one order of magnitude higher than that of with $O_2^{\bullet-}$ (2.7×10^3 mol^{-1} dm^3 s^{-1} [79] and 5.8×10^2 mol^{-1} dm^3 s^{-1} [80], respectively). Addition of $HO_2^{\bullet}$ to the aromatic ring results in a hydroxy-hydroperoxycyclohexadienyl radical. After O_2 addition to this latter species again fragmentation products, aliphatic aldehydes, carboxylic acids and finally CO_2 and H_2O form [81]. However, model calculations of *Altarawneh et al.* demonstrated that the reaction rate coefficient of the H-abstraction of $HO_2^{\bullet}$ is with at leas two orders of magnitude higher than that of $HO_2^{\bullet}$ addition [82]. Thus, H-abstraction of $HO_2^{\bullet}$ to yield H_2O_2 and phenoxyl radical dominates over the addition reaction.

$HO_2^{\bullet}$ may also recombine with phenoxyl radicals. The formed instable product might stabilize due dehydration, and the further transformation of the formed quinones results in 1,2-dihydroxybenzene or ring-opening products [83].

2.5. H_2O_2 formation during the VUV photolysis of aqueous solutions

The recombination (29, 30) and disproportionation reactions (31–33) of the radicals generated during the VUV photolysis of aqueous solutions may lead to H_2O_2 production:

$2\ HO^{\bullet} \rightarrow H_2O_2$ $\quad k_{29} = 5.5 \times 10^9\ mol^{-1}\ dm^3\ s^{-1}$ [29] (29)

$H^{\bullet} + HO_2^{\bullet} \rightarrow H_2O_2$ $\quad k_{30} = 9.7 \times 10^7\ mol^{-1}\ dm^3\ s^{-1}$ [84] (30)

$2\ HO_2^{\bullet} \rightarrow H_2O_2 + O_2$ $\quad k_{31} = 8.3 \times 10^5\ mol^{-1}\ dm^3\ s^{-1}$ [69] (31)

$2\ O_2^{\bullet-} + 2\ H_2O \rightarrow O_2 + H_2O_2 + 2\ HO^-$ $\quad k_{32} < 0.3\ mol^{-1}\ dm^3\ s^{-1}$ [69] (32)

$O_2^{\bullet-} + HO_2^{\bullet} + H_2O \rightarrow O_2 + H_2O_2 + HO^-$ $\quad k_{33} = 9.7 \times 10^7\ mol^{-1}\ dm^3\ s^{-1}$ [69] (33)

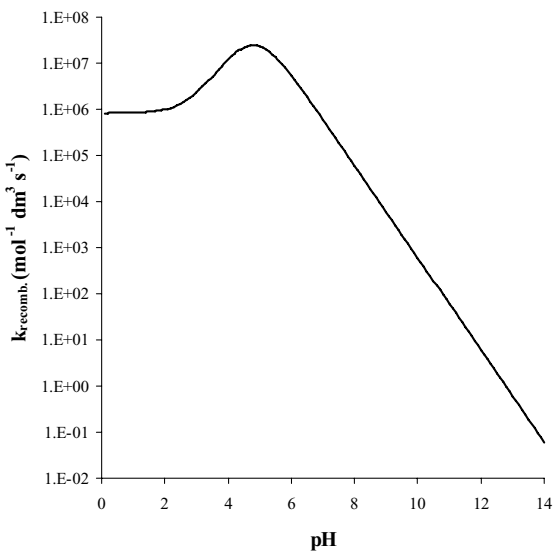

Fig. 7. The reaction rate constant of the recombination reaction of $HO_2^{\bullet}/O_2^{\bullet-}$ as a function of the solution pH [69].

However, the minor or negligible H_2O_2 concentration ($c_{H_2O_2}$) measured during the VUV photolysis of pure water under deoxygenated conditions suggests that the recombination reactions of $HO^{\bullet}$ (29) take place only in a minor extent [68, 85, 86].

Additionally, the significance of reaction (30) is reduced because of the low concentration of $H^{\bullet}$ in the presence of dissolved O_2, while that of reaction (32) because of the low value of rate constant k_{32}. Thus, it can be stated that in pure water H_2O_2 is mainly formed in the recombination reaction of $HO_2^{\bullet}/O_2^{\bullet-}$. It has to be noticed, that the reaction rate constant of this reaction ($k_{\text{recomb.}}$) depends strongly on the pH of the solution (Fig. 7) [69].

The possibility of H_2O_2 formation is reduced by the reaction of $HO_2^{\bullet}$ with $HO^{\bullet}$:

$$HO_2^{\bullet} + HO^{\bullet} \rightarrow O_2 + H_2O \qquad k_{34} = 6.6 \times 10^9 \text{ mol}^{-1} \text{ dm}^3 \text{ s}^{-1} \text{ [87]} \quad (34)$$

H_2O_2 can be decomposed by reaction with $HO^{\bullet}$ (35) or with $H^{\bullet}$ (36) (this latter reaction being of lower significance in the presence of O_2 because of the low concentration of $H^{\bullet}$) and in a minor extent by its VUV photolysis (37) [68]. The quantum yield of the photolysis has been estimated to be 0.98 ± 0.05 at 254 nm [88], while in the presence of organic compounds it was determined to be 0.50 [89].

$$H_2O_2 + HO^{\bullet} \rightarrow HO_2^{\bullet} + H_2O \qquad k_{35} = 2.7 \times 10^7 \text{ mol}^{-1} \text{ dm}^3 \text{ s}^{-1} \text{ [29]} \quad (35)$$

$$H_2O_2 + H^{\bullet} \rightarrow HO^{\bullet} + H_2O \qquad k_{36} = 3.6 \times 10^7 \text{ mol}^{-1} \text{ dm}^3 \text{ s}^{-1} \text{ [90]} \quad (36)$$

$$H_2O_2 + h\nu \rightarrow 2\ HO^{\bullet} \quad (37)$$

The presence of organic contaminants influences the $c_{H_2O_2}$ since the reaction of these molecules with $HO^{\bullet}$ increases the concentration of $R^{\bullet}$ (8), and also reduces the probability of the reaction of H_2O_2 and $HO^{\bullet}$ (35). Additionally, the decomposition of $ROO^{\bullet}$, generated from $R^{\bullet}$ in the presence of dissolved O_2 (13), may lead to $HO_2^{\bullet}$ production (38) [91], but they may also furnish tetroxides (ROOOOR) by recombination (39). $HO_2^{\bullet}/O_2^{\bullet-}$ can lead to H_2O_2 formation not only through reactions (31 and 33) but also through H-abstraction from an organic compound (40). According to the works of *von Sonntag and Schuchmann* [91] and *Quici et al.* [92] the decomposition of the unstable tetroxides with the formation of ketones (R'R"C=O) (41) results again in H_2O_2.

$$RHOO^{\bullet} \rightarrow R + HO_2^{\bullet} \quad (38)$$

$$2\ ROO^{\bullet} \rightarrow ROOOOR \quad (39)$$

$$RH + HO_2^{\bullet} \rightarrow R^{\bullet} + H_2O_2 \quad (40)$$

$$ROOOOR \rightarrow 2\ R'R''C{=}O + H_2O_2 \quad (41)$$

The tetroxides formed from secondary peroxyl radicals may also produce oxyl radicals (42). The rearrangement of the latter species result in their tautomers, the α-hydroxyalkyl radicals (43), while the reaction of these radicals with dissolved O_2 may produce $HO_2^{\bullet}$ again (44) [91]:

$$R'R''HCOOOOCHR''R' \rightarrow 2\ R'R''HCO^{\bullet} + O_2 \quad (42)$$

$$R'R''HCO^{\bullet} \rightarrow R'R''C^{\bullet}OH \quad (43)$$

$$R'R''C^{\bullet}OH + O_2 \rightarrow R'R''C{=}O + HO_2^{\bullet} \quad (44)$$

3. Objectives

Since pharmaceuticals are usually reported to be recalcitrant water contaminants, four nonsteroidal anti-inflammatory drugs (IBU, KETO, NAP and DICL) were chosen as target molecules of VUV photolysis and PhOH as a model compound.

$HO_2^{\bullet}/O_2^{\bullet-}$ are the most important oxygen containing species (ROS) along with $HO^{\bullet}$. The concentration of H_2O_2 ($c_{H_2O_2}$) refers to their concentration ($c_{HO_2^{\bullet}/O_2^{\bullet-}}$) and therefore, the $c_{H_2O_2}$ was planned to be measured during the VUV photolysis of the target molecules.

As it could be seen from Section 2.3.1 and Fig. 8, dissolved O_2 affects the radical set from several routes. Therefore, the aim of this study was to investigate the effect of the presence of O_2 on the initial transformation of the pollutants, on the formation and transformation of their main aromatic by-products and on their mineralization. To study the relatively increasing effect of dissolved O_2, experiments were planned in solutions containing the contaminant molecules in two different initial concentrations.

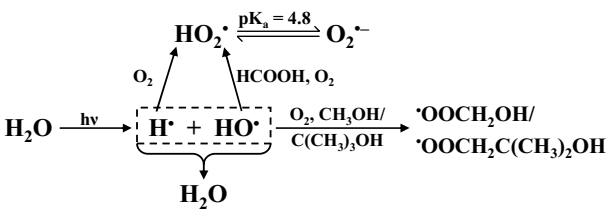

Fig. 8. The effect of different radical transfers on the radical set generated during the VUV photolysis of water.

In the presence of both dissolved O_2 and formate ions, all of primary reactive species of VUV photolysis ($HO^{\bullet}$ and $H^{\bullet}/e_{aq}^{-}$) transform to $HO_2^{\bullet}/O_2^{\bullet-}$ (Fig. 8). Additionally, altering the pH of the solution the ratio of $HO_2^{\bullet}$ and $O_2^{\bullet-}$ might also be influenced. Thus, the experiments aimed at the investigation of the effects of $HO_2^{\bullet}$ and $O_2^{\bullet-}$ on the initial transformation rates of the target compounds.

In the presence of both dissolved O_2 and radical scavengers (methanol or *tert*-butanol), peroxyl radicals ($^{\bullet}OOCH_2OH$ and $^{\bullet}OOCH_2C(CH_3)_2OH$) are present in the solution along with $HO_2^{\bullet}/O_2^{\bullet-}$ (Fig. 8). The aim of this study was to compare the initial transformation of the pollutant molecules in the presence of formate ions and in the presence of radical scavengers, and the reactivity of these ROS with each other.

The radical set is affected also by the contaminants themselves, and therefore the VUV photolysis of the target molecules was planned to be executed in four different initial concentrations.

Since no information was found in the literature concerning the VUV degradation of IBU, KETO, NAP or DICL, the aim of this work was also to give suggestions for the chemical structures of the formed aromatic by-products and to give a tentative mechanism of their formation.

Considering the VUV transformation of DICL, the investigation of the effect of the contaminant molecule and the treated multicomponent solutions on the cell proliferation and migratory responses of freshwater ciliate *Tetrahymena pyriformis* was also planned.

4. Materials and methods

4.1. Chemicals and reagents

Table V. The purity and the producer of the used chemicals.

chemical	purity	producer
1,2-DHB	≥ 99%	Fluka
1,4-DHB	99.5%	Riedel-de Häen
2-propanol	HPLC gradient grade, 99.8%	Scharlau
acetonitrile	ultra gradient HPLC grade	J.T.Baker
tert-butanol	100%	VWR
CH_3COOH	HPLC grade	Scharlau
CH_3OH	HiPerSolv CHROMANORM, 99.8%	VWR
DICL	n.r.*	Sigma
PhOH	99%	Sigma
HCl	AnalaR NORMAPUR, 37%	VWR
HCOOH	AnalaR NORMAPUR, 99–100%	VWR
HCOONa	n.r.	Reanal
HNO_3	AnalaR NORMAPUR, 68.5%	VWR
H_2O_2	puriss, ~ 30%	Fluka
H_2O_2-urea adduct	~ 30%	Fluka
H_3PO_4	85%	SAFC
IBU	> 99%	Fluka
$KMnO_4$	n.r.	Reanal
K-oxalate	n.r.	Reanal
KETO	n.r.	Sigma-Aldrich
NaH_2PO_4	≥ 99%	Spektrum 3D
Na_2HPO_4	≥ 99%	Fluka
$NaNO_3$	99.2%	VWR
NaOH	AnalaR NORMAPUR, 99%	VWR
Na-oxalate	n.r.	Reanal
NAP	98%	Fluka

*not reported

All the chemicals used were analytical grade (Table V) and were applied without further purification. The solutions were prepared in ultrapure Milli-Q water (MILLIPORE Milli-Q Direct 8/16 or MILLIPORE Synergy185). The parameters of the water gained from the first system were the followings: permeate conductivity: 13.3 μS cm^{-1}, resistivity: 18.2 MΩ cm, total organic carbon (TOC) content: 2 ppb.

The resistivity of the water gained from the second system was 18 MΩ cm. Some photolytic measurements of DICL were preformed in phosphate-buffered solution (PB). PB of pH = 7.4 contained 1.1×10^{-3} mol dm^{-3} NaH_2PO_4 and 1.9×10^{-3} mol dm^{-3} Na_2HPO_4 in Milli-Q water. The initial concentration (c_0) of the used radical transfers were chosen in order to ensure the reaction rates of $HO^\bullet$ and these compounds ($r_0 = k \times c_0 \times [HO^\bullet]_{SS}$) to be in nearly the same order of magnitude (see k_{16}, k_{17}, k_{21} and k_{22}; $[HO^\bullet]_{SS}$ being the steady-state concentration of $HO^\bullet$). The c_0 values of HCOOH, HCOONa, CH_3OH and $C(CH_3)_3OH$ were therefore 0.50, 0.05, 0.1 and 0.50 mol dm^{-3}, respectively. Additionally, the radical scavengers (methanol and *tert*-butanol) were applied also in concentrations ($c_{rad.\ scav.}$) of 1 mol dm^{-3} and 0.05 mol dm^{-3}, respectively.

4.2. Spectrophotometric determination of the H_2O_2 concentration

The concentration of H_2O_2 ($c_{H_2O_2}$), formed during the photolysis of H_2O in the presence of PhOH, IBU or KETO was measured with H_2O_2 test kits from Merck (valid in the range $4.41 \times 10^{-7} - 1.76 \times 10^{-4}$ mol dm^{-3}), which is based on the redox reaction between H_2O_2 and Cu(II) ions in the presence of phenanthroline (7, 45–47). This reaction results in a yellow or orange complex that can be determined spectrophotometrically at 455 ± 4 nm ($\varepsilon_{454\ nm} = 14300 \pm 200$ mol^{-1} dm^3 cm^{-1}) [93]. Samples were analyzed either in a Perkin Elmer, Lambda 16 or in an Agilent 8453 diode array spectrophotometer.

$$H_2O_2 + H_2O \rightleftharpoons H_3O^+ + HO_2^- \qquad pK_a = 11.6\ [94] \quad (45)$$

$$Cu^{2+} + HO_2^- \rightarrow Cu^+ + HO_2^\bullet \qquad (46)$$

$$Cu^{2+} + O_2^{\bullet-} \rightarrow Cu^+ + O_2 \qquad (47)$$

The five points calibration of the test kit was done with H_2O_2-urea adduct or simply H_2O_2. The exact concentration of the aqueous solution of the adduct and the

H_2O_2 solution were determined by titration with $KMnO_4$ (standardized with potassium or sodium oxalate solution). The calibration curve of this $c_{H_2O_2}$ measuring method was reported not to be affected by coexisting organic compounds and organic peroxides [93]. Thus, the equation established between the absorbance of the samples and their $c_{H_2O_2}$ in pure H_2O could also be used in the case of solutions containing PhOH, IBU, KETO or their decomposition products. This was confirmed in control experiments.

$c_{H_2O_2}$ in four samples (for IBU and KETO) was calculated using the calibration curve or the standard addition method. In the latter case, 4 cm^3 of standard 1.34×10^{-4} mol dm^{-3} H_2O_2 solution (made from the urea adduct) was added to 4 cm^3 of irradiated sample solution. In the knowledge of the exact concentration of the standard solution, $c_{H_2O_2}$ for the sample could be calculated. The difference between the results of calculations using the calibration curve or the standard addition method was within the error of $c_{H_2O_2}$ determination. The standard deviation of the measurements performed with the H_2O_2 test kit was less than ± 10% of the stated values [68].

4.3. Reactor configurations

Two types of experimental setups were used for the VUV investigations. Most of the measurements were performed in the apparatus depicted in Fig. 9, containing a Radium Xeradex™ xenon excimer lamp (of 20 W electrical input power) emitting at 172±14 nm. The lamp was placed at the center of a water-cooled, triple-walled tubular reactor. The inner wall of the reactor was made of Suprasil® quartz. The treated solution (250 cm^3) was circulated at 375 cm^3 min^{-1} in a 2-mm thick layer within the two inner walls of the reactor and in the reservoir by a Heidolph Pumpdrive 5001 peristaltic pump. The reactor and the reservoir were thermostated at 25.0±0.5 °C. N_2 (> 99.99% purity; Messer) or O_2 (> 99.99% purity; Messer) was bubbled (855–600 cm^3 min^{-1}) through the solution in the reservoir to achieve

deoxygenated or O_2-saturated conditions, respectively. The injection of N_2 was started 30, while the injection of O_2 15 min before each experiment, and was continued until the end of the irradiation.

The pH of the irradiated solutions was measured with an inoLab pH 730p instrument, the measuring electrode being introduced directly into the reservoir.

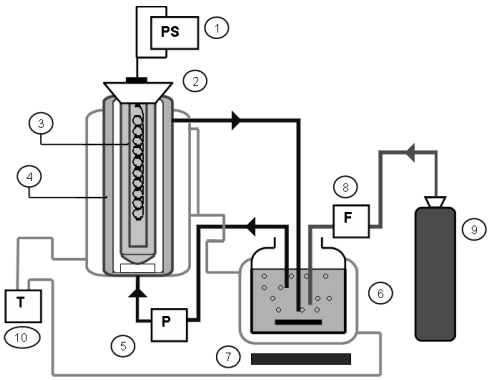

Fig. 9. Scheme of the 20 W photochemical apparatus 1: power supply; 2: teflon packing ring; 3: xenon excimer lamp; 4: reactor; 5: peristaltic pump; 6: reservoir; 7: magnetic stirrer; 8: flow meter; 9: O_2 or N_2 bottle and 10: thermostat.[1]

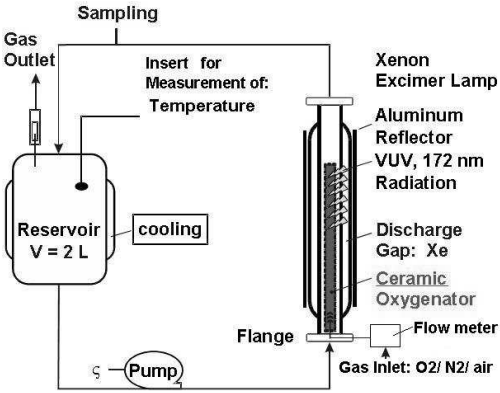

Fig. 10. Scheme of the 100 W photochemical apparatus containing a ceramic gassing unit [95].

The formation of H_2O_2 during the VUV photolysis of IBU and KETO was followed in the other apparatus, containing a 100 W xenon excimer flow-through

[1] Reprinted from *Science of the Total Environment*, 468–469, Arany, E.; Láng, J.; Somogyvári, D.; Láng, O.; Alapi, T.; Ilisz, I.; Gajda-Schrantz, K.; Dombi, A.; Kőhidai, L.; Hernádi, K., *Vacuum ultraviolet photolysis of diclofenac and the effect of the treated aqueous solutions on the proliferation and migratory responses of Tetrahymena pyriformis*, 996–1006, 2014, with permission from Elsevier.

photoreactor (Fig. 10). The photon flux of this lamp was reported to be (2,07 ± 0,08) × 10^{-5} mol_{photon} s^{-1} [96]. The inner electric connection of this reactor was a central metal wire and its outer electric connection was an aluminum reflector (foil). The electric connections were linked to an ENI plasma generator (model HPG-2). This lamp emitted also a quasi-monochromatic, incoherent radiation ($\lambda_{max.}$ = 172±14 nm) with an electrical efficiency of ~ 8–10% [97, 98].

Due to the low penetration depth of 172 nm light in H_2O the aqueous solution within the cylindrical xenon excimer flow-through photoreactor consists of a non-irradiated O_2-saturated bulk solution and a thin-walled hollow cylindrical irradiated volume (V_{irr}) near the quartz/H_2O interface. Within V_{irr}, dissolved O_2 reacts rapidly with $H^{\bullet}/e_{aq}^{-}$ and $R^{\bullet}$ (5, 6 and 13), resulting in a permanent O_2 deficit within this tiny volume [99, 100]. To reduce this effect and facilitate the transfer of O_2 directly into the irradiation zone, a ceramic gassing unit was mounted axially within the xenon excilamp [95].

In this case, 2 dm^3 of liquid was transferred into the reservoir and continuously recirculated through the xenon excimer flow-through lamp at a flow rate of 8 to 9 dm^3 min^{-1}. The reservoir was cooled externally with tap water. Additionally, 240 cm^3 of residual water remained within the pump and the teflon tubes, resulting in 2.240 dm^3 total treated volume. The flow rate of the injected gases was adjusted to ~ 1 dm^3 min^{-1}, with a gas pressure of ~ 0.5 bar. To saturate the solution with O_2, the liquid was recirculated for 30 min before ignition of the lamp. During both the saturation and the irradiation phases the gas was injected continuously.

All the presented results are the averages of 2–5 experiments; the error bars show the standard deviation of the measured values.

4.4. Gas chromatography

The photon flux of the 20 W light source was determined by means of methanol actinometry [96]. The methanol containing samples were analyzed on an Agilent Technologies 6890N Network GC System with an Agilent Technologies 5973

Network Mass Selective Detector. Helium was used as carrier gas at a flow rate of 1 cm^3 min^{-1} and at 0.58 bar. Methanol was separated from its VUV degradation products (*e.g.* formic acid, ethylene glycol or formaldehyde) on an Agilent 19091N-133 HP-INNOWax (0.25 mm × 30 m × 0.25 μm) column using the following heating profile: the temperature was kept at 60 °C for 3 min, than raised to 100 °C with a slope of 40 °C min^{-1} and kept there for 1 min, further it was raised to 220 °C with a slope of 40 °C min^{-1} and kept there for another 1 min. In each case 0.1 μl sample was injected using the split mode with a split ratio of 50.

4.5. Solid phase extraction

Solid phase extraction (SPE) was used for sample concentration before performing the MS measurements in the case of IBU and KETO. 20 cm^3 sample solution was extracted in each case on C_{18} SPE cartridges with the help of a BAKER spe-12G apparatus (prod. no. 7018-94). The cartridges were conditioned with 2 cm^3 of 1% acetic acid and methanol in 1:1 ratio, followed by 1 cm^3 Milli-Q water. After the addition of the sample solution the cartridges were left to dry for ten minutes and washed with 1 cm^3 4% 2-propanol solution. The elution of the target molecules was performed with 1 cm^3 of 1% acetic acid and methanol in 1:1 ratio.

4.6. High-performance liquid chromatography with mass spectrometry

Samples containing the pollutant molecules were analyzed on an Agilent 1100 series LCMSD VL system consisting of a binary pump, a micro vacuum degasser, a diode array detector, a thermostated column compartment, a 1956 MSD and ChemStation data managing software (Agilent Technologies). In case of the NSAIDs, 1% aqueous acetic acid and acetonitrile were used in 1:1 ratio as eluent, at a flow rate of 0.8 cm^3 min^{-1} either on a LiChroCART C_{18} (4 × 125 mm, 5 μm) or on a Kinetex Phenomenex C_{18} (4.6 × 100 mm, 2.6 μm) column. In the case of PhOH, methanol and

Milli-Q water were used in 7:13 ratio, at a flow rate of 0.8 cm^3 min^{-1} on a LiChroCART C_{18} (4.6 × 150 mm, 5 μm) column. The quantification wavelengths for the UV detector were 210 and 280 nm in the case of PhOH, 220 and 260 nm in the case of IBU, 260 nm in the case of KETO, 230 and 242 nm in the case of NAP and 240, 273 and 280 nm in the case of DICL containing solutions. For MS detection, a 1956 MSD with quadrupole analyzer and electrospray ionization was operated in the negative ion mode when measuring IBU, three of its by-products (A_{IBU}, B_{IBU} and D_{IBU}), KETO, three of its by-products (B_{KETO}, C_{KETO} and D_{KETO}), one by-product of NAP (B_{NAP}), DICL and its by-products (A_{DICL}, B_{DICL} and C_{DICL}), and in the positive ion mode when measuring one by-product of IBU (C_{IBU}), one by-product of KETO (A_{KETO}), NAP and two of its by-products (A_{NAP} and C_{NAP}). N_2 was used as drying gas (300 °C, 12 dm^3 min^{-1}) and the fragmentor voltage was 70 V (except for the measurement of C_{DICL}, where a fragmentor voltage of 80 V was applied). The nebulizer pressure was 2.4 bar in the case of measuring IBU and KETO, while it was 3.4 bar in the case of measuring NAP and DICL containing solutions. The capillary voltage was 3000 V (except in the case of measuring DICL containing solutions, where it was 1000 V).

4.7. Adsorbable organic halogen content measurements

The adsorbable organic halogen (AOX) contents of DICL containing solutions were determined using an APU2 sample preparation module (Analytik Jena AG) and a multi X 2500 instrument (Analytik Jena AG). During sample preparation, 30 cm^3 of solution was passed at a flow rate of 3 cm^3 min^{-1} through two quartz tubes containing 2 × 50 mg active carbon in the APU2 module. Inorganic halogens were washed from the surface of the carbon with a solution containing 0.2 mol dm^{-3} $NaNO_3$ and 0.14 mol dm^{-3} HNO_3. The carbon-containing columns were then burned in O_2 (> 99.99% purity; Messer,) stream at 950 °C and their halogen content was measured with a microcoulometric method in the multi X 2500 instrument.

4.8. Total organic carbon content measurements

The TOC content of the solutions was measured using a multi N/C 3100 instrument (Analytik Jena AG). The TOC content was determined as the difference between the total carbon (TC) and total inorganic carbon (TIC) contents. 2 cm^3 10 v/v % H_3PO_4 was added to 0.500 cm^3 solution to release the TIC of the sample in the form of CO_2. A further 0.500-cm^3 sample was then burned in O_2 (> 99.995% purity; Messer) stream at 800 °C. The CO_2 formed reflected the TC content of the sample. In both cases the amount of CO_2 was measured with a nondispersive infrared absorption detector.

4.9. Kinetic modeling

Performing a nonlinear model fit on the concentrations measured during the HPLC analyses, with the help of Mathematica 8 (Wolfram) software, the formal *k'* values of the degradation of the investigated compounds were determined. It should be mentioned that our system is very inhomogeneous, in spite of the continuous stirring. The VUV photons are absorbed in a very thin water layer (< 0.1 mm) and therefore only a thin-walled hollow cylindrical volume of solution is irradiated, near the quartz/water interface. Further, the experimental setup consisted of a partly-irradiated reactor and a reservoir, the determined (apparent) *k'* values therefore referring to the overall transformation rate of the target molecules under the experimental conditions applied.

4.10. Proliferation inhibition assays

For measuring the proliferation inhibiting effect of the VUV-treated DICL containing samples, 10^3 cells $well^{-1}$ were placed in the core blocks of 60 wells in 96-well microtiter plates (Sarstedt AG) and incubated with the samples at 28 °C for 24 h. The cells were subsequently fixed with 4% formaldehyde (Reanal) containing PB and

counted with an impedimetric CASY TT cell counter (Innovatis-Roche). The inhibitory effects of VUV-treated samples were determined by normalizing the numbers of cells in the treated sample wells to the cell numbers in the negative control wells. These wells contained cell culture medium (containing 0.1% (w/w) yeast extract (Difco) and 1% (w/w) Bactotriptone (Difco) in distilled water) with the appropriate volume proportion of PB. Measurements were performed in quintuplicate and repeated three times.

Samples from the VUV photolysis of DICL solutions prepared in PB were then diluted to 1%, 5% and 25% (v/v) in the cell culture medium. Cells were incubated with 1–90 v/v% of PB in culture medium for 24 h, and the number and morphology of the cells were then evaluated under a microscope (Zeiss Axio Observer).

4.11. Chemotaxis assay

Directed migratory response of motile cells to the gradient of a dissolved chemical is called chemotaxis. Chemotactic characterization of a substance includes the description of the elicited effect, which can be positive, *i.e.* attractant, or negative, *i.e.* repellent, as well as the time and concentration dependences of the induced response. The chemotactic responses elicited by the VUV-treated DICL containing samples were measured in a two-chamber multichannel capillary assay device [101] for which the optimal incubation time was found to be 15 min [102]. Samples were placed in the upper chamber of the device, whereas cells (10^4) were loaded into the lower chamber. The number of positive responder cells was determined with a CASY TT cell counter (Innovatis-Roche), following a 15-min incubation at 28 °C and fixation with 4% formaldehyde containing PB.

Samples were diluted to 0.1%, 0.01%, 0.001%, 0.0001%, 0.00001% and 0.000001% (v/v) in cell culture medium. Control runs with pure culture medium in the upper chamber served for the normalization of cell numbers. The ratio obtained designated the Chemotaxis Index (Chtx. Ind.). Measurements were carried out in quadruplicate.

5. Results and discussion

5.1. Methanol actinometry

At the beginning of the measurements the photon flux of the 20 W light source was determined by means of methanol actinometry [96]. According to the work of Oppenländer and Schwarzwälder, the photon flux of the lamp (P) is proportional to the initial VUV-induced degradation rate of methanol ($k^0_{\text{obs.}}$) in aqueous solution, as it is presented in Eq. VII. The factor 0.946 refers to the production of methanol by the disproportionation reaction of hydroxymethyl radicals ($^{\bullet}CH_2OH$) (48), which slows down the $HO^{\bullet}$-induced transformation of methanol (21); V_R is the total irradiated volume (250 cm^3); Φ_{H_2O} is the total quantum yield of water photolysis (0.42 [62]); ζ_{H_2O} is the fraction of photons absorbed by water; Φ_{CH_3OH} is the total quantum yield of methanol photolysis (0.88 [62]) and ζ_{CH_3OH} is the fraction of photons absorbed by methanol. Since the k' values of Fig. 22 and the r_0 (= $k' \times c_0$) values of Tables VI, VIII–X (Sections 5.2–5.5) were calculated to refer to the overall transformation rate of the target molecules, the $k^0_{\text{obs.}}$ values calculated here refer also to the overall transformation of methanol, and V_R, although inhomogeneously irradiated, is considered to be the total volume of the solution. Thus, the k' and $k^0_{\text{obs.}}$ values are consistent with each other.

$$P = \frac{1}{0.946} \times k^0_{\text{obs.}} \times \frac{V_R}{\Phi_{H_2O} \times \zeta_{H_2O} + \Phi_{CH_3OH} \times \zeta_{CH_3OH}} \qquad \text{(VII)}$$

$$2\ ^{\bullet}CH_2OH \rightarrow CH_3OH + CH_2O \qquad (48)$$

The ζ_{H_2O} and ζ_{CH_3OH} values were calculated from the molar absorption coefficients of water and methanol at 172 nm (ε_{H_2O} = 10 mol^{-1} dm^3 cm^{-1}, ε_{CH_3OH} = 162 mol^{-1} dm^3 cm^{-1}, respectively [62]), the initial concentration of methanol ($c^0_{CH_3OH}$) and the concentration of water (c_{H_2O}), which was considered to be 55.6 mol dm^{-3} in such diluted solutions (Eqs. VIII and IX).

$$\zeta_{CH_3OH} = \frac{\varepsilon_{CH_3OH} \times c^0_{CH_3OH}}{\varepsilon_{CH_3OH} \times c^0_{CH_3OH} + \varepsilon_{H_2O} \times c_{H_2O}} \quad \text{(VIII)}$$

$$\zeta_{H_2O} = 1 - \zeta_{CH_3OH} \quad \text{(IX)}$$

The P may be determined from the $k^0_{obs.}$ values, which are nearly constant over a definite $c^0_{CH_3OH}$ range. At lower $c^0_{CH_3OH}$ the degradation of methanol may be represented with a pseudo-first-order rate constant, instead of a zero-order rate constant ($k^0_{obs.}$), while at higher $c^0_{CH_3OH}$, the VUV photolysis of methanol (49–52) competes with the VUV photolysis of water (2, 3) and the $HO^\bullet$-initiated degradation of methanol (21), increasing the $k^0_{obs.}$ values [96] (the $\Phi_{\lambda = 185\ nm}$ values represent the quantum yield of the processes at 185 nm). The $k^0_{obs.}$ was determined therefore to be 5.1×10^{-6} mol dm^{-3} s^{-1} (Fig. 11) and the photon flux of the 20 W xenon excimer lamp was calculated to be $(3.0 \pm 0.1) \times 10^{-6}$ mol$_{photon}$ s^{-1}.

$CH_3OH + h\nu \rightarrow CH_3O^\bullet + H^\bullet$ $\Phi_{\lambda = 185\ nm} = 0.69$ [62] (49)

$CH_3OH + h\nu \rightarrow {}^\bullet CH_2OH + H^\bullet$ $\Phi_{\lambda = 185\ nm} = 0.08$ [62] (50)

$CH_3OH + h\nu \rightarrow CH_2O + H_2$ $\Phi_{\lambda = 185\ nm} = 0.06$ [62] (51)

$CH_3OH + h\nu \rightarrow CH_3^\bullet + HO^\bullet$ $\Phi_{\lambda = 185\ nm} = 0.05$ [62] (52)

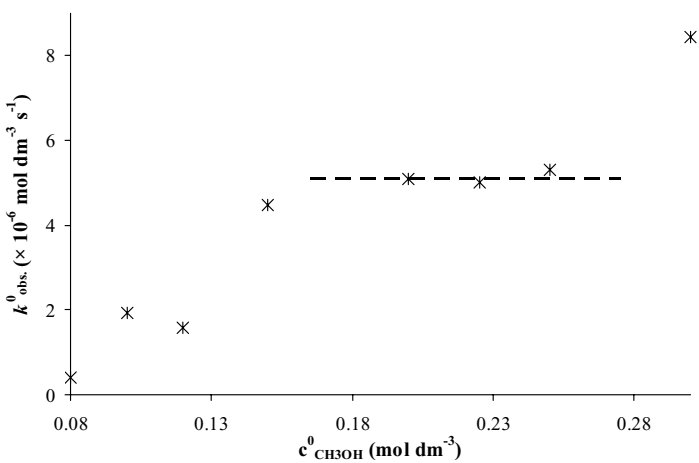

Fig. 11. The initial VUV-induced degradation rates of methanol as a function of the initial methanol concentration, using the 20 W xenon excimer lamp.

Since the energy of the 172 nm photons ($E^{172\ \mathrm{nm}}$) is 6.96 × 10^5 J $\mathrm{mol_{photon}}^{-1}$, the electrical power of this lamp may be calculated ($P_{\mathrm{el.}}$ = 2.1 W; Eq. X), which means a realistic electrical efficiency of ~ 10%.

$$P_{\mathrm{el.}} = P \times E^{172\,\mathrm{nm}} = 3\times10^{-6}\ \mathrm{mol_{photon}\ s^{-1}} \times 6.96\times10^{5}\ \mathrm{J\ mol_{photon}}^{-1} = 2.1\ \mathrm{W} \qquad \text{(X)}$$

5.2. The effects of dissolved O_2

5.2.1. H_2O_2 formation during the VUV photolysis of the contaminant molecules

Although the formation of H_2O_2 during the irradiation of PhOH was measured in the reactor depicted in Fig. 9, and during the irradiation of IBU or KETO in the reactor shown in Fig. 10, it was experienced in each case that the initial transformation of the contaminant molecules increases the $c_{H_2O_2}$ (Fig. 12) [68]. (The $c_{H_2O_2}$ values measured during the VUV photolysis of the NSAIDs were significantly higher than the values obtained in the case of PhOH likely because of the difference between the electric input power of the light sources (100 W *vs.* 20 W). While the difference between the $c_{H_2O_2}$ values in the case of IBU and KETO are likely due to the difference between the chemical structures and the number of carbon atoms of these compounds.)

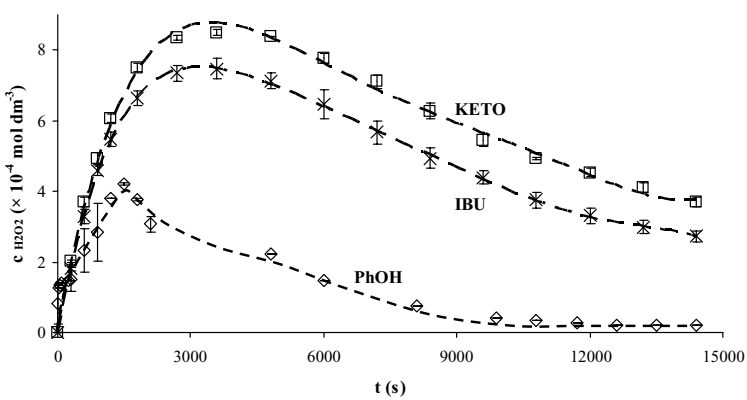

Fig. 12. H_2O_2 formation during the VUV irradiation of PhOH, IBU or KETO containing (c_0 = 1.0 × 10^{-4} mol dm^{-3}), O_2 saturated solutions.

The increase of the $c_{H_2O_2}$ in the presence of the previously mentioned organic contaminants is in accordance with the results concerning the VUV-induced mineralization of oxalic acid or methanol [85, 86] and make reasonable the assumption that the $c_{H_2O_2}$ increases also during the VUV photolysis of NAP and DICL. The reason of the increased values of $c_{H_2O_2}$ may be that these organic contaminants are able to remove $HO^{\bullet}$ and $H^{\bullet}/e_{aq}^{-}$ from the solvent cage and transform to $R^{\bullet}$ (8, 53).

$$RH + H^{\bullet} \rightarrow R^{\bullet} + H_2 \qquad (53)$$

On the one hand, H_2O_2 may be generated through the formation and decomposition of tetroxides, generated from these radicals (13, 39 and 41). The formation of ketones (41) may occur through formation of six- or five-membered transition states (Figs. 13 and 14, where Ph represents the aromatic ring) [91, 92]. As evidence of the above reaction mechanisms, 4-isobutylacetophenone was detected to form during the VUV transformation of IBU (Section 5.6.1).

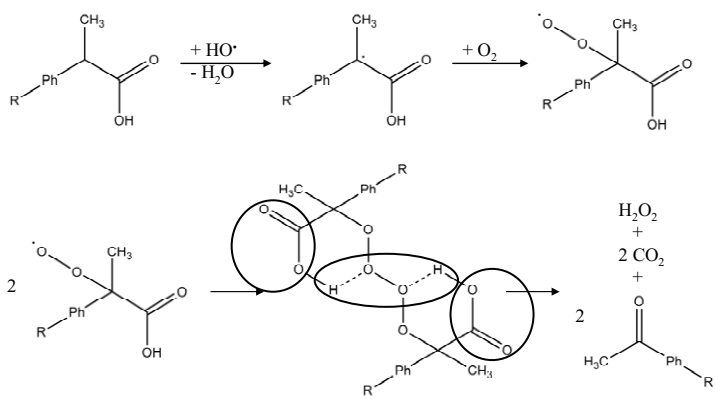

Fig. 13. Split off of H_2O_2 from tetroxides formed by the recombination of tertiary peroxyl radicals.

On the other hand, the $c_{HO_2^{\bullet}/O_2^{\bullet-}}$ is also increased in the presence of organic contaminants (38, 44), which could be the second reason of the increased $c_{H_2O_2}$, due to the reactions (31, 33 and 40). Thus, the former results (Fig. 12) support the

assumption that during the initial VUV transformation of the studied contaminant molecules the $c_{HO_2^{\bullet}/O_2^{\bullet-}}$ increases. Although the reactivity of $HO_2^{\bullet}/O_2^{\bullet-}$ is usually reported to be lower than that of $H^{\bullet}$ [70], in an elevated concentration they may also contribute to the degradation of organic contaminants [68]. Therefore it is reasonable to investigate thoroughly the effects of $HO_2^{\bullet}/O_2^{\bullet-}$ on the VUV decomposition of pollutants.

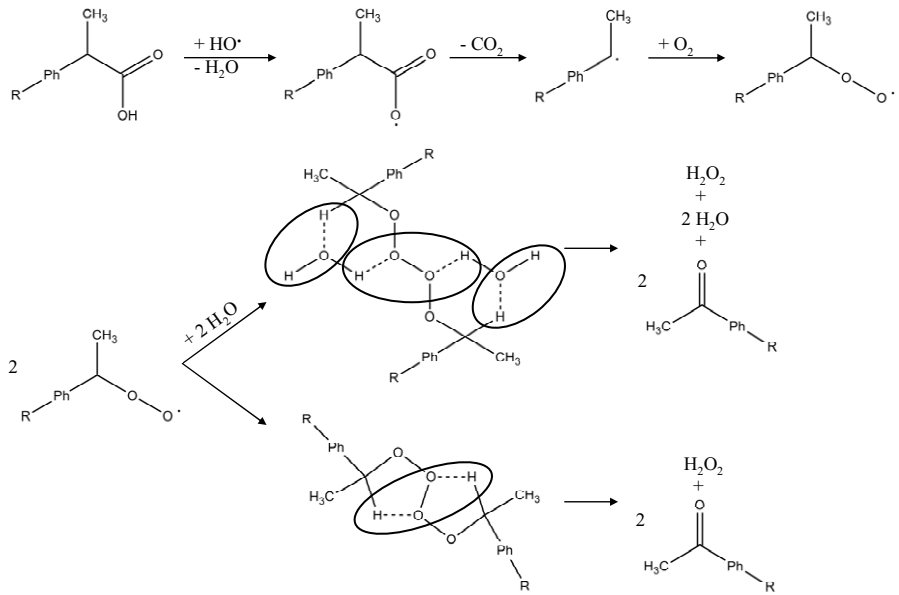

Fig. 14. Split off of H_2O_2 from tetroxides formed by the recombination of secondary peroxyl radicals.

5.2.2. The effects of dissolved O_2 on the initial transformation of the contaminant molecules

Although the reactivity of $HO_2^{\bullet}/O_2^{\bullet-}$ is usually reported to be lower than that of $H^{\bullet}$ [70], in an elevated concentration they may also contribute to the degradation of organic contaminants. Additionally, dissolved O_2 could prevent the recombination of $H^{\bullet}/e_{aq}^{-}$ and $HO^{\bullet}$ (2, 3, 5 and 6), and at the same time may hinder the regeneration of the target molecules (8–15). The increase of the initial transformation rates (r_0) of the

studied compounds was expected therefore, in the presence of O_2. The results supported the above assumptions in the case of the model compound (PhOH) (Fig. 15). The regeneration of PhOH during the disproportionation reactions of either $DHCD^{\bullet}$ or $HCD^{\bullet}$ was presented in Fig. 6. Along the former explanations, the reaction of $HO_2^{\bullet}$ (present in O_2 saturated solutions instead of $H^{\bullet}$) with PhOH also leads to the degradation of the latter (Fig. 6), therefore it seems that the contribution of oxidative $HO_2^{\bullet}/O_2^{\bullet-}$ to the transformation of PhOH is much more significant than that of $H^{\bullet}/e_{aq}^{-}$.

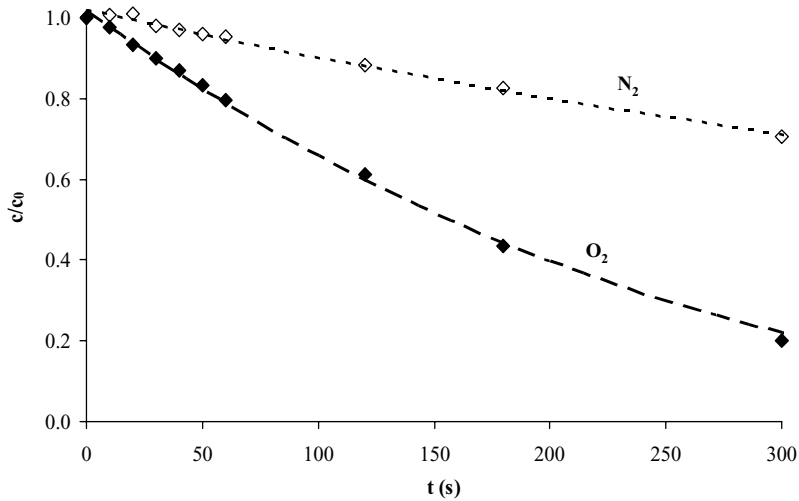

Fig. 15. The VUV photolysis of PhOH ($c_0 = 1.0 \times 10^{-4}$ mol dm^{-3}) in the presence and absence of dissolved O_2.

Contrary to the expectations, the r_0 values were significantly higher in the absence of O_2, when NAP containing solutions were irradiated (Fig. 16) [39]. Moreover, the differences between the r_0 values determined in O_2-saturated or deoxygenated solutions didn't depend on the c_0 values of NAP.

The effect of dissolved O_2 was investigated therefore in the case of the three other NSAIDs as well. As it can be deduced from Table VI, the absence of O_2 enhanced the VUV photolysis of IBU in 1.0×10^{-5} mol dm^{-3} concentrated solutions, but it had no significant effect in any other case.

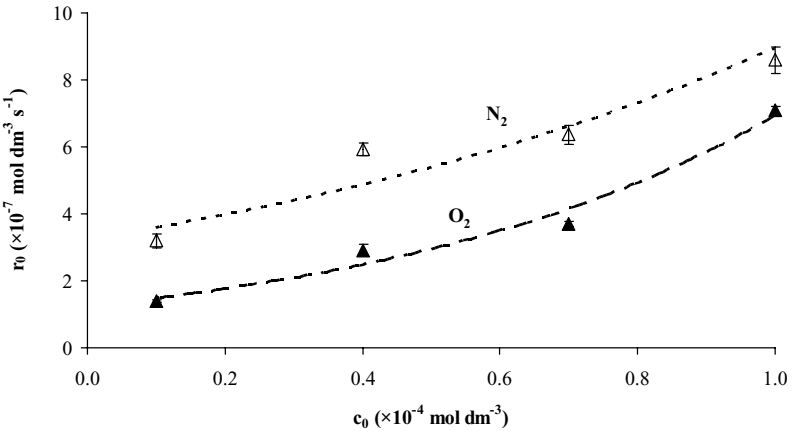

Fig. 16. The initial VUV transformation rates of NAP solutions of different initial concentrations, in the presence and absence of dissolved O_2.[2]

Table VI. The initial VUV transformation rates of the investigated compounds in the presence and absence of dissolved O_2.

comp.	gas	r_0 (× 10^{-7} mol dm^{-3} s^{-1})	
		$c_0 = 1.0 \times 10^{-5}$ mol dm^{-3}	$c_0 = 1.0 \times 10^{-4}$ mol dm^{-3}
PhOH	O_2	2.4 ± 0.05	4.4 ± 0.10
	N_2	1.9 ± 0.05	1.2 ± 0.03
IBU	O_2	1.2 ± 0.07	5.3 ± 0.20
	N_2	1.6 ± 0.06	5.2 ± 0.30
KETO	O_2	2.8 ± 0.10	10.0 ± 0.30
	N_2	2.7 ± 0.04	10.3 ± 0.40
NAP	O_2	1.4 ± 0.04	6.8 ± 0.20
	N_2	3.2 ± 0.20	8.6 ± 0.40
DICL	O_2	1.9 ± 0.05	5.7 ± 0.30
	N_2	1.8 ± 0.08	5.5 ± 0.08

Since the reaction of $H^{\bullet}/e_{aq}^{-}$ with O_2 (5, 6) or with an organic compound are competitive processes, the role of dissolved O_2 was investigated in solutions containing the contaminant molecules both in 1.0×10^{-5} mol dm^{-3} and 1.0×10^{-4} mol dm^{-3}. Although the value of the reaction rate constant of the reaction with $H^{\bullet}$ is reported only in the case of PhOH and IBU (Table III), it might be supposed that also the other three values are in nearly the same order of magnitude as the *k* values of

[2] Reprinted from *Journal of Hazardous Materials,* 262, Arany, E.; Szabó, R.K.; Apáti, L.; Alapi, T.; Ilisz, I.; Mazellier, P.; Dombi, A.; Gajda-Schrantz, K., *Degradation of naproxen by UV, VUV photolysis and their combination*, 151–157, 2013, with permission from Elsevier.

their reactions with $HO^{\bullet}$ or the values of k_5 and k_6. Additionally, the concentration of dissolved O_2 (c_{O_2} = 1.25 × 10^{-3} mol dm^{-3}) was with one or two orders of magnitude higher than the applied c_0 values. If the c_0 was 1.0 × 10^{-5} mol dm^{-3}, the rate of the reaction of $H^{\bullet}/e_{aq}^{-}$ with O_2 (5, 6) was therefore ~ 100 times higher and in the other case ~ 10 times higher than the rate of the reaction of $H^{\bullet}/e_{aq}^{-}$ with the studied compounds. Thus, the effects of dissolved O_2 were more pronounced in the case of using a c_0 of 1.0 × 10^{-5} mol dm^{-3}.

In the case of NAP and 1.0 × 10^{-5} mol dm^{-3} IBU solutions it might be supposed that $H^{\bullet}/e_{aq}^{-}$ also contribute to the degradation of the target molecules. In the presence of dissolved O_2 the transformation of these reactive intermediates to less reactive $HO_2^{\bullet}/O_2^{\bullet-}$ might hinder the degradation of the contaminants [39].

In the case of KETO, DICL and 1.0 × 10^{-4} mol dm^{-3} IBU solutions also the contribution of $H^{\bullet}/e_{aq}^{-}$ to the transformation of the organic substrates might be underlined. However, in this case it is likely that the concentration of $H^{\bullet}/e_{aq}^{-}$, which decreased in the presence of O_2, was compensated by the increased concentration of ROS [103].

Additionally, in the case of the NSAIDs the significance of dissolved O_2 in hindering the regeneration of the contaminant molecules seemed not to be relevant, maybe because of the rapid further transformation of $R^{\bullet}$, RH-$R^{\bullet}$ and $(RHOH)^{\bullet}$.

5.2.3. The effects of dissolved O_2 on the degradation by-products and the mineralization of the contaminant molecules

Dissolved O_2 also affected the formation and transformation of VUV photoproducts of the contaminant molecules (Section 5.6). During the photolysis of the target compounds four aromatic by-products of IBU and KETO (A_{IBU} – D_{IBU} and A_{KETO} – D_{KETO}, respectively – see their tentative structures in Sections 5.6.1 and 5.6.2), three by-products of NAP and DICL (A_{NAP} – C_{NAP} and A_{DICL} – C_{DICL}, respectively – see their tentative structures in Sections 5.6.3 and 5.6.4) and two by-

products of PhOH (1,2- and 1,4-dihydroxybenzene (1,2-DHB and 1,4-DHB, respectively) – identified with the help of standards) were detected. Among these photoproducts, the concentration of A_{IBU}, B_{IBU}, B_{KETO}, C_{KETO}, D_{KETO}, A_{NAP}, C_{NAP}, A_{DICL} and 1,2-DHB was higher in the presence of dissolved O_2, while the concentration of C_{IBU}, A_{KETO}, B_{DICL}, C_{DICL} and 1,4-DHB in the absence of O_2 (like in Fig. 17). The concentration of D_{IBU} was nearly the same both under oxygenated or deoxygenated conditions, while B_{NAP} was detected only in O_2 saturated solutions.

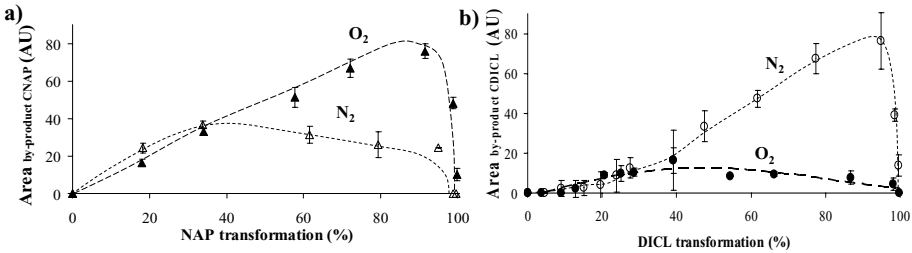

Fig. 17. The effects of dissolved O_2 on the VUV formation and transformation of a) by-product C_{NAP} and b) by-product C_{DICL} ($c_0 = 1.0 \times 10^{-4}$ mol dm^{-3}).

Although the formation of the detected by-products of the NSAIDs is probably not a one-step process (see Section 5.6), the reactions between the radicals generated during the VUV photolysis and the target molecules may be the rate determining steps of their formation. If the reaction rate of a radical and an organic compound is higher than that of the radical and the by-product (which can be considered as a result of the reaction between the radical and the contaminant), the radical enhances the formation of the by-product. Similarly, if the reaction rate of a radical and an organic compound is lower than that of the radical and the by-product, the radical contributes mainly to the transformation of the by-product. In other words, the concentration of a by-product is elevated if a radical contributes to its formation, and it is lower if a radical enhances its transformation.

In O_2-saturated solutions $HO_2^{\bullet}/O_2^{\bullet-}$ are present along $HO^{\bullet}$, while in deoxygenated solutions $H^{\bullet}/e_{aq}^{-}$. According to the ratio of the by-products in the presence and in the absence of O_2, mentioned above (*e.g.* in Fig. 17) it is likely that $HO_2^{\bullet}/O_2^{\bullet-}$ contributed to the formation of A_{IBU}, B_{IBU}, B_{KETO}, C_{KETO}, D_{KETO}, A_{NAP},

B_{NAP}, C_{NAP}, A_{DICL} and 1,2-DHB and to the transformation of C_{IBU}, A_{KETO}, B_{DICL}, C_{DICL} and 1,4-DHB. Similarly, $H^{\bullet}/e_{aq}^{-}$ could contribute to the formation of C_{IBU}, A_{KETO}, B_{DICL}, C_{DICL} and 1,4-DHB and to the transformation of A_{IBU}, B_{IBU}, B_{KETO}, C_{KETO}, D_{KETO}, A_{NAP}, B_{NAP}, C_{NAP}, A_{DICL} and 1,2-DHB.

Chlorine-containing compounds, and therefore also the VUV degradation by-products of DICL may have toxic effects. Hence, the AOX contents of the irradiated solutions ($c_0 = 1.0 \times 10^{-4}$ mol L^{-1}) were also measured. As it can be seen from Fig. 18, the rate of dehalogenation did not depend on the presence or absence of O_2. The reason of this might be on the one hand, that the initial degradation rates of DICL were very similar in oxygenated and deoxygenated solutions (Table VI). On the other hand, the concentration of by-product A_{DICL} was higher in the presence, while that of B_{DICL} and C_{DICL} in the absence of dissolved O_2 (Fig. 17b) [103].

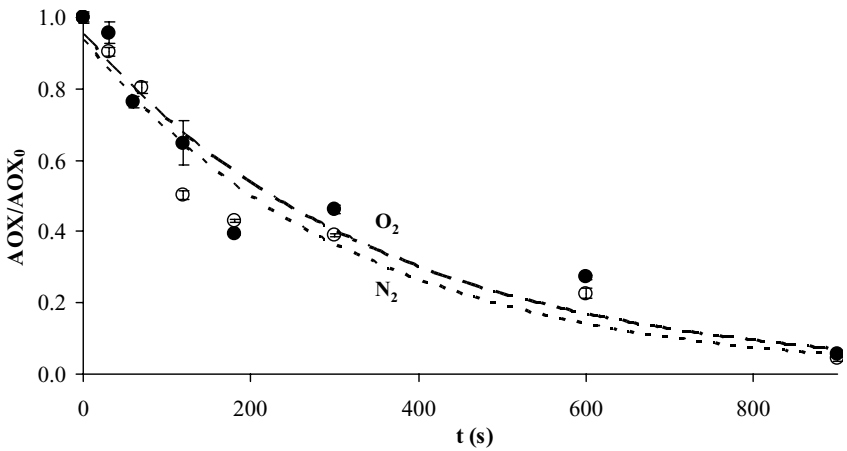

Fig. 18. The effect of dissolved O_2 on the dehalogenation of DICL ($c_0 = 1.0 \times 10^{-4}$ mol dm^{-3}).[3]

Similarly to NAP-containing solutions (Fig. 19), the mineralization of the NSAIDs was significantly more efficient in the presence of dissolved O_2 (Table VII). In oxygenated solutions the total mineralization of the contaminants was reached after 2 h of VUV irradiation (with the exception of IBU, where 25% of the initial

[3] Reprinted from *Science of the Total Environment*, 468–469, Arany, E.; Láng, J.; Somogyvári, D.; Láng, O.; Alapi, T.; Ilisz, I.; Gajda-Schrantz, K.; Dombi, A.; Kőhidai, L.; Hernádi, K., *Vacuum ultraviolet photolysis of diclofenac and the effect of the treated aqueous solutions on the proliferation and migratory responses of Tetrahymena pyriformis*, 996–1006, 2014, with permission from Elsevier.

TOC content of the solution was detected even after 2 h of treatment). However, in solutions purged with N_2, only a 10–45% mineralization could be reached within the applied irradiation time. This would suggest that in deoxygenated solutions, some undetected recalcitrant by-products were formed. In the absence of O_2, the recombination of the $R^{\bullet}$ formed in the reaction of the NSAIDs and $HO^{\bullet}$ is highly likely and may result in dimers and oligomers of the target molecules, analogously to the transformation of other organic contaminants [70, 103, 104].

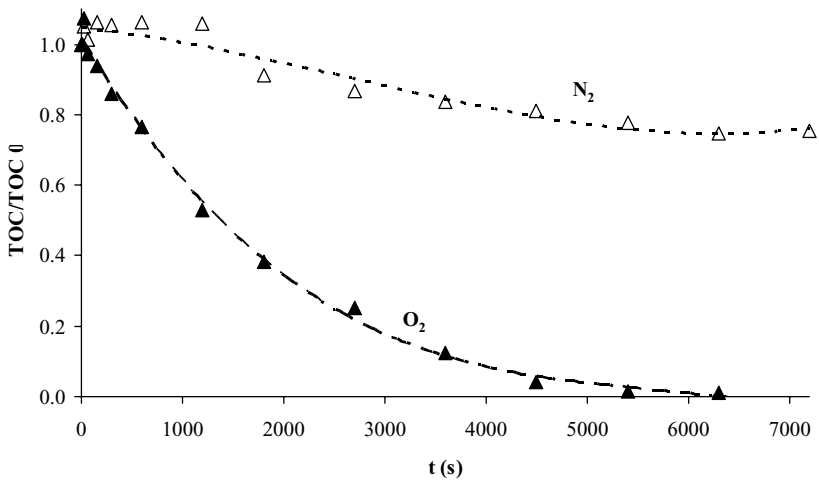

Fig. 19. The effect of dissolved O_2 on the mineralization of NAP ($c_0 = 1.0 \times 10^{-4}$ mol dm^{-3}).

Table VII. The degree of mineralization of the studied NSAIDs after 2 h of VUV irradiation in oxygenated and deoxygenated solutions.

comp.	mineralization (%)	
	O_2	N_2
IBU	75	20
KETO	100	10
NAP	100	25
DICL	100	45

As a proof of these assumptions, *m/z* values much higher than the *m/z* values of the target molecules were detected during the VUV photolysis of deoxygenated solutions. However, their exact structures could not be determined since they were not the multiples of the *m/z* values of the original molecules. Presumably, not two

identical molecules were bounded to each other in these cases, but maybe some fragments of the contaminants.

The degradation of such dimers/oligomers is much more difficult than that of the original molecule, which could explain the low efficiency of TOC loss in deoxygenated solutions (Fig. 19, Table VII). The essential role of dissolved O_2 during the effective decontamination of NSAID-containing solutions should therefore be underlined.

5.3. The effects of $HO_2^{\bullet}/O_2^{\bullet-}$ on the transformation of the target compounds

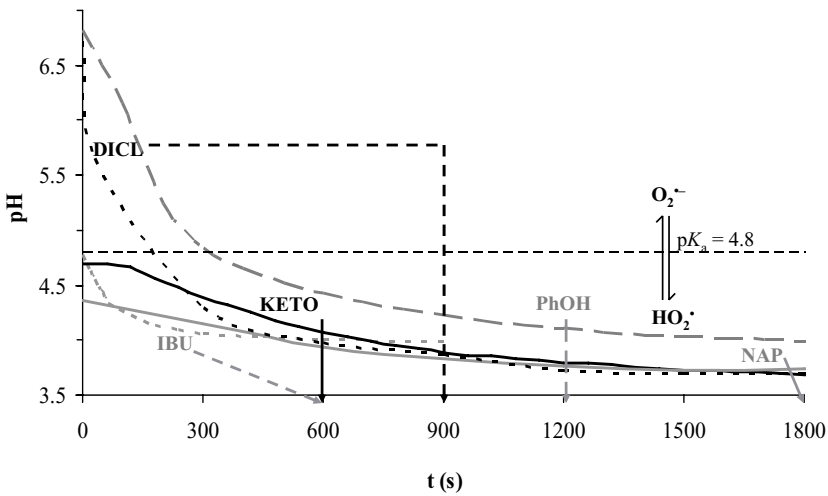

Fig. 20. The decrease of the pH of the O_2 saturated, VUV irradiated solutions. The arrows show the treatment time needed for the complete transformation of the compounds. The broken line depicts the pH, where the concentration of $HO_2^{\bullet}$ and $O_2^{\bullet-}$ is equal.

The ratio of $HO_2^{\bullet}$ and $O_2^{\bullet-}$, formed during the VUV irradiation of O_2 saturated aqueous solutions, is affected by the pH. Above the pK_a of $HO_2^{\bullet}$ (4.8 [69]) the predominance of $HO_2^{\bullet}$ over $O_2^{\bullet-}$ should be taken into consideration. This was the case during the VUV photolysis of IBU, KETO and NAP (Fig. 20). However, due to the higher pK_a of PhOH (9.88 [105]), compared to the pK_a values of the NSAIDs (Table I) and the usage of the sodium salt of DICL, in the case of irradiating PhOH or

DICL, $HO_2^{\bullet}$ was mainly present in the form of its conjugate base-pair till the 70–80% transformation of these contaminant molecules.

To settle which form of $HO_2^{\bullet}/O_2^{\bullet-}$ plays the greater role in the transformation of the studied compounds, their VUV photolysis was investigated also in the presence of formate ions and dissolved O_2 both at lower (~ 3.9) and higher pH (~ 10.5). As it was expounded in Section 2.3.2, if both formate ions and O_2 are present in the solution, almost all primary radicals of VUV photolysis can be converted to $HO_2^{\bullet}/O_2^{\bullet-}$ (16–20). If the pH is adjusted to ~3.9, 90% of the radicals appear in form of $HO_2^{\bullet}$, while using a pH of ~ 10.5, they are almost completely transformed to $O_2^{\bullet-}$. The comparison of Tables VI and VIII reveals that the conversion of highly reactive $HO^{\bullet}$ to less reactive $HO_2^{\bullet}/O_2^{\bullet-}$ decreased significantly (with nearly one order of magnitude in most cases) the transformation rates of the contaminants. Additionally, the values of Table VIII suggest that during the transformation of PhOH and NAP, the contribution of $HO_2^{\bullet}$, while in the case of IBU and KETO, the contribution of $O_2^{\bullet-}$ was higher among $HO_2^{\bullet}/O_2^{\bullet-}$. According to the expectations, it seems that the reaction rate of $HO_2^{\bullet}/O_2^{\bullet-}$ and organic compounds depends highly on the structure of the target molecule.

Table VIII. The initial VUV transformation rates of the investigated compounds in case of converting the majority of the radicals to $HO_2^{\bullet}$ or to $O_2^{\bullet-}$.

comp.	r_0 **(× 10^{-8} mol dm^{-3} s^{-1})**	
	$HO_2^{\bullet}$	**$O_2^{\bullet-}$**
PhOH	13.0 ± 1.00	1.1 ± 0.10
IBU	2.2 ± 0.20	5.2 ± 0.20
KETO	3.2 ± 0.05	8.8 ± 0.30
NAP	2.2 ± 0.20	1.1 ± 0.03

Because of the low solubility of DICL below pH = 5.8 (Fig. 2), the effect of $HO_2^{\bullet}$ could not be investigated by using formate ions as radical transfers and adjusting the pH around 3.9, as it was studied in the case of the other target molecules. However, the VUV photolysis of DICL was performed also in the presence of phosphates, to adjust the pH to be in the range 6.9–7.2. Under such

conditions $HO_2^{\bullet}/O_2^{\bullet-}$ was present mainly in the form of $O_2^{\bullet-}$ during the whole treatment. Using longer irradiation times (t > 180 s, Fig. 21a), in the case of DICL dissolved in Milli-Q water, the majority of $O_2^{\bullet-}$ could be converted to $HO_2^{\bullet}$. Comparing the VUV photolysis of DICL and the formation and transformation of its by-products in oxygenated solutions, in the presence and absence of PB, may give therefore an insight into the role of $HO_2^{\bullet}/O_2^{\bullet-}$ also in this case. As it can be seen in Fig. 21a, the decay of DICL was slightly increased in Milli-Q water after 180 s of irradiation and the concentrations of the by-products were higher in the presence of PB [103].

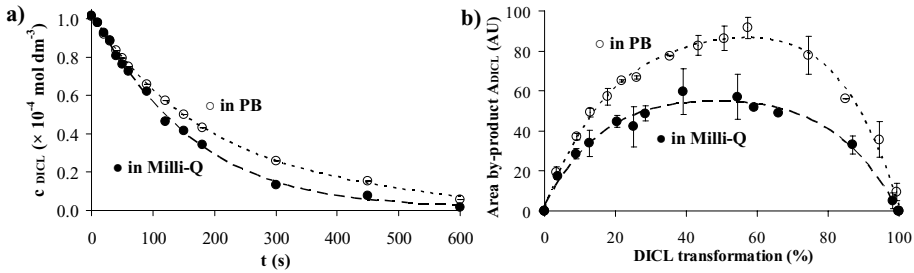

Fig. 21. The effects of PB a) on the degradation of DICL and b) on the formation and transformation of by-product A_{DICL} ($c_0 = 1.0 \times 10^{-4}$ mol dm^{-3}) in oxygenated solutions.

Both $H_2PO_4^-$ and HPO_4^{2-} are reported to be $HO^{\bullet}$ scavengers [106]. It is essential therefore, to calculate their effects on the DICL degradation kinetics. The reaction rate constants of HPO_4^{2-} and $H_2PO_4^-$: $k_{HPO_4^{2-}}$ [106-108] and $k_{H_2PO_4^-}$ [108, 109] are 2–6 orders of magnitude lower than that of DICL (k_{DICL}, Table III):

$$HPO_4^{2-} + HO^{\bullet} \rightarrow HPO_4^{\bullet-} + OH^- \qquad k_{HPO_4^{2-}} = 1.5 \times 10^5 - 5 \times 10^6 \text{ mol}^{-1} \text{ dm}^3 \text{ s}^{-1} \quad (54)$$

$$H_2PO_4^- + HO^{\bullet} \rightarrow H_2PO_4^{\bullet} + OH^- \qquad k_{H_2PO_4^-} = 2 \times 10^4 - 1 \times 10^7 \text{ mol}^{-1} \text{ dm}^3 \text{ s}^{-1} \quad (55)$$

The reaction rates of DICL (r_{DICL}), HPO_4^{2-} ($r_{HPO_4^{2-}}$) and $H_2PO_4^-$ ($r_{H_2PO_4^-}$) may be calculated from the reaction rate constants and the initial concentrations of DICL, HPO_4^{2-} and $H_2PO_4^-$, since these concentration values were roughly equal to their actual concentrations ([DICL], [HPO_4^{2-}] and [$H_2PO_4^-$], respectively), at the beginning of the photolysis:

$$\frac{r_{DICL}}{r_{HPO_4^{2-}}} = \frac{k_{DICL} \times [HO^{\bullet}] \times [DICL]}{k_{HPO_4^{2-}} \times [HO^{\bullet}] \times [HPO_4^{2-}]} \quad \text{(XI)}$$

$$63 < \frac{r_{DICL}}{r_{HPO_4^{2-}}} < 8421 \quad \text{(XII)}$$

$$\frac{r_{DICL}}{r_{H_2PO_4^-}} = \frac{k_{DICL} \times [HO^{\bullet}] \times [DICL]}{k_{H_2PO_4^-} \times [HO^{\bullet}] \times [H_2PO_4^-]} \quad \text{(XIII)}$$

$$55 < \frac{r_{DICL}}{r_{H_2PO_4^-}} < 109091 \quad \text{(XIV)}$$

As Eqs. (XII and XIV) demonstrates, both $r_{HPO_4^{2-}}$ and $r_{H_2PO_4^-}$ were significantly lower than r_{DICL}. Therefore, the majority of $HO^{\bullet}$ is likely to react with DICL rather than with HPO_4^{2-} or $H_2PO_4^-$. These findings could explain the negligible difference found between the degradation rates of DICL in Milli-Q water and in PB at the beginning of the photolysis (Fig. 21a) [103].

The experiences that the concentrations of aromatic by-products were higher in the presence of PB (where $HO_2^{\bullet}/O_2^{\bullet-}$ is mainly present in the form of $O_2^{\bullet-}$) than in the samples prepared in Milli-Q water (where $HO_2^{\bullet}/O_2^{\bullet-}$ is mainly present in the form of $HO_2^{\bullet}$ after 180 s of photolysis) (Fig. 21b) and that the degradation rate of DICL was lower in the presence of phosphates, using longer irradiation times (Fig. 21a), may suggest that the reaction rates of DICL and its by-products with $O_2^{\bullet-}$ are probably lower than those of their reactions with $HO_2^{\bullet}$ [103].

5.4. The effects of radical scavengers on the transformation of the target compounds

Methanol and *tert*-butanol are usually considered as $HO^{\bullet}$ scavengers and therefore, their effects were investigated during the VUV photolysis of the studied NSAIDs and PhOH, respectively. According to the expectations, the presence of both dissolved O_2 and radical scavengers decreased significantly the initial VUV

transformation rates of the studied molecules (c_0 = 1.0 × 10^{-4} mol dm^{-3}) (Table IX) due to the conversion of highly reactive $HO^{\bullet}$ to less reactive $^{\bullet}OOCH_2OH$ or $^{\bullet}OOCH_2C(CH_3)_2OH$.

Table IX. The initial VUV transformation rates of the investigated compounds (c_0 = 1.0 × 10^{-4} mol dm^{-3}) in the presence of dissolved O_2 and both dissolved O_2 and radical scavengers (methanol in the case of the NSAIDs and *tert*-butanol in the case of PhOH).

comp.	$c_{rad.\ scav.}$ (mol dm^{-3})	r_0 (× 10^{-7} mol dm^{-3} s^{-1})
PhOH	–	4.40 ± 0.10
	0.05	0.83 ± 0.01
	0.50	0.55 ± 0.02
IBU	–	5.30 ± 0.20
	0.10	2.90 ± 0.10
KETO	–	10.00 ± 0.30
	0.10	9.10 ± 0.20
	1.00	5.40 ± 0.20
NAP	–	6.80 ± 0.20
	0.10	2.06 ± 0.07
	1.00	1.37 ± 0.03
DICL	–	5.70 ± 0.30
	0.10	3.75 ± 0.05
	1.00	2.21 ± 0.05

At the beginning of the reactions the actual concentrations of the solutes can be considered roughly equal to their initial concentrations. Using these concentrations and the reaction rate constants reported in Table III, as well as k_{21} and k_{22}, the reaction rates of these compounds and $HO^{\bullet}$ may be calculated. The c_0 values were chosen in order to ensure the reaction rates of $HO^{\bullet}$ and the radical scavengers to be ~ 2 orders of magnitude higher than that of $HO^{\bullet}$ and the target molecules, *i.e.* that almost all $HO^{\bullet}$ react with the radical scavengers instead of with the contaminants. Exceptions were the usage of 1.00 mol dm^{-3} CH_3OH (where the reaction rate of $HO^{\bullet}$ and methanol was ~ 3 orders of magnitude higher than that of $HO^{\bullet}$ and the NSAIDs) and the usage of 0.05 mol dm^{-3} *tert*-butanol (where the ratio of the reaction rate of $HO^{\bullet}$ and phenol and that of $HO^{\bullet}$ and the radical scavenger was only 36).

If the ratio of the initial transformation rates of the studied molecules are compared in the presence of dissolved O_2 and in the presence of both O_2 and formate ions (to convert the radicals to $HO_2^{\bullet}/O_2^{\bullet-}$) ($r_0$ (O_2)/r_0 ($HO_2^{\bullet}$) or r_0 (O_2)/r_0 ($O_2^{\bullet-}$)) with the ratio of the transformation rates in the presence of dissolved O_2 and in the presence of both O_2 and radical scavengers (CH_3OH or *tert*-butanol) (r_0 (O_2)/r_0 (lower $c_{rad.\ scav.}$) or r_0 (O_2)/r_0 (higher $c_{rad.\ scav.}$)), it may be noticed that the former values are significantly (in almost all cases with one order of magnitude) higher than the latter ones (Table X). The only exception is the case of irradiating PhOH in the presence of both O_2 and formate ions at acidic pH. The reason of the former surprising observation might be that the contribution of the peroxyl radicals (formed in the presence of both O_2 and the radical scavengers: $^{\bullet}OOCH_2OH$ and $^{\bullet}OOCH_2C(CH_3)_2OH$, respectively) to the transformation of the contaminants may be higher than that of $HO_2^{\bullet}/O_2^{\bullet-}$ (formed in the presence of both O_2 and formate ions). The contribution of these peroxyl radicals to the degradation of organic pollutants should therefore not be neglected and methanol and *tert*-butanol should also be considered as radical transfers instead of radical scavengers. The relatively low value of r_0 (O_2)/r_0 ($HO_2^{\bullet}$) in case of irradiating PhOH suggests that the reaction rate constants of $HO_2^{\bullet}$ are lower in case of the NSAIDs than that of PhOH (2.7×10^3 dm^3 mol^{-1} s^{-1} [79]). Therefore, the contribution of $HO_2^{\bullet}$ to the degradation of the contaminants seems to be negligible in the case of the studied drugs and it seems to have a minor significance in the case of PhOH.

Table X. The ratio of the initial VUV transformation rates of the investigated compounds in the presence of different radical transfers (among the radical scavengers, methanol was used in the case of the NSAIDs and *tert*-butanol in the case of PhOH).

comp.	**r_0 (O_2)/ r_0 ($HO_2^{\bullet}$)**	**r_0 (O_2)/ r_0 ($O_2^{\bullet-}$)**	**r_0 (O_2)/ r_0 (lower $c_{rad.\ scav.}$)**	**r_0 (O_2)/ r_0 (higher $c_{rad.\ scav.}$)**
PhOH	3.4	40.0	5.3	8.0
IBU	24.1	10.2	1.8	n.m.*
KETO	31.3	11.4	1.1	1.9
NAP	30.9	60.2	3.3	5.0
DICL	n.m.	n.m.	1.5	2.6

*not measured

5.5. The effects of the initial concentration of the target compounds

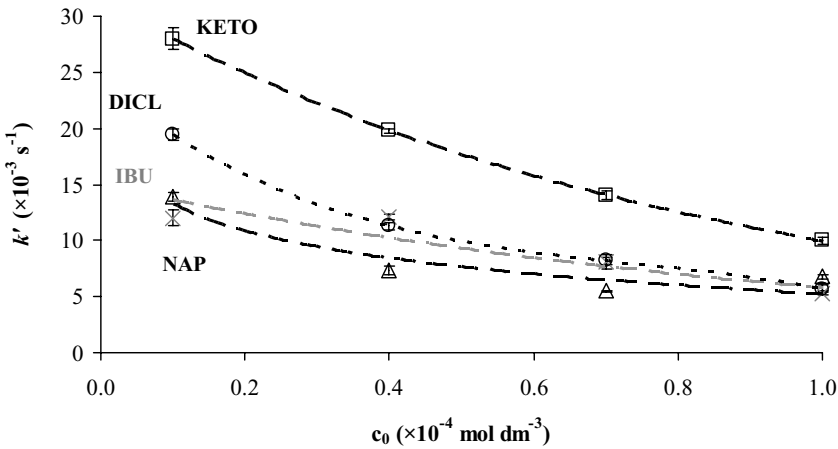

Fig. 22. The apparent reaction rate constants of the studied NSAIDs as a function of their initial concentrations, in the presence of dissolved O_2.

If the c_0 is fixed, the pseudo-first-order approach is suitable for the description of the degradation kinetics of the VUV photolysis of the investigated contaminants. However, in oxygenated solutions, the apparent first-order rate constants (k') decreased in almost all cases with the increase of the c_0 (Fig. 22). The reason of these observations might be that at higher c_0, more reactive species are involved in reactions with the NSAIDs and the steady-state concentration of the radicals ($[\text{radicals}]_{SS}$) therefore decreases. Thus, our observation that k' (= $k \times [\text{radicals}]_{SS}$, where k is the second-order rate constant of the reaction of the NSAIDs with the radicals) decreases with the increase of c_0 can be explained by the decrease in $[\text{radicals}]_{SS}$ along with the constant value of k [39, 103]. Although it was measured only in the case of two c_0, similar tendency was experienced also in the case of PhOH (see Table VI), the k' being 4.4×10^{-3} s^{-1} if the c_0 was 1.0×10^{-4} mol dm^{-3} and 24×10^{-3} s^{-1} if the c_0 was chosen to be 1.0×10^{-5} mol dm^{-3}. These results correlate well with the work of *Sato et al.* [110].

5.6. Possible reaction mechanism of the VUV decomposition of the treated NSAIDs based on the experiments

5.6.1. Possible reaction mechanism of the VUV decomposition of ibuprofen

The mechanism of the VUV photolysis of PhOH was presented in Section 2.4 (Fig. 6), this section focuses therefore on the decomposition of the studied NSAIDs. The HPLC-MS results permitted suggestions concerning the chemical structures of the aromatic by-products of the treated drugs. Among the four by-products of IBU photolysis (A_{IBU} – D_{IBU}, Figs. 24 and 25) one (C_{IBU}) could be detected using the positive and the others using the negative ion mode. The *m/z* value of A_{IBU} was found to be 221 (see Fig. A2 in the Appendix). Therefore, its molecular mass should be 222, which differs by 16 from the molecular mass of IBU (206) (Fig. A1).

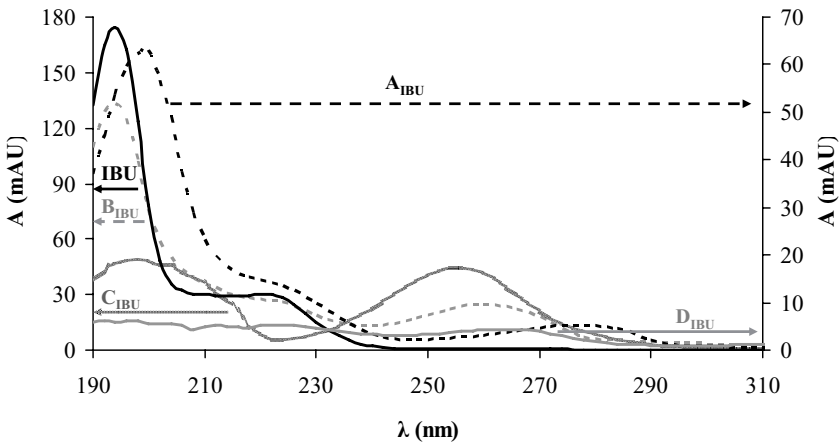

Fig. 23. UV absorbance of IBU and of by-products A_{IBU}, B_{IBU}, C_{IBU} and D_{IBU}.

The diode array UV detector of the used HPLC automatically measured the UV absorbance of the chromatographic peaks. Therefore, the UV spectra of IBU and its aromatic by-products could be compared. The UV absorbance spectrum of A_{IBU} displayed some similarities with that of IBU, although a bathochromic shift of the absorbance maxima was observed and a tertiary maximum around 275 nm was

detected (Fig. 23). Since electron-donating substituents (like OH groups, characterized with a positive mesomeric effect) are reported to induce bathochromic shifts [111] and the atomic mass of O is 16, it was presumed, that this by-product is a monohydroxylated derivative of IBU (Fig. 24, A_{IBU}). The formation of such derivatives was reported also during gamma radiolysis [34, 112], photocatalysis [113, 114], sonolysis, sonophotocatalysis [113], the photo-Fenton treatment [115], using chemical oxidants ($KMnO_4$, H_2O_2 or $K_2Cr_2O_7$) or heating [116], but also during the biodegradation of IBU in the white-rot fungi *Trametes versicolor* [117].

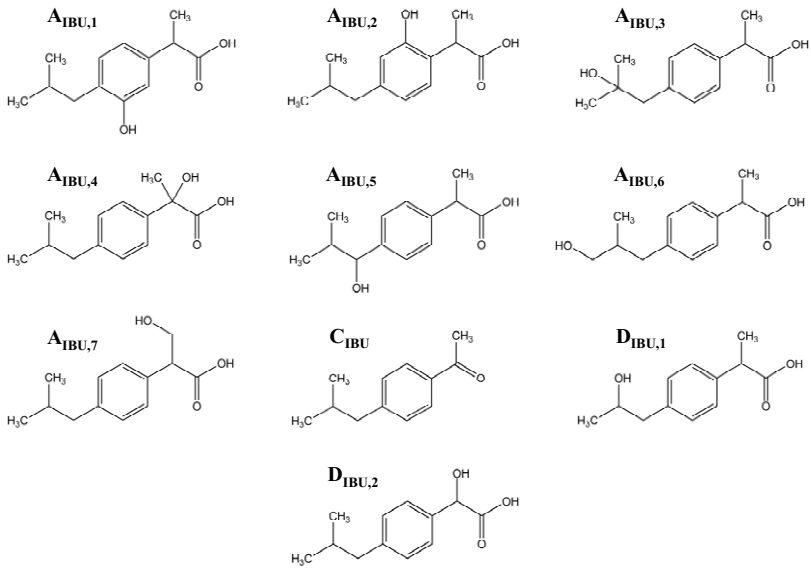

Fig. 24. Possible chemical structures of by-products A_{IBU}, C_{IBU} and D_{IBU}.

The *m/z* value of by-product B_{IBU} (237) differed by 16 from the *m/z* value of the former compound (221) (Fig. A3) and its UV absorbance spectrum displayed similarities with that of IBU and A_{IBU} (in this case the absorbance maxima of the tertiary maximum was found around 260 nm) (Fig. 23). It is likely therefore that this by-product is a dihydroxylated derivative of IBU (Fig. 25). Such products form also during gamma radiolysis [34], photocatalysis, sonolysis, sonophotocatalysis [113] and during the biodegradation of IBU in *Trametes versicolor* [117].

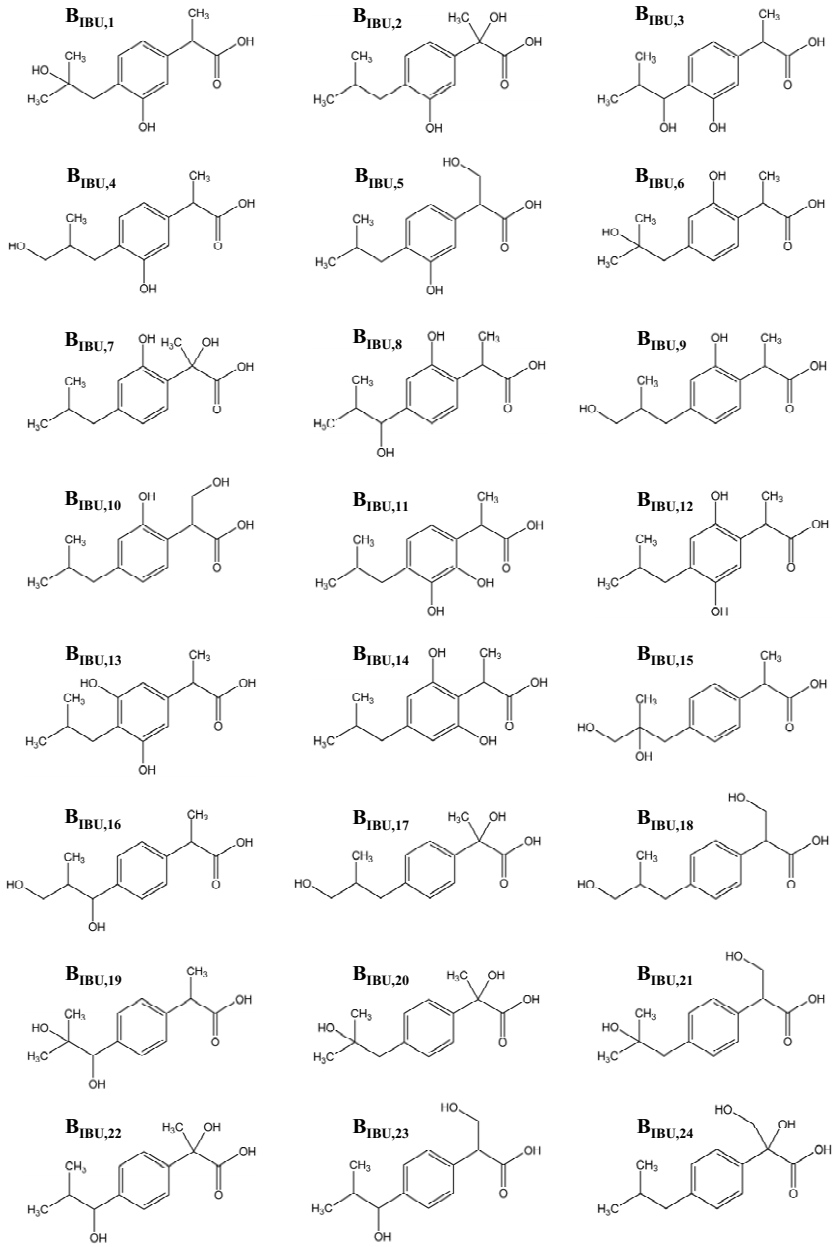

Fig. 25. Possible chemical structures of by-product B_{IBU}.

However, *Mendez-Arriaga et al.* proposed the formation of a hydroxylated peroxy acid *(m/z* = 237) during the photocatalytic and photo-Fenton treatment of IBU

[114, 115]. The generation of such molecule during the VUV photolysis might be interpreted by a hydrogen abstraction reaction from the carboxyl group of a monohydroxylated IBU derivative, followed by a recombination reaction between the formed radical and $HO^{\bullet}$. However, $HO^{\bullet}$ usually abstracts $H^{\bullet}$ from the carbon atoms of the aliphatic chains instead from oxygen atoms (in accordance with the higher energy of the O-H bond (463 kJ mol^{-1}) compared to that of the C-H bond (413 kJ mol^{-1}) [118]), like in its reactions with methanol (21, 56).

$$CH_3OH + HO^{\bullet} \rightarrow CH_3O^{\bullet} + H_2O \qquad k_{56} = 7.3 \times 10^7\ mol^{-1}\ dm^3\ s^{-1}\ [119]\ (56)$$

In this case (56) the possibility of the formation of methoxy radicals ($CH_3O^{\bullet}$) is only 7% [120]. Therefore, the generation of a dihydroxylated product is more likely during VUV photolysis than the formation of a hydroxylated peroxy acid.

The molecular mass of C_{IBU} (176, calculated from its *m/z* value (177), Fig. A4) differed by 30 from the molecular mass of IBU (206) (Fig. A1) and its UV spectrum differed significantly from that of IBU (Fig. 23). It might be supposed that in this case the decarboxylation of IBU occurred, and from the generated radical ($R_{IBU}^{\bullet}$) the ketone 4-isobutylacetophenone was formed (Fig. 24, C_{IBU}), altering significantly the chromophore of the parent compound. Although C_{IBU} might also be 1-isobutyl-4-isopropylbenzene (its *m/z* value would be 177), the formation of such by-product is mechanistically unlikely, because neither the elimination of a $HO_2^{\bullet}$ (followed by H_2 addition) from IBU, nor the recombination of a methyl radical with $R_{IBU}^{\bullet}$ is probable. It should be mentioned, that the formation of 4-isobutylacetophenone was reported also during gamma radiolysis of oxygenated IBU solutions [34], sonolysis, sonophotocatalysis [113], UV and UV/VUV photolysis [12, 43, 121, 122], electro-Fenton and photoelectro-Fenton treatment [123], using chemical oxidants ($KMnO_4$, H_2O_2 or $K_2Cr_2O_7$) or heating [116].

The molecular mass of D_{IBU} (208, calculated from its *m/z* value (207), Fig. A5) differed by 2 from the molecular mass of IBU (206) (Fig. A1) and it had only a weak absorption (with an intensity maximum around 260 nm) in the 190–310 nm region (Fig. 23). It is supposed therefore, that in this case a methyl group was substituted

with a hydroxyl group, resulting in 2-[4-(2-hydroxypropyl)phenyl]propanoic acid (Fig. 24, $D_{IBU,1}$) or hydroxy(4-isobutylphenyl)acetic acid (Fig. 24, $D_{IBU,2}$). The formation of such by-product was experienced also during sonolysis, photocatalysis and sonophotocatalysis [124].

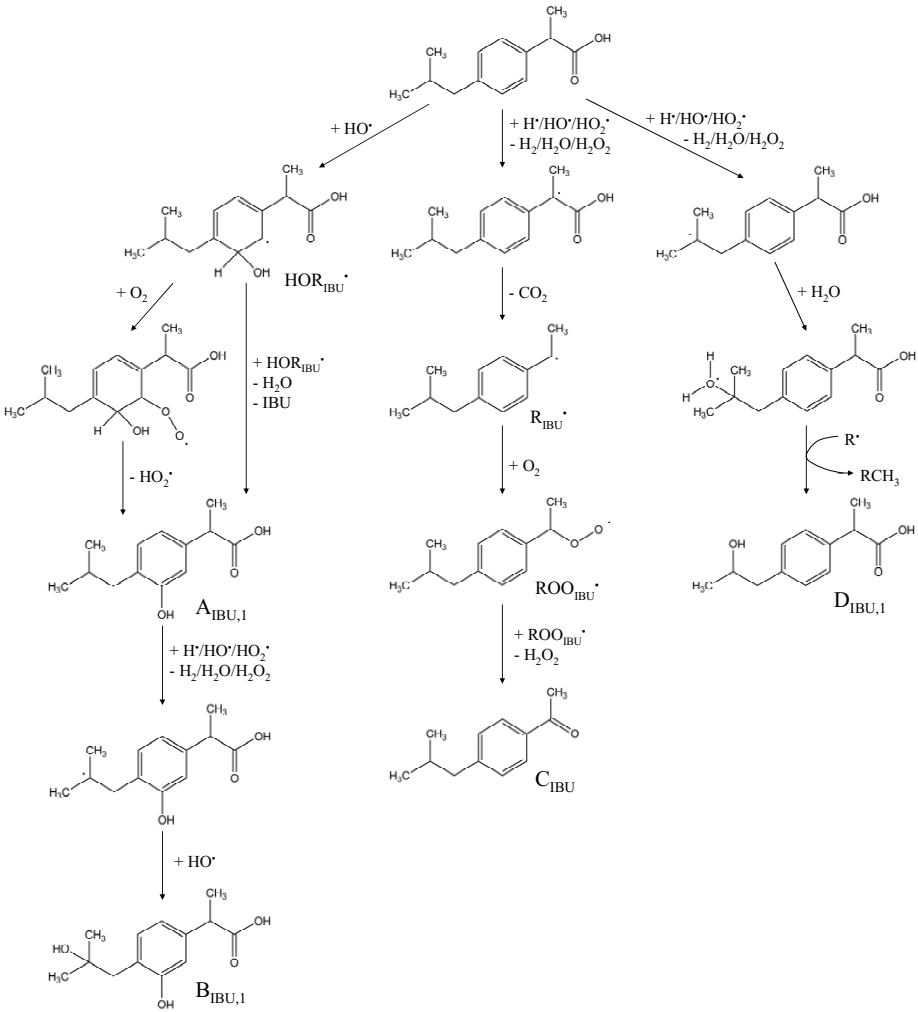

Fig. 26. Possible pathway of formation of by-products $A_{IBU,1}$, $B_{IBU,1}$, C_{IBU} and $D_{IBU,1}$.

The degradation of IBU during photocatalysis, electro-Fenton and photoelectro-Fenton treatment is supposed to be initiated by hydroxylation followed by a

decarboxylation step [114, 123, 124]. Similar transformation pathways might happen also during VUV photolysis. Hydroxylation might take place in the ring [34], but also in the side chains [112, 113, 115-117]. The former pathway might be interpreted by the addition of a $HO^{\bullet}$ to the ring, resulting in a hydroxycyclohexadienyl-type radical ($HOR_{IBU}^{\bullet}$, similarly to the hydroxylation mechanism of PhOH, Fig. 6). After the addition of an O_2 molecule to this radical and the elimination of a $HO_2^{\bullet}$, or the dismutation of the $HOR_{IBU}^{\bullet}$, 2-(3-hydroxy-4-isobutylphenyl)propanoic acid ($A_{IBU,1}$) and 2-(2-hydroxy-4-isobutylphenyl)propanoic acid ($A_{IBU,2}$) might be formed (Fig. 26). The latter pathway might be induced by the H-abstraction reactions of $H^{\bullet}$, $HO^{\bullet}$ or $HO_2^{\bullet}$. The recombination reactions of the generated carbon-centered radicals with $HO^{\bullet}$ could result in 2-[4-(2-hydroxyisobutyl)phenyl]propanoic acid ($A_{IBU,3}$), 2-hydroxy-2-(4-isobutylphenyl)propanoic acid ($A_{IBU,4}$), 2-[4-(1-hydroxyisobutyl) phenyl]propanoic acid ($A_{IBU,5}$), 2-[4-(3-hydroxyisobutyl)phenyl]propanoic acid ($A_{IBU,6}$) or 3-hydroxy-2-(4-isobutylphenyl)propanoic acid ($A_{IBU,7}$) (Fig. 24). Since the stability of carbon-centered radicals increases in the order: primary < secondary < tertiary [125], the probability of $A_{IBU,5}$ formation is lower than that of $A_{IBU,3}$ and $A_{IBU,4}$, but higher than that of $A_{IBU,6}$ and $A_{IBU,7}$. However, further investigations are needed to decide which structure corresponds to by-product A_{IBU} during the VUV photolysis of IBU.

It has to be mentioned, that similarly to the hydroxylation of PhOH during its VUV photolysis, the rate of hydroxylation of IBU is supposed to be higher in the presence of dissolved O_2 since IBU is regenerated during the disproportionation reaction of $HOR_{IBU}^{\bullet}$ under deoxygenated conditions.

The formation of dihydroxylated IBU by-products might be interpreted by the hydroxylation of the monohydroxylated IBU derivatives (Fig. 26). Thus, by-products hydroxylated both in the side chains and in the aromatic rings, dihydroxylated only in the aromatic rings or only in the side chains may be generated. 2-[3-hydroxy-4-(2-hydroxy-isobutyl)phenyl]propanoic acid ($B_{IBU,1}$), 2-hydroxy-2-(3-hydroxy-4-isobutylphenyl)propanoic acid ($B_{IBU,2}$), 2-[3-hydroxy-4-(1-hydroxy-isobutyl)phenyl)

propanoic acid ($B_{IBU,3}$), 2-[3-hydroxy-4-(3-hydroxy-isobutyl)phenyl]propanoic acid ($B_{IBU,4}$), 3-hydroxy-2-(3-hydroxy-4-isobutylphenyl)propanoic acid ($B_{IBU,5}$), 2-[2-hydroxy-4-(2-hydroxy-isobutyl)phenyl]propanoic acid ($B_{IBU,6}$), 2-hydroxy-2-(2-hydroxy-4-isobutylphenyl)propanoic acid ($B_{IBU,7}$), 2-[2-hydroxy-4-(1-hydroxy-isobutyl)phenyl)propanoic acid ($B_{IBU,8}$), 2-[2-hydroxy-4-(3-hydroxy-isobutyl)phenyl] propanoic acid ($B_{IBU,9}$) and 3-hydroxy-2-(2-hydroxy-4-isobutylphenyl) propanoic acid ($B_{IBU,10}$) may form the first group. 2-[2,3-dihydroxy-4-(2-methylpropyl) phenyl]propanoic acid ($B_{IBU,11}$), 2-[2,5-dihydroxy-4-(2-melthylpropyl)phenyl] propanoic acid ($B_{IBU,12}$), 2-[3,5-dihydroxy-4-(2-melthylpropyl)phenyl]propanoic acid ($B_{IBU,13}$) and 2-[2,6-dihydroxy-4-(2-melthylpropyl)phenyl]propanoic acid ($B_{IBU,14}$) may be species from the second group. Finally, 2-[4-(2,3-dihydroxy-2-methylpropyl)phenyl]propanoic acid ($B_{IBU,15}$), 2-[4-(1,3-dihydroxy-2-methylpropyl) phenyl]propanoic acid ($B_{IBU,16}$), 2-hydroxy-2-[4-(3-hydroxy-2-methylpropyl)phenyl] propanoic acid ($B_{IBU,17}$), 3-hydroxy-2-[4-(3-hydroxy-2-methylpropyl)phenyl] propanoic acid ($B_{IBU,18}$), 2-[4-(1,2-dihydroxy-2-methylpropyl)phenyl]propanoic acid ($B_{IBU,19}$), 2-hydroxy-2-[4-(2-hydroxy-2-methylpropyl)phenyl]propanoic acid ($B_{IBU,20}$), 3-hydroxy-2-[4-(2-hydroxy-2-methylpropyl)phenyl]propanoic acid ($B_{IBU,21}$), 2-hydroxy-2-[4-(1-hydroxy-2-methylpropyl)phenyl]propanoic acid ($B_{IBU,22}$), 3-hydroxy-2-[4-(1-hydroxy-2-methylpropyl)phenyl]propanoic acid ($B_{IBU,23}$) and 2,3-dihydroxy-2-[4-(2-methylpropyl)phenyl]propanoic acid ($B_{IBU,24}$) may compose the third group. Also in this case, further investigations are needed to decide which structure corresponds to by-product B_{IBU} during the VUV photolysis of IBU.

If $H^{\bullet}$, $HO^{\bullet}$ or $HO_2^{\bullet}$ abstracts H atom from the second C atom of the propanoic acid side chain, CO_2 molecule might eliminate from the formed carbon-centered radical. Thus, another carbon-centered radical ($R_{IBU}^{\bullet}$) could be generated. In oxygenated solutions the addition of an O_2 to this species would result in a peroxyl radical ($ROO_{IBU}^{\bullet}$). After the recombination of two $ROO_{IBU}^{\bullet}$ a H_2O_2 molecule might eliminate from the formed tetroxide according to the Bennett mechanisms [91]. This would result in 4-isobutylacetophenone (C_{IBU}, Fig. 26). Although the recombination reaction of $R_{IBU}^{\bullet}$ and $HO_2^{\bullet}$ could result in a hydroperoxide, which might also lead to

the formation of 4-isobutylacetophenone through its dehydration, the former pathway seems to be the relevant, since no hydroperoxide was detected among the VUV transformation products of IBU.

The fact that the concentration of A_{IBU}, B_{IBU} and C_{IBU} was significantly higher in the presence of dissolved O_2 correlates well with the tentative formation mechanisms listed above.

Even the substitution of a methyl group of IBU with a hydroxyl group is likely to be initiated by H-abstraction from the tertiary C atoms of the side chains of IBU. After the addition of a H_2O molecule and the elimination of a methyl radical ($CH_3^{\bullet}$) 2-[4-(2-hydroxypropyl)phenyl]propanoic acid ($D_{IBU,1}$) or hydroxy[(4-isobutyl) phenyl]acetic acid ($D_{IBU,2}$) might be generated (Fig. 26). This mechanism is in accordance with the finding that the concentration of D_{IBU} was nearly the same both in the presence and absence of dissolved O_2.

Based on the electronegativity values of C, H and O atoms, Fig. 27 depicts the distribution of electrons in IBU. Since $HO^{\bullet}$ is an electrophile radical and the electron density is higher on the tertiary C atom of the isobutyl side chain than on the propanoic acid side chain, it is likely that hydrogen abstraction occurs more favorably from the isobutyl chain. Therefore, it is more reasonable that the substitution reactions take place at this chain, resulting in 2-[4-(2-hydroxyisobutyl) phenyl]propanoic acid ($A_{IBU,3}$) rather than in 2-hydroxy-2-(4-isobutylphenyl) propanoic acid ($A_{IBU,4}$) and in 2-[4-(2-hydroxypropyl)phenyl]propanoic acid ($D_{IBU,1}$) rather than in hydroxy[(4-isobutyl)phenyl] acetic acid ($D_{IBU,2}$).

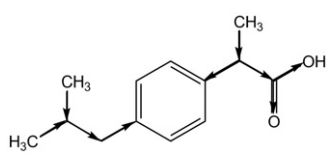

Fig. 27. The distribution of electrons in IBU, the arrows indicating the increasing electron density.

5.6.2. Possible reaction mechanism of the VUV decomposition of ketoprofen

Among the four photoproducts of KETO (A_{KETO} – D_{KETO}, Fig. 29) one (A_{KETO}) could be detected using the positive and the others using the negative ion mode. The molecular mass of A_{KETO} (210, calculated from its *m/z* value (211), Fig. A7) differs by 44 from the molecular mass of KETO (254, Fig. A6). Additionally, the UV spectrum of A_{KETO} showed similarities with that of KETO (Fig. 28), suggesting that the change in the structure of the parent compound did not alter significantly the structure of the chromophore. It is presumed therefore, that A_{KETO} is the decarboxylated derivative of KETO, the 3-ethylbenzophenone (Fig. 29, A_{KETO}). Such by-product was reported to form also during radiolysis [126], heterogeneous photocatalysis [127], photolysis using UV, UV/VUV light [43, 122, 128-132] or simulated sunlight [131], ozonolysis and the combined O_3/UV treatment of KETO [133].

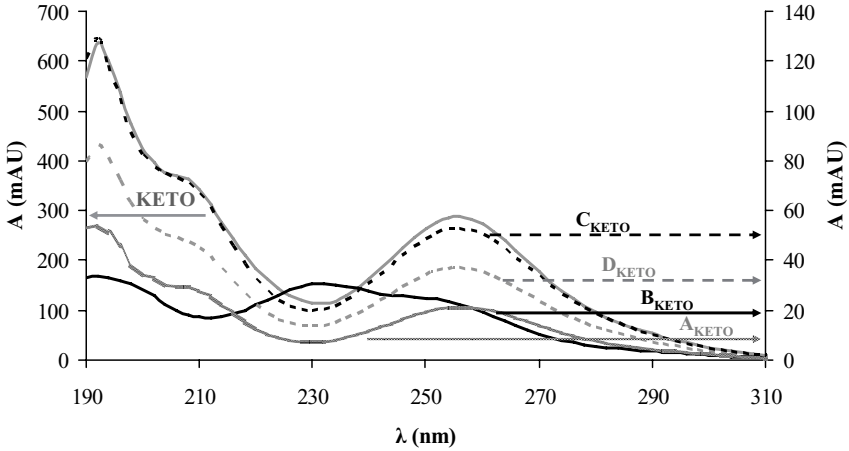

Fig. 28. UV absorbance of KETO and of by-products A_{KETO}, B_{KETO}, C_{KETO} and D_{KETO}.

The molecular mass of B_{KETO} (242, calculated from its *m/z* value (241), Fig. A8) differed by 32 from the molecular mass of A_{KETO} (210). Obvious differences were found also between the UV spectra of these two compounds (Fig. 28). Thus, it might be interpreted that after the decarboxylation of KETO the addition of an O_2 molecule

or the recombination with a $HO_2^{\bullet}$ occurred, resulting in 3-(1-hydroperoxyethyl) benzophenone (Fig. 29, B_{KETO}). In this case the mesomeric effect of O might result in a resonance structure (Fig. 30) that could alter the conjugated system and therefore the UV absorbance of the chromophore. 3-(1-hydroperoxyethyl)benzophenone was found also between the UV and UV/VUV photoproducts of KETO [43, 122, 128, 132], during heterogeneous photocatalysis [127], radiolysis [126], ozonolysis and the combined O_3/UV treatment of this contaminant [133].

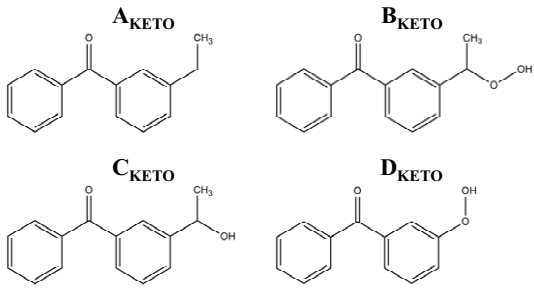

Fig. 29. Possible chemical structures of by-products A_{KETO}, B_{KETO}, C_{KETO} and D_{KETO}.

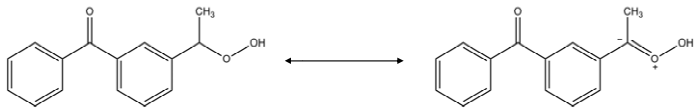

Fig. 30. Two resonance structures of B_{KETO}.

From the *m/z* value of C_{KETO} in the negative ion mode (225) (Fig. A9) the molecular mass of this compound was established to be 226, which differs by 16 from molecular mass of A_{KETO} (210). Additionally, the UV spectrum of C_{KETO} was similar to that of KETO and A_{KETO} (Fig. 28). Therefore, it is likely that C_{KETO} contains one more O atom than A_{KETO}. Thus, C_{KETO} is likely to be 3-(1-hydroxyethyl)benzophenone (Fig. 29, C_{KETO}), which was detected also during the radiolysis [126], UV and UV/VUV photolysis [43, 122, 128-132], ozonolysis and combined O_3/UV treatment [133] and photocatalytic treatment of KETO [127].

The molecular mass of D_{KETO} (214, calculated from its *m/z* value (213), Fig. A10) differed by 40 from the molecular mass of KETO (254) and by 4 from the molecular mass of A_{KETO} (210). Although no published results were found in the

literature concerning the formation of such by-product, it is proposed that in this case, after the decarboxylation of KETO, also the loss of an ethyl group occurred and after the recombination with a $HO_2^{\bullet}$ or the addition of an O_2 molecule, 3-hydroperoxybenzophenone was generated (Fig. 29, D_{KETO}). Although in this case the dihydroxylation of benzophenone is also imaginable, it is considered not to be very likely, since no monohydroxylated derivatives were detected. Additionally, the UV spectrum of D_{KETO} was similar to that of KETO, A_{KETO} and C_{KETO} (Fig. 28). In this case a mesomeric rearrangement of a nonbonding electron pair of the O atom would not result in the stabilization of the conjugated system, in contrast with B_{KETO}, and therefore it is not likely to happen, resulting in the nearly unchanged UV spectrum of D_{KETO}, comparing to that of KETO, A_{KETO} or C_{KETO}.

Decarboxylation is suggested to be among the first steps during the degradation of KETO [43, 128, 129, 134-136]. Analogously to the formation pathway of $R_{IBU}^{\bullet}$, during the VUV photolysis of KETO this process might be interpreted by the H-abstraction reaction of $H^{\bullet}$, $HO^{\bullet}$ or $HO_2^{\bullet}$ from the second C atom of the propanoic acid side chain, followed by the elimination of a CO_2 molecule, to result in a carbon-centered radical ($R_{KETO}^{\bullet}$). This radical might abstract a H atom from another molecule (RH) and thus, 3-(1-hydroperoxyethyl)benzophenone (A_{KETO}) might be generated (Fig. 31).

In oxygenated solutions the former process might compete with the recombination of $R_{KETO}^{\bullet}$ with a $HO_2^{\bullet}$ or with the addition of molecular O_2 to $R_{KETO}^{\bullet}$ to result in a peroxyl radical ($ROO_{KETO}^{\bullet}$). Both reactions could lead to the production of 3-(1-hydroperoxyethyl)benzophenone (B_{KETO}), the former reaction directly, while the latter one after a H-abstraction reaction. After the recombination of two $ROO_{KETO}^{\bullet}$ and the elimination of an O_2 molecule, the disproportionation of two oxyl radicals ($RO_{KETO}^{\bullet}$) might result in 3-(1-hydroxyethyl)benzophenone (C_{KETO}) and 3-acetylbenzophenone [91] (Fig. 31). Unfortunately, the generation of this latter compound was not detected during the VUV photolysis of KETO.

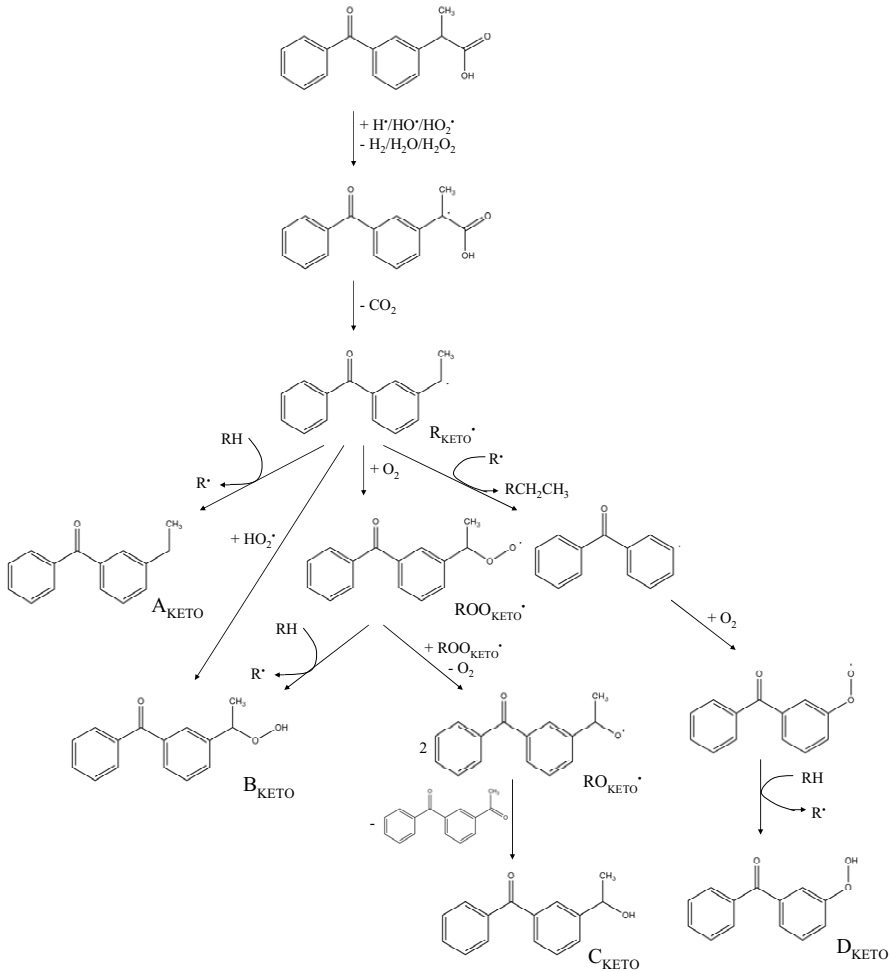

Fig. 31. Possible pathway of formation of by-products A_{KETO}, B_{KETO}, C_{KETO} and D_{KETO}.

A reaction with another radical might result in the deethylation of $R_{KETO}^{\bullet}$. The recombination of the formed radical with $HO_2^{\bullet}$ or O_2 addition to this radical and H-abstraction from the generated other peroxyl radical could give rise to 3-hydroperoxybenzophenone (D_{KETO}). These assumptions correlate well with the experience that the concentration of B_{KETO}, C_{KETO} and D_{KETO} was significantly higher in the presence of dissolved O_2 and that of A_{KETO} in deoxygenated solutions.

5.6.3. Possible reaction mechanism of the VUV decomposition of naproxen

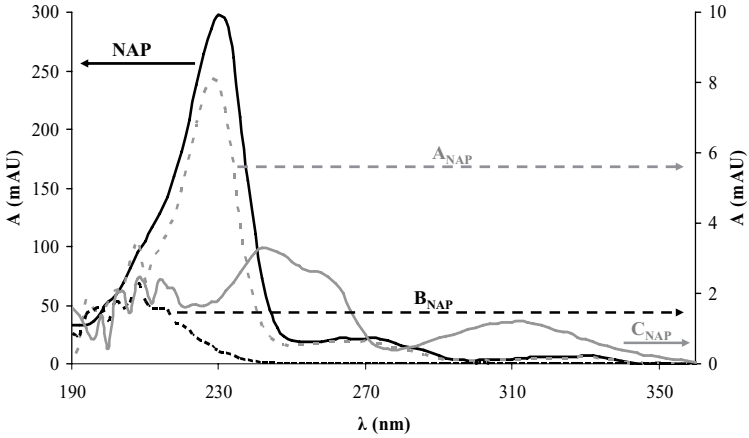

Fig. 32. UV absorbance of NAP and of by-products A_{NAP}, B_{NAP} and C_{NAP}.

Among the three by-products of NAP (A_{NAP} – C_{NAP}, Fig. 33) one (B_{NAP}) could be detected using the negative and the others using the positive ion mode. The molecular mass of A_{NAP} (184, calculated from its *m/z* value (185), Fig. A12) differed by 46 from the molecular mass of NAP (230, Fig. A11). Additionally, the UV spectrum of A_{NAP} was similar to that of NAP (Fig. 32). Thus, this compound might be formed through the decarboxylation and dehydrogenation of NAP. 2-methoxy-6-vinylnaphthalene (Fig. 33, A_{NAP}) was found to be produced also during UV photolysis [39, 137, 138].

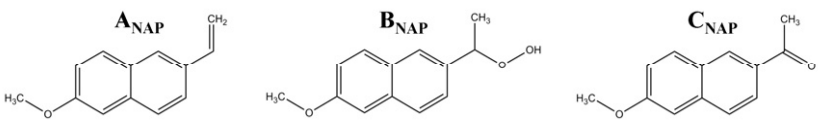

Fig. 33. Possible chemical structures of by-products A_{NAP}, B_{NAP} and C_{NAP}.

The molecular mass of B_{NAP} (218, calculated from its *m/z* value (217), Fig. A13) differed by 12 from the molecular mass of NAP (230). Therefore, in this case O_2 addition or recombination reaction with $HO_2^{\bullet}$ might have followed a decarboxylation

step, resulting in 1-(6-methoxynaphthalene-2-yl)ethylhydroperoxide (Fig. 33, B_{NAP}). Similarly to the case of B_{KETO}, the difference between the UV spectra of B_{NAP} and NAP might be attributed to the mesomeric rearrangement of a nonbonding electron pair of the O atom (Fig. 34). This compound was also detected among the UV photoproducts of NAP [39, 122, 137, 138].

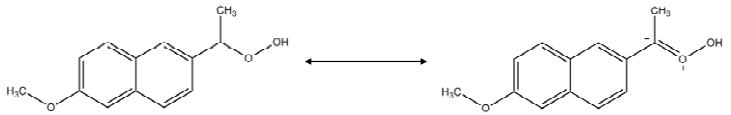

Fig. 34. Two resonance structures of B_{NAP}.

The molecular mass of C_{NAP} (200, calculated from its *m/z* value (201), Fig. A14) differed by 30 from the molecular mass of NAP (230) and by 18 from the molecular mass of B_{NAP} (218). Additionally, the UV spectrum of this compound showed obvious differences from that of NAP (Fig. 32). It might be suggested therefore that in this case 1-(2-methoxynaphthalene-6-yl)ethanone was formed (Fig. 33, C_{NAP}), which is a well-known by-product of NAP UV photolysis [39, 122, 137-139].

The main step of the formation of the by-products is reported to be the decarboxylation [39, 122, 138, 139], which is in accordance with the above results, since all the proposed structures are the decarboxylated derivatives of NAP. This mechanism might be initiated also in this case by a H-abstraction reaction of $H^{\bullet}$, $HO^{\bullet}$ or $HO_2^{\bullet}$ from the second C atom of the propanoic acid side chain. The elimination of a CO_2 molecule from this radical would result in a carbon-centered radical ($R_{NAP}^{\bullet}$). If a radical (a $R^{\bullet}$, a $H^{\bullet}$, a $HO^{\bullet}$ or a $HO_2^{\bullet}$) abstracts H from $R_{NAP}^{\bullet}$, 2-methoxy-6-vinylnaphthalene (A_{NAP}) might form (Fig. 35).

Recombination reaction of $R_{NAP}^{\bullet}$ with $HO_2^{\bullet}$ or O_2 addition to this radical might compete with the former process, resulting in 1-(6-methoxynaphthalene-2-yl)ethylhydroperoxide (B_{NAP}) directly or through the H-abstraction reaction the peroxyl radical $ROO_{NAP}^{\bullet}$, respectively – similarly to the formation of B_{KETO} (Fig. 35).

Either the elimination of a H_2O molecule from B_{NAP} [122] or the recombination of two $ROO_{NAP}^{\bullet}$, followed by H_2O_2 elimination could result in 1-(2-

methoxynaphthalene-6-yl)ethanone (C_{NAP}), similarly to the formation of C_{IBU} (Fig. 35). The facts that the concentration of C_{NAP} was significantly lower in deoxygenated solutions and B_{NAP} was detected only in the presence of dissolved O_2 support the former formation pathways.

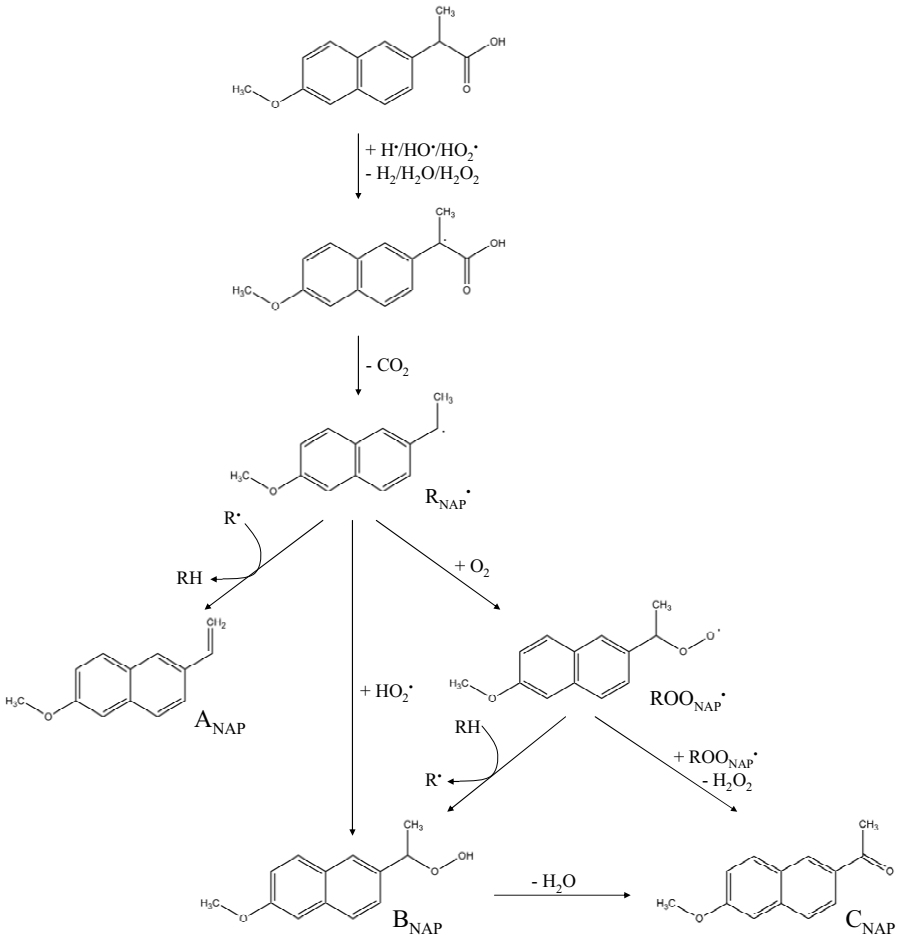

Fig. 35. Possible pathway of formation of by-products A_{NAP}, B_{NAP} and C_{NAP}.

5.6.4. Possible reaction mechanism of the VUV decomposition of diclofenac

In the negative ion mode, DICL was observed with an *m/z* value of 294, with two isotope peaks at 296 and 298 in nearly 9:3:1 ratio, which indicated the replacement of one or two ^{35}Cl by ^{37}Cl (Fig. A15). Among the by-products of DICL (A_{DICL} – C_{DICL}, Fig. 37) in the case of A_{DICL} (the *m/z* value being 310) were detected two isotope peaks (with *m/z* values of 312 and 314) in 9:3:1 ratio, suggesting that this compound also contains two Cl atoms (Fig. A16). On the one hand, the difference between the *m/z* value of A_{DICL} and that of DICL was 16 and on the other hand, their UV absorbance spectra were very similar to each other (the maxima and minima in the absorbance of the two compounds were to be found at very similar wavelengths; Fig. 36). Therefore, it seems reasonable that A_{DICL} is a hydroxylated derivative of DICL (Fig. 37, A_{DICL}) [103].

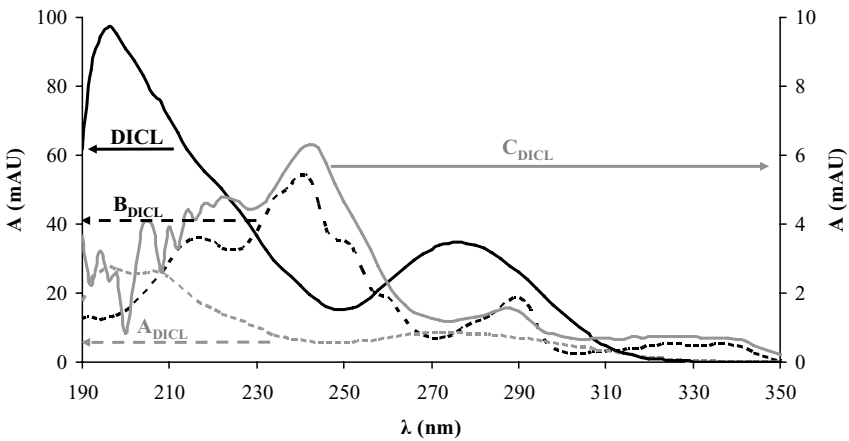

Fig. 36. UV absorbance of DICL and of by-products A_{DICL}, B_{DICL} and C_{DICL}.[4]

Hydroxylation could occur not only on the aromatic rings, resulting in 5-hydroxydiclofenac ($A_{DICL,1}$), 3-hydroxydiclofenac ($A_{DICL,2}$), 3'-hydroxydiclofenac ($A_{DICL,3}$) or 4'-hydroxydiclofenac ($A_{DICL,4}$) [60, 124, 140, 141], but also on the second

[4] Reprinted from ibid. with permission from Elsevier.

carbon atom of the acetic acid side chain to result in 2-[2-(2,6-dichlorophenylamino) phenyl](hydroxy)acetic acid ($A_{DICL,5}$) [140] or on the nitrogen atom to furnish in 2-[2-(2,6-dichlorophenyl)(hydroxyamino)phenyl](hydroxy)acetic acid ($A_{DICL,6}$) [17] (Fig. 37). During radiolysis and the photo-Fenton treatment $A_{DICL,1}$ has been hypothesized to be the most probable structure [60, 142]. However, during the H_2O_2/UV treatment and radiolysis of DICL [25, 143] the formation of $A_{DICL,2}$ and $A_{DICL,4}$ has been reported together with $A_{DICL,1}$, due to the relative unselectivity of $HO^{\bullet}$ [144]. Further investigations are therefore needed to decide which structure corresponds to by-product A_{DICL} during the VUV photolysis of DICL [103].

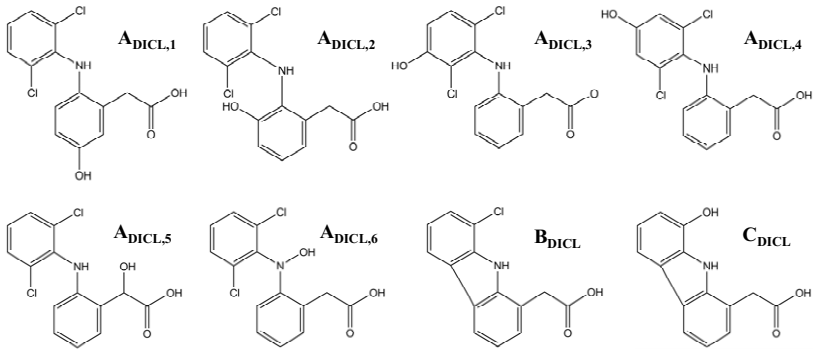

Fig. 37. Possible chemical structures of by-products A_{DICL}, B_{DICL} and C_{DICL}.[5]

The difference between the *m/z* value of by-product B_{DICL} (258) and that of DICL (294) was 36. Additionally, one isotope peak (*m/z* = 260) was also detected with an isotope ratio of 3:1 (Fig. A17), suggesting that this by-product contains only one Cl atom. Furthermore, the UV absorbance spectrum of B_{DICL} differed significantly from that of DICL (Fig. 36). These results suggested that HCl was probably eliminated from DICL to lead to the formation of 1-(8-chlorocarbazolyl)acetic acid (Fig. 37, B_{DICL}) [103], a well-known UV-photolytic and photocatalytic degradation product of DICL [50, 145, 146].

The difference between the *m/z* value of by-product C_{DICL} (240) and that of B_{DICL} was 18 (258) (Fig. A18). The lack of the isotope peaks in this case suggested that C_{DICL} contains no Cl atoms. Additionally, the UV absorbance spectra of these two

[5] Reprinted from ibid. with permission from Elsevier.

compounds were very similar to each other (Fig. 36). It is likely therefore, that C_{DICL} is the OH-substituted derivative of 1-(8-chlorocarbazolyl)acetic acid (B_{DICL}), the 1-(8-hydroxycarbazolyl)acetic acid (Fig. 37, C_{DICL}) [103]. The former substitution appears also in the literature [50, 145, 146].

$HO^{\bullet}$ is an electrophilic radical, it usually attacks therefore at the electron-dense sites of aromatic rings, *e.g.* on carbon atoms 5, 3, 3' and 4' in DICL. Analogously to the mechanisms postulated for the formation of 5-hydroxydiclofenac in $HO^{\bullet}$-initiated reactions [60, 106, 144] or the hydroxylation reactions of PhOH and IBU (Figs. 6 and 26), the hydroxylation of DICL is reasonable to be initiated by the addition of $HO^{\bullet}$ to the aromatic ring (*e.g.* to position 3, as interpreted by Fig. 38) to result in a hydroxycyclohexadienyl-type radical ($HOR_{DICL}^{\bullet}$). After the addition of an O_2 molecule and the elimination of a $HO_2^{\bullet}$, or the disproportionation of two $HOR_{DICL}^{\bullet}$, 3-hydroxydiclofenac ($A_{DICL,2}$) may be formed [103]. Since the dismutation reaction regenerates DICL, the rate of hydroxylation should be lower in the absence of O_2, similarly to the case of PhOH and IBU. This assumption correlates well with the fact that A_{DICL} was detected in significantly lower concentration in deoxygenated solutions than in the O_2-saturated conditions, both in the presence and absence of PB.

The mechanism of the hydroxylation of the amino group or the acetic acid side chain may be interpreted by H-abstraction reaction initiated by $H^{\bullet}$, $HO^{\bullet}$ or $HO_2^{\bullet}$, followed by recombination with $HO^{\bullet}$, similarly to the formation of $A_{IBU,3}$, $A_{IBU,4}$, $A_{IBU,5}$, $A_{IBU,6}$ and $A_{IBU,7}$.

During the transformation $HOR_{DICL}^{\bullet}$, O_2 addition and HCl elimination seem to be competitive processes. The latter process could result in ring closure. The formed radical might stabilize through a reaction with another radical (a $R^{\bullet}$, a $H^{\bullet}$ or a $HO^{\bullet}$), to result in 1-(8-chlorocarbazolyl)acetic acid (B_{DICL}) [103]. The lower concentration of B_{DICL} under O_2-saturated conditions might be explained by the mentioned competition kinetics. Similar mechanisms can be proposed for the formation of B_{DICL} as a result of the reactions of DICL with $H^{\bullet}$, $HO_2^{\bullet}$ or e_{aq}^{-}, the latter reaction being of

lower significance because of the low quantum yield of e_{aq}^- formation during the VUV photolysis of water (Fig. 38).

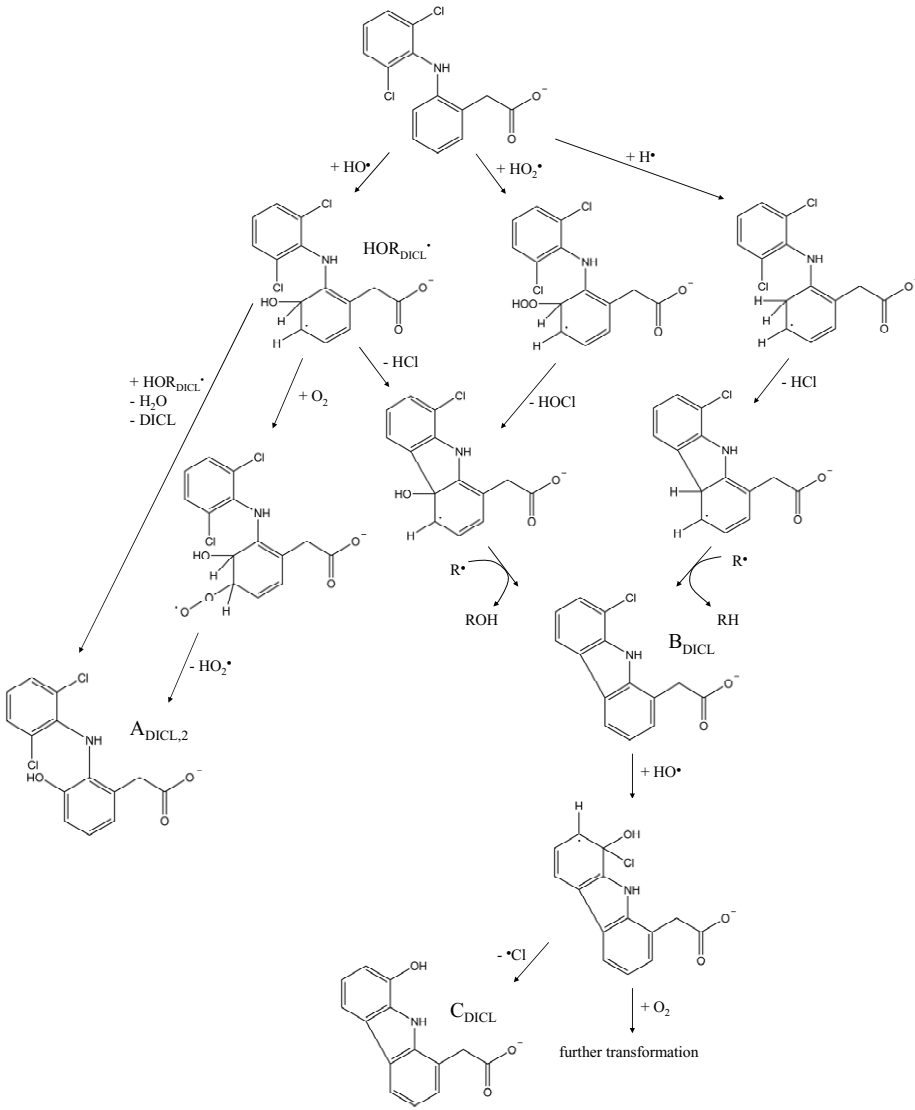

Fig. 38. Possible pathway of formation of by-products $A_{DICL,2}$, B_{DICL} and C_{DICL}.

The generation of C_{DICL} might be interpreted by a $HO^{\bullet}$ addition to B_{DICL}, followed by a $^{\bullet}Cl$ elimination reaction. However, in O_2-saturated solutions, the

addition of O_2 might compete with the latter process (Fig. 38), which could explain the higher concentration of the by-product C_{DICL} in deoxygenated Milli-Q water than that under N_2 purged conditions (Fig. 17b) [103].

5.7. Cell biological effects of VUV-treated solutions of diclofenac on the freshwater ciliate *Tetrahymena*

As it was mentioned in Section 2.1, the investigated pharmaceuticals have toxic side effects. Therefore, in the case of DICL the VUV irradiated, multicomponent samples were characterized also via the proliferation and migratory responses of the bioindicator eukaryotic ciliate *Tetrahymena pyriformis*, to have an insight in the environmental risk of the parent compound and its degradation by-products [103]. (The details of biological investigation see in the paper.)

The proliferation-inhibiting effect of the untreated sample (2.5×10^{-5} mol dm^{-3} DICL in PB) was ~ 13%, in accordance with the previous results of *Láng and Kőhidai* [6]. Treated samples taken after definite periods of irradiation exerted slight, but significant proliferation-inhibiting effects. Depending on the c_{O_2}, the irradiation time *vs.* proliferation inhibition curves of 25% (v/v) diluted samples displayed different shapes. *E.g.* in samples irradiated for 10–90 s, the inhibitory effect increased in the presence of dissolved O_2 and it decreased in deoxygenated solutions (Fig. 39). The significantly higher concentration of by-product A_{DICL} under O_2-saturated conditions might correlate with these results [103]. Previous findings concerning the toxic effects of the solutions treated by gamma radiolysis towards *Vibrio fischeri*, where the toxicity of the by-products formed under oxidative conditions was higher than that of the by-products generated under reductive conditions [25], are in accordance with these results.

Considering the longer treatments, when samples saturated with O_2 were irradiated for 2400–3600 s, the inhibitory potential of the samples decreased, reaching only 8% at 3600 s. In contrast, in the inhibition of deoxygenated samples was nearly the same within this time interval (Fig. 39). The significantly more

efficient mineralization achieved under the oxygenated conditions correlate with these results: after 3000 s of treatment 70% of DICL was mineralized in the presence, while only ~ 25% in the absence of dissolved O_2. Further, the TOC diminution reached 75% after 3600 s in oxygenated, while it did not exceed 45% even after 7000 s of irradiation in deoxygenated solution. Moreover, in solutions purged with N_2, the formation of di- and oligomeric by-products were assumed (see Section 5.2.3), which could not be detected with the applied analytical methods [104, 147], but which could contribute significantly to the mixture toxicity [103].

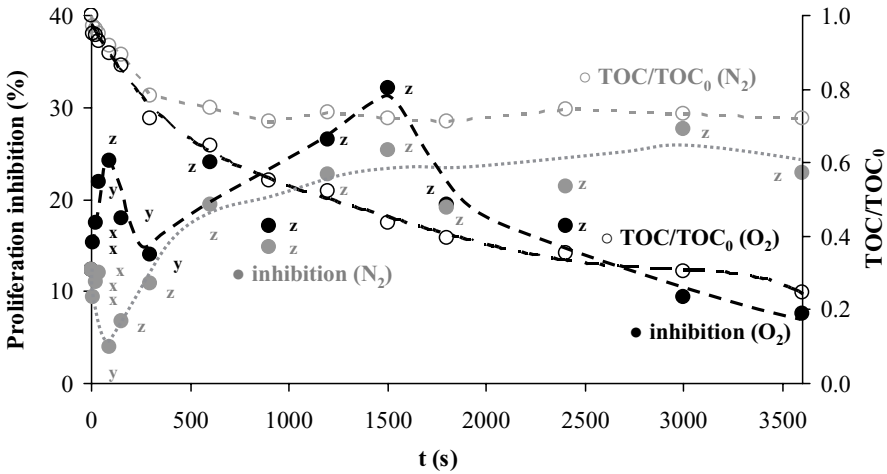

Fig. 39. Time course of the mineralization and the proliferation-inhibiting ability during the VUV photolysis of DICL under O_2-saturated or deoxygenated conditions. Filled symbols represent diminution of TOC compared to TOC_0 throughout the treatment, open symbols correspond to the toxic potential of samples expressed as proliferation inhibition. Significance levels correspond to: x: $p<0.05$; y: $p<0.01$; z: $p<0.001$.[6]

The proliferation-inhibiting capacity of AOP treated samples usually increase before decreasing, during the treatments. *E.g.* the maximal toxic potential of the intermediate samples was 5 or 6-fold higher than that of the parent compound during the direct photolysis or photocatalytic degradation of DICL [148, 149]. However, the maximal intermediate proliferation-inhibiting capacity measured during the VUV photolysis of DICL was significantly lower than previously reported results: it was only about 2 times higher than that of the parent compound (about 30%) under both

[6] Reprinted from ibid. with permission from Elsevier.

oxygenated and deoxygenated conditions. This moderate toxicity enhancement may also underline the adequacy of VUV photolysis [103].

The impact of the VUV-treated samples in sublethal concentrations (10^{-5}% (v/v) – 1% (v/v)) on the migratory response of *Tetrahymena* was also investigated beside their proliferation-inhibiting effects. The use of such has the advantage, that Behavioral changes, *e.g.* avoidance reactions, are in most cases 10–100 times more sensitive and less time-consuming indicators of the biological impact of a pollutant than acute or chronic toxicity assays are, which could point out the importance of behavioral assays [150]. Untreated samples in 1% (v/v) dilution exhibited a strong chemorepellent character, in accordance with the previous findings of *Láng and Kőhidai* [6]. Similarly, treated samples acted also predominantly as chemorepellents [103].

In summary, the cell-biological investigations showed that the VUV treatment of DICL containing solutions are more efficient in the elimination of both the parent compound and the toxic degradation products if they are performed under O_2-saturated conditions.

6. Conclusions

During this work the VUV photolysis of four NSAIDs (IBU, KETO, NAP and DICL) and PhOH, as model compound, were performed.

At the beginning of the measurements the photon flux of the 20 W xenon excimer lamp was determined by means of methanol actinometry [96] and was found to be $(3.0 \pm 0.1) \times 10^{-6}$ mol_{photon} s^{-1}.

The VUV photolysis of oxygenated PhOH, IBU and KETO solutions showed that during the initial transformation of the contaminant molecules the $c_{H_2O_2}$ increases, which could be a proof for the increase of the concentration of $HO_2^{\bullet}/O_2^{\bullet-}$ ($c_{HO_2^{\bullet}/O_2^{\bullet-}}$). Although the reactivity of $HO_2^{\bullet}/O_2^{\bullet-}$ is usually reported to be lower than that of $H^{\bullet}$ [70], in an elevated concentration they may also contribute to the degradation of organic contaminants.

Along the generation of $HO_2^{\bullet}/O_2^{\bullet-}$, dissolved O_2 could also prevent the recombination of $H^{\bullet}/e_{aq}^{-}$ and $HO^{\bullet}$ (2, 3, 5 and 6), and at the same time may hinder the regeneration of the contaminants (8–15). These effects resulted in the increase of the initial transformation rate of PhOH in the presence of O_2. Additionally, the reaction of $HO_2^{\bullet}$ (present in O_2 saturated solutions instead of $H^{\bullet}$) with PhOH also leads to the degradation of the latter, therefore it seems that the contribution of oxidative $HO_2^{\bullet}/O_2^{\bullet-}$ to the transformation of PhOH is much more significant than that of $H^{\bullet}/e_{aq}^{-}$.

In contrast, in the case of NAP and 1.0×10^{-5} mol dm^{-3} IBU solutions, the r_0 values of the contaminants were significantly higher in the absence of O_2. These results suggested that in this case the contribution of reductive $H^{\bullet}/e_{aq}^{-}$ to the transformation of the target molecules is much more significant than that of $HO_2^{\bullet}/O_2^{\bullet-}$.

It should be mentioned, that in the case of KETO, DICL and 1.0×10^{-4} mol dm^{-3} IBU solutions the r_0 values didn't depend on the c_{O_2}. Thus, it seems that in this case the concentration of $H^{\bullet}/e_{aq}^{-}$, which decreased in the presence of O_2, was compensated by the increased concentration of ROS.

Dissolved O_2 also affected the formation and transformation of the VUV photoproducts of the contaminant molecules. The results suggested that $HO_2^{\bullet}/O_2^{\bullet-}$ contributed to the formation of by-products A_{IBU}, B_{IBU}, B_{KETO}, C_{KETO}, D_{KETO}, A_{NAP}, B_{NAP}, C_{NAP}, A_{DICL} and 1,2-DHB and to the transformation of C_{IBU}, A_{KETO}, B_{DICL}, C_{DICL} and 1,4-DHB. Similarly, $H^{\bullet}/e_{aq}^{-}$ could contribute to the formation of C_{IBU}, A_{KETO}, B_{DICL}, C_{DICL} and 1,4-DHB and to the transformation of A_{IBU}, B_{IBU}, B_{KETO}, C_{KETO}, D_{KETO}, A_{NAP}, B_{NAP}, C_{NAP}, A_{DICL} and 1,2-DHB.

The presence of dissolved O_2 was found to be essential during the effective decontamination of NSAID-containing solutions, since it seems that in deoxygenated solutions some undetected recalcitrant by-products (maybe the dimers and oligomers of the target molecules) were formed.

With the addition of both formate ions and O_2 under acidic or basic conditions, the role of $HO_2^{\bullet}$ or $O_2^{\bullet-}$ could be investigated, respectively. In the case of DICL VUV photolyses were performed in solutions prepared both in Milli-Q water and phosphate buffer. The results suggested that in the case of PhOH, NAP and DICL, the contribution of $HO_2^{\bullet}$, while in the case of IBU and KETO, the contribution of $O_2^{\bullet-}$ was higher among $HO_2^{\bullet}/O_2^{\bullet-}$. From these findings it might be supposed that the reaction rate of $HO_2^{\bullet}/O_2^{\bullet-}$ and organic compounds depends highly on the structure of the target molecule.

The comparison of the ratios of the initial transformation rates of the studied molecules in the presence of dissolved O_2 and in the presence of both O_2 and formate ions (to convert the radicals to $HO_2^{\bullet}/O_2^{\bullet-}$) with the ratios of the transformation rates in the presence of dissolved O_2 and in the presence of both O_2 and radical scavengers (CH_3OH or *tert*-butanol) suggested that the contribution of peroxyl radicals ($^{\bullet}OOCH_2OH$ and $^{\bullet}OOCH_2C(CH_3)_2OH$) to the transformation of the contaminants may be higher than that of $HO_2^{\bullet}/O_2^{\bullet-}$. Methanol and *tert*-butanol therefore, should also be considered as radical transfers instead of radical scavengers. Additionally, the contribution of $HO_2^{\bullet}$ to the degradation of the contaminants seems to have a minor

significance only in the case of PhOH and to be negligible in case of the studied drugs.

In oxygenated solutions, the apparent first-order rate constants ($k' = k \times [\text{radicals}]_{SS}$) decreased in almost all cases with the increase of the c_0. The reason of these observations might be that along the constant value of k, the steady-state concentration of the reactive radicals decreases with the increase of c_0.

During the VUV photolysis of the investigated NSAIDs four aromatic by-products of IBU and KETO and three by-products of NAP and DICL were detected. With the help of the HPLC-MS analysis, suggestions could be given for the chemical structures of these compounds. At the same time, a tentative mechanism of the VUV photolysis of the studied drugs could be given. H-abstraction, $HO^{\bullet}/H^{\bullet}$-addition and decarboxylation reactions, as well as the reactions of the peroxyl radicals (formed from the target molecules) are the key steps during the VUV degradation of the studied NSAIDs. Some of these reactions take place only in oxygenated solutions, while others both in the presence and absence of dissolved O_2. The formation of the by-products of KETO and NAP could be interpreted with the reactions of the aliphatic chains, the formation of the by-products of DICL with the reactions of the aromatic rings [103], while the formation of the by-products of IBU with the reactions of both the aromatic ring and the aliphatic chains.

DICL and the VUV irradiated, multicomponent samples inhibited the proliferation of the bioindicator eukaryotic ciliate *Tetrahymena pyriformis* and exhibited a strong chemorepellent character. However, O_2-saturated conditions seemed to be more efficient in the decrease of the toxic effect of the parent compound and its degradation by-products.

References

[1] Fent, K.; Weston, A.A.; Caminada, D., *Ecotoxicology of human pharmaceuticals*, Aquatic Toxicology, 76 (2), 122-159, 2006.

[2] Cleuvers, M., *Mixture toxicity of the anti-inflammatory drugs diclofenac, ibuprofen, naproxen, and acetylsalicylic acid*, Ecotoxicology and Environmental Safety, 59 (3), 309-315, 2004.

[3] Osada, M.; Nomura, T., *The levels of prostaglandins associated with the reproductive-cycle of the scallop, Patinopecten yessoensis*, Prostaglandins, 40 (3), 229-239, 1990.

[4] Oaks, J.L.; Gilbert, M.; Virani, M.Z.; Watson, R.T.; Meteyer, C.U.; Rideout, B.A.; Shivaprasad, H.L.; Ahmed, S.; Chaudhry, M.J.I.; Arshad, M.; Mahmood, S.; Ali, A.; Khan, A.A., *Diclofenac residues as the cause of vulture population decline in Pakistan*, Nature, 427, 630-633, 2004.

[5] Gajda-Schrantz, K.; Arany, E.; Illés, E.; Szabó, E.; Pap, Zs.; Takács, E.; Wojnárovits, L., *Advanced oxidation processes for ibuprofen removal and ecotoxicological risk assessment of degradation intermediates*, in: Carter, W.C.; Brown, B.R. (Eds.) Ibuprofen: Clinical pharmacology, medical uses and adverse effects, Nova Science Publishers, Inc., Hauppauge, New York, 2013, pp. 159–232.

[6] Láng, J.; Kőhidai, L., *Effects of the aquatic contaminant human pharmaceuticals and their mixtures on the proliferation and migratory responses of the bioindicator freshwater ciliate Tetrahymena*, Chemosphere, 89 (5), 592-601, 2012.

[7] la Farré, M.; Ferrer, I.; Ginebreda, A.; Figueras, M.; Olivella, L.; Tirapu, L.; Vilanova, M.; Barceló, D., *Determination of drugs in surface water and wastewater samples by liquid chromatography–mass spectrometry: methods and preliminary results including toxicity studies with Vibrio fischeri*, Journal of Chromatography A, 938, 187–197, 2001.

[8] Naidoo, V.; Wolter, K.; Cromarty, D.; Diekmann, M.; Duncan, N.; Meharg, A.A.; Taggart, M.A.; Venter, L.; Cuthbert, R., *Toxicity of non-steroidal anti-*

inflammatory drugs to Gyps vultures: a new threat from ketoprofen, Biology Letters, 6 (3), 339-341, 2010.

[9] Pomati, F.; Castiglioni, S.; Zuccato, E.; Fanelli, R.; Vigetti, D.; Rossetti, C.; Calamari, D., *Effects of a complex mixture of therapeutic drugs at environmental levels on human embryonic cells*, Environmental Science & Technology, 40 (7), 2442-2447, 2006.

[10] Quinn, B.; Gagne, F.; Blaise, C., *An investigation into the acute and chronic toxicity of eleven pharmaceuticals (and their solvents) found in wastewater effluent on the cnidarian, Hydra attenuata*, Science of the Total Environment, 389 (2-3), 306-314, 2008.

[11] Quinn, B.; Gagne, F.; Blaise, C., *Evaluation of the acute, chronic and teratogenic effects of a mixture of eleven pharmaceuticals on the cnidarian, Hydra attenuata*, Science of the Total Environment, 407 (3), 1072-1079, 2009.

[12] Vione, D.; Maddigapu, P.R.; De Laurentiis, E.; Minella, M.; Pazzi, M.; Maurino, V.; Minero, C.; Kouras, S.; Richard, C., *Modelling the photochemical fate of ibuprofen in surface waters*, Water Research, 45 (20), 6725–6736, 2011.

[13] Shaw, L.R.; Irwin, W.J.; Grattan, T.J.; Conway, B.R., *The effect of selected water-soluble excipients on the dissolution of paracetamol and ibuprofen*, Drug Development and Industrial Pharmacy, 31 (6), 515–525, 2005.

[14] Meloun, M.; Bordovska, S.; Galla, L., *The thermodynamic dissociation constants of four non-steroidal anti-inflammatory drugs by the least-squares nonlinear regression of multiwavelength spectrophotometric pH-titration data*, Journal of Pharmaceutical and Biomedical Analysis, 45 (4), 552–564, 2007.

[15] Benitez, F.J.; Real, F.J.; Acero, J.L.; Roldan, G., *Removal of selected pharmaceuticals in waters by photochemical processes*, Journal of Chemical Technology and Biotechnology, 84 (8), 1186-1195, 2009.

[16] Packer, J.L.; Werner, J.J.; Latch, D.E.; McNeill, K.; Arnold, W.A., *Photochemical fate of pharmaceuticals in the environment: Naproxen, diclofenac, clofibric acid, and ibuprofen*, Aquatic Sciences, 65 (4), 342–351, 2003.

[17] Huber, M.M.; Canonica, S.; Park, G.-Y.; von Gunten, U., *Oxidation of pharmaceuticals during ozonation and Advanced Oxidation Processes*, Environmental Science & Technology, 37, 1016–1024, 2003.

[18] Avdeef, A.; Berger, C.M.; Brownell, C., *pH-metric solubility. 2: Correlation between the acid-base titration and the saturation shake-flask solubility-pH methods*, Pharmaceutical Research, 17 (1), 85–89, 2000.

[19] Chowhan, Z.T., *pH-solubility profiles of organic carboxilic acids and their salts*, Journal of Pharmaceutical Sciences, 67 (9), 1257-1260, 1978.

[20] Vieno, N., *Occurrence of pharmaceuticals in Finnish sewage treatment plants, surface waters and their elimination in drinking water treatment processes*, PhD Thesis, University of Technology, Tampere, Finland, 2007.

[21] Bonin, J.; Janik, I.; Janik, D.; Bartels, D.M., *Reaction of the hydroxyl radical with phenol in water up to supercritical conditions*, Journal of Physical Chemistry A, 111 (10), 1869–1878, 2007.

[22] Cooper, W.J.; Snyder, S.A.; Mezyk, S.P.; Peller, J.R.; Nickelson, M.G., *Reaction rates and mechanisms of advanced oxidation processes for water reuse*, Water Reuse Foundation, Alexandria, Egypt, 2010.

[23] Jones, G.K., *Applications of radiation chemistry to understand the fate and transport of emerging pollutants of concern in coastal waters*, PhD Thesis, North Caroline State University, Rayleigh, North Caroline, USA, 2007.

[24] Illés, E.; Takács, E.; Dombi, A.; Gajda-Schrantz, K.; Gonter, K.; Wojnárovits, L., *Radiation induced degradation of ketoprofen in dilute aqueous solution*, Radiation Physics and Chemistry, 81 (9), 1479-1483, 2012.

[25] Yu, H.; Nie, E.; Xu, J.; Yan, S.; Cooper, W.J.; Song, W., *Degradation of diclofenac by advanced oxidation and reduction processes: Kinetic studies, degradation pathways and toxicity assessments*, Water Research, 47, 1909–1918, 2013.

[26] Field, R.J.; Raghavan, N.V.; Brummer, J.G., *A pulse radiolysis investigation of the reactions of $BrO_2^{\bullet}$ with $Fe(CN)_6^{4-}$, Mn(II), phenoxide ion, and phenol.*, Journal of Physical Chemistry, 86, 2443–2449, 1982.

[27] Adams, G.E.; Boag, J.W.; Currant, J.; Michael, B.D., *Absolute rate constants for the reaction of the hydroxyl radical with organic compounds*, in: Ebert, M.; Keene, J.P.; Swallow, A.J.; Baxendale, J.H. (Eds.) Pulse Radiolysis, Academic Press, New York, 1965, pp. 131–143.

[28] Lai, C.C.; Freeman, G.R., *Solvent effects on the reactivity of solvated electrons with organic solutes in methanol water and ethanol water mixed-solvents*, Journal of Physical Chemistry, 94 (1), 302–308, 1990.

[29] Buxton, G.V.; Greenstock, C.L.; Helman, W.P.; Ross, A.B., *Critical review of rate constants for reactions of hydrated electrons, hydrogen atoms and hydroxyl radicals ($^{\bullet}OH/^{\bullet}O^{-}$) in aqueous solution*, Journal of Physical and Chemical Reference Data, 17, 513–886, 1988.

[30] Ye, M.; Madden, K.P.; Fessenden, R.W.; Schuler, R.H., *Azide as a scavenger of hydrogen atoms*, Journal of Physical Chemistry, 90, 5397–5399, 1986.

[31] Smaller, B.; Avery, E.C.; Remko, J.R., *EPR pulse radiolysis studies of the hydrogen atom in aqueous solution. I. Reactivity of the hydrogen atom.*, Journal of Chemical Physics, 55, 2414–2418, 1971.

[32] Das, R.; Vione, D.; Rubertelli, F.; Maurino, V.; Minero, C.; Barbati, S.; Chiron, S., *Modelling On Photogeneration Of Hydroxyl Radical In Surface Waters And Its Reactivity Towards Pharmaceutical Wastes*, in: Paruya, S.; Kar, S.; Roy, S. (Eds.) International Conference on Modeling, Optimization, and Computing, Amer Inst Physics, Melville, 2010, pp. 178–185.

[33] Aruoma, O.I.; Halliwell, B., *The iron-binding and hydroxyl radical scavenging action of anti-inflammatory drugs*, Xenobiotica, 18 (4), 459-470, 1988.

[34] Illés, E.; Takács, E.; Dombi, A.; Gajda-Schrantz, K.; Rácz, G.; Gonter, K.; Wojnárovits, L., *Hydroxyl radical induced degradation of ibuprofen*, Science of the Total Environment, 447, 286-292, 2013.

[35] Real, F.J.; Benitez, F.J.; Acero, J.L.; Sagasti, J.J.P.; Casas, F., *Kinetics of chemical oxidation of the pharmaceuticals primidone, ketoprofen, and diatrizoate in ultrapure and natural waters*, Industrial & Engineering Chemistry Research, 48, 3380–3388, 2009.

[36] Parij, N.; Nagy, A.M.; Neve, J., *Linear and nonlinear competition plots in the deoxyribose assay for determination of rate constants for reaction of nonsteroidal aniinflammatory drugs with hydroxyl radicals*, Free Radical Research, 23 (6), 571–579, 1995.

[37] Pereira, V.J.; Linden, K.G.; Weinberg, H.S., *Evaluation of UV irradiation for photolytic and oxidative degradation of pharmaceutical compounds in water*, Water Research, 41, 4413–4423, 2007.

[38] Peuravuori, J.; Pihlaja, K., *Phototransformations of selected pharmaceuticals under low-energy UVA-vis and powerful UVB-UVA irradiations in aqueous solutions-the role of natural dissolved organic chromophoric material*, Analytical and Bioanalytical Chemistry, 394 (6), 1621–1636, 2009.

[39] Arany, E.; Szabó, R.K.; Apáti, L.; Alapi, T.; Ilisz, I.; Mazellier, P.; Dombi, A.; Gajda-Schrantz, K., *Degradation of naproxen by UV, VUV photolysis and their combination*, Journal of Hazardous Materials, 262, 151–157, 2013.

[40] Moore, D.E.; Chappuis, P.P., *A comparative study of the photochemistry of the non-steroidal anti-inflammatory drugs, naproxen, benoxaprofen and indomethacin*, Photochemistry and Photobiology, 47 (2), 173–180, 1988.

[41] Audureau, J.; Filiol, C.; Boule, P.; Lemaire, J., *Photolysis and photo-oxidation of phenol in aqueous solution*, Journal de Chimie Physique et de Physico-Chimie Biologique, 73 (6), 613–620, 1976.

[42] Alapi, T., *Kisnyomású higanygőzlámpák alkalmazása szerves víz- és légszennyezők lebontásában (Applications of low-pressure mercury vapor lamps for decompositing organic pollutants in water and air)*, PhD Thesis, University of Szeged, Szeged, Hungary, 2007.

[43] Szabó, R.K.; Megyeri, C.; Illés, E.; Gajda-Schrantz, K.; Mazellier, P.; Dombi, A., *Phototransformation of ibuprofen and ketoprofen in aqueous solutions*, Chemosphere, 84 (11), 1658–1663, 2011.

[44] Yuan, F.; Hu, C.; Hu, X.X.; Qu, J.H.; Yang, M., *Degradation of selected pharmaceuticals in aqueous solution with UV and UV/H_2O_2*, Water Research, 43 (6), 1766–1774, 2009.

[45] Pereira, V.J.; Weinberg, H.S.; Linden, K.G.; Singer, P.C., *UV degradation kinetics and modeling of pharmaceutical compounds in laboratory grade and surface water via direct and indirect photolysis at 254 nm*, Environmental Science & Technology, 41 (5), 1682-1688, 2007.

[46] Costanzo, L.L.; Guidi, G.d.; Condorelli, G.; Cambria, A.; Fama, M., *Molecular mechanism of drug photosensitization - II. photohaemolysis sensitized by ketoprofen*, Photochemistry and Photobiology, 50 (3), 359–365, 1989.

[47] Marotta, R.; Spasiano, D.; Di Somma, I.; Andreozzi, R., *Photodegradation of naproxen and its photoproducts in aqueous solution at 254 nm: A kinetic investigation*, Water Research, 47 (1), 373-383, 2013.

[48] Boreen, A.L.; Arnold, W.A.; McNeill, K., *Photodegradation of pharmaceuticals in the aquatic environment: A review*, Aquatic Sciences, 65 (4), 320-341, 2003.

[49] Poiger, T.; Buser, H.R.; Muller, M.D., *Photodegradation of the pharmaceutical drug diclofenac in a lake: Pathway, field measurements, and mathematical modeling*, Environmental Toxicology and Chemistry, 20 (2), 256-263, 2001.

[50] Moore, D.E.; Roberts-Thomson, S.; Zhen, D.; Duke, C.C., *Photochemical studies on the anti-inflammatory drug diclofenac*, Photochemistry and Photobiology, 52 (4), 685–690, 1990.

[51] Buser, H.R.; Poiger, T.; Muller, M.D., *Occurrence and fate of the pharmaceutical drug diclofenac in surface waters: Rapid photodegradation in a lake*, Environmental Science & Technology, 32 (22), 3449-3456, 1998.

[52] Canonica, S.; Meunier, L.; von Gunten, U., *Phototransformation of selected pharmaceuticals during UV treatment of drinking water*, Water Research, 42 (1-2), 121-128, 2008.

[53] Andreozzi, R.; Raffaele, M.; Nicklas, P., *Pharmaceuticals in STP effluents and their solar photodegradation in aquatic environment*, Chemosphere, 50, 1319–1330, 2003.

[54] Gagnon, C.; Lajeunesse, A.; Cejka, P.; Gagne, F.; Hausler, R., *Degradation of selected acidic and neutral pharmaceutical products in a primary-treated wastewater by disinfection processes*, Ozone: Science & Engineering, 30 (5), 387–392, 2008.

[55] Meunier, L.; Canonica, S.; von Gunten, U., *Implications of sequential use of UV and ozone for drinking water quality*, Water Research, 40 (9), 1864-1876, 2006.

[56] Kim, I.; Yamashita, N.; Tanaka, H., *Photodegradation of pharmaceuticals and personal care products during UV and UV/H_2O_2 treatments*, Chemosphere, 77 (4), 518-525, 2009.

[57] Spinks, J.W.T.; Woods, R.J., *An Introduction to Radiation Chemistry*, 3rd ed. ed., Wiley-Interscience, New York, USA, 1990.

[58] Buxton, G.V., *The radiation chemistry of liquid water: Principles and applications*, in: Mozumder, A.; Hatano, Y.; Dekker, M. (Eds.) Charged particle and photon interaction with matter, CRC Press, New York, USA, 2004, pp. 331–363.

[59] Hashimoto, S.; Miyata, T.; Kawakami, W., *Radiation-induced decomposition of phenol in flow system*, Radiation Physics and Chemistry, 16 (1), 59-65, 1980.

[60] Homlok, R.; Takács, E.; Wojnárovits, L., *Elimination of diclofenac from water using irradiation technology*, Chemosphere, 85 (4), 603-608, 2011.

[61] Oppenländer, T., *Photochemical purification of water and air*, Wiley-VCH, Weinheim, 2003.

[62] Heit, G.; Neuner, A.; Saugy, P.-Y.; Braun, A.M., *Vacuum-UV (172 nm) actinometry. The quantum yield of the photolysis of water*, Journal of Physical Chemistry A, 102 (28), 5551–5561, 1998.

[63] Hart, E.J.; Anbar, M., *The hydrated electron*, Wiley-Interscience, New York, 1970.

[64] László, Zs., *Vákuum-ultraibolya fotolízis alkalmazhatóságának vizsgálata környezeti szennyezők lebontására (Investigation of applicability of VUV photolyis for degradation of organic pollutants)*, PhD Thesis, University of Szeged, Szeged, Hungary, 2001.

[65] Noyes, R.M., *Models relating molecular reactivity and diffusion in liquids*, Journal of the American Chemical Society, 78 (21), 5486–5490, 1956.

[66] Noyes, R.M., *Kinetics of competitive processes when reactive fragments are produced in pairs*, Journal of the American Chemical Society, 77 (8), 2042–2045, 1955.

[67] Thomas, J.K., *Rates of reaction of the hydroxyl radical*, Transactions of the Faraday Society, 61, 702–707, 1965.

[68] Arany, E.; Oppenländer, T.; Gajda-Schrantz, K.; Dombi, A., *Influence of H_2O_2 formed in situ on the photodegradation of ibuprofen and ketoprofen*, Current Physical Chemistry, 2 (3), 286–293, 2012.

[69] Bielski, B.H.J.; Cabelli, D.E.; Arudi, R.L.; Ross, A.B., *Reactivity of HO_2/O_2^- radicals in aqueous solution*, Journal of Physical and Chemical Reference Data, 14 (4), 1041–1100, 1985.

[70] Gonzalez, M.G.; Oliveros, E.; Wörner, M.; Braun, A.M., *Vacuum-ultraviolet photolysis of aqueous reaction systems*, Journal of Photochemistry and Photobiology, C: Photochemistry Reviews, 5, 225–246, 2004.

[71] Bielski, B.H.J.; Cabelli, D.E.; Arudi, R.L.; Ross, A.B., *Reactivity of HO_2/O_2^- radicals in aqueous-solution*, Journal of Physical and Chemical Reference Data, 14 (4), 1041-1100, 1985.

[72] Leitner, N.K.V.; Dore, M., *Hydroxyl radical induced decomposition of aliphatic acids in oxygenated and deoxygenated aqueous solutions*, Journal of Photochemistry and Photobiology, A: Chemistry, 99, 137-143, 1996.

[73] Ilan, Y.; Rabani, J., *On some fundamental reactions in radiation chemistry: Nanosecond pulse radiolysis*, International Journal for Radiation Physics and Chemistry, 8, 609-611, 1976.

[74] Rabani, J.; Klug-Roth, D.; Henglein, A., *Pulse radiolytic investigations of $OHCH_2O_2$ radicals*, Journal of Physical Chemistry, 78 (21), 2089–2093, 1974.

[75] von Piechowski, M.; Thelen, M.A.; Hoigne, J.; Buehler, R.E., *tert-butanol as an OH-scavenger in the pulse radiolysis of oxygenated aqueous systems*, Berichte der Bunsengesellschaft für physikalische Chemie, 96 (10), 1448–1454, 1992.

[76] Köhler, G.; Solar, S.; Getoff, N.; Holzwarth, A.R.; Schaffner, K., *Relationship between the quantum yields of electron photoejection and fluorescence of aromatic carboxylate anions in aqueous solution*, Journal of Photochemistry, 28 (3), 383–391, 1985.

[77] Grabner, G.; Köhler, G.; Marconi, G.; Monti, S.; Venuti, E., *Photophysical properties of methylated phenols in nonpolar solvents*, Journal of Physical Chemistry, 94 (9), 3609–3613, 1990.

[78] Gadosy, T.A.; Shukla, D.; Johnston, L.J., *Generation, characterization, and deprotonation of phenol radical cations*, Journal of Physical Chemistry A, 103 (44), 8834–8839, 1999.

[79] Kozmér, Zs.; Arany, E.; Alapi, T.; Takács, E.; Wojnárovits, L.; Dombi, A., *Determination of the rate constant of hydroperoxyl radical reaction with phenol*, Radiation Physics and Chemistry, 102, 135-138, 2014.

[80] Tsujimoto, Y.; Hashizume, H.; Yamazaki, M., *Superoxide radical scavenging activity of phenolic compounds*, International Journal of Biochemistry, 25, 491–494, 1993.

[81] Getoff, N., *Radiation-induced degradation of water pollutants – state of the art*, Radiation Physics and Chemistry, 47 (4), 581–593, 1996.

[82] Altarawneh, M.; Al-Muhtaseb, A.A.H.; Dlugogorski, B.Z.; Kennedy, E.M.; Mackie, J.C., *Rate constants for hydrogen abstraction reactions by the hydroperoxyl radical from methanol, ethenol, acetaldehyde, toluene and phenol*, Journal of Computational Chemistry, 32, 1725–1733, 2011.

[83] Skokov, S.; Kazakov, A.; Dryer, F.L., *A theoretical study of oxidation of phenoxy and benzyl radicals by HO_2*, in: The 4th Joint Meeting of the U.S. Sections of the Combustion Institute, Drexel University, Philadelphia, PA, 2005.

[84] Feng, P.Y.; Brynjolfsson, A.; Halliday, J.W.; Jarrett, R.D., *High-intensity radiolysis of aqueous ferrous sulfate-cupric sulfate-sulfuric acid solutions*, Journal of Physical Chemistry, 74, 1221–1227, 1970.

[85] Azrague, K.; Bonnefille, E.; Pradines, V.; Pimienta, V.; Oliveros, E.; Maurette, M.-T.; Benoit-Marquié, F., *Hydrogen peroxide evolution during V-UV photolysis of water*, Photochemical & Photobiological Sciences, 4, 406–408, 2005.

[86] Robl, S.; Worner, M.; Maier, D.; Braun, A.M., *Formation of hydrogen peroxide by VUV-photolysis of water and aqueous solutions with methanol*, Photochemical & Photobiological Sciences, 11 (6), 1041-1050, 2012.

[87] Elliot, A.J.; Buxton, G.V., *Temperature dependence of the reactions OH + O_2^- and OH + HO_2 in water up to 200°C*, Journal of the Chemical Society, Faraday Transactions, 88, 2465–2470, 1992.

[88] Hunt, J.P.; Taube, H., *The photochemical decomposition of hydrogen peroxide. Quantum yields, tracer and fractionation effects*, Journal of the American Chemical Society, 74, 5999–6002, 1952.

[89] Baxendale, J.H.; Wilson, J.A., *The photolysis of hydrogen peroxide at high light intensities*, Transactions of the Faraday Society, 53, 344–356, 1957.

[90] Mezyk, S.P.; Bartels, D.M., *Direct EPR measurement of Arrhenius parameters for the reactions of $H^\bullet$ atoms with H_2O_2 and $D^\bullet$ atoms with D_2O_2 in aqueous solution*, Journal of the Chemical Society, Faraday Transactions, 91, 3127–3132, 1995.

[91] von Sonntag, C.; Schuchmann, H.-P., *The elucidation of peroxyl radical reactions in aqueous solution with the help of radiation-chemical methods*, Angewandte Chemie International Edition, 30, 1229–1253, 1991.

[92] Quici, N.; Litter, M.I.; Braun, A.M.; Oliveros, E., *Vacuum-UV-photolysis of aqueous solutions of citric and gallic acids*, Journal of Photochemistry and Photobiology, A: Chemistry, 197, 306–312, 2008.

[93] Kosaka, K.; Yamada, H.; Matsui, S.; Echigo, S.; Shishida, K., *Comparison among the methods for hydrogen peroxide measurements to evaluate Advanced Oxidation Processes: application of a spectrophotometric method using copper(II) ion and 2,9-dimethyl-1,10-phenanthroline*, Environmental Science & Technology, 32, 3821–3824, 1998.

[94] Staehelin, J.; Hoigne, J., *Decomposition of ozone in water: Rate of initiation by hydroxide ions and hydrogen peroxide*, Environmental Science & Technology, 16, 676-681, 1982.

[95] Oppenländer, T.; Walddörfer, C.; Burgbacher, J.; Kiermeier, M.; Lachner, K.; Weinschrott, H., *Improved vacuum-UV (VUV)-initiated photomineralization of organic compounds in water with a xenon excimer flow-through photoreactor (Xe_2* lamp, 172 nm) containing an axially centered ceramic oxygenator*, Chemosphere, 60, 302–309, 2005.

[96] Oppenländer, T.; Schwarzwalder, R., *Vacuum-UV oxidation (H_2O-VUV) with a xenon excimer flow-through lamp at 172 nm: Use of methanol as actinometer for VUV intensity measurement and as reference compound for OH-radical competition kinetics in aqueous systems*, Journal of Advanced Oxidation Technologies, 5 (2), 155-163, 2002.

[97] Eliasson, B.; Kogelschatz, U., *UV excimer radiation from dielectric-barrier discharges*, Applied Physics B: Lasers and Optics, 46, 299–303, 1988.

[98] Kogelschatz, U., *Excimer lamps: history, discharge physics and industrial applications*, in: Tarasenko, V.F.; Mayer, G.V.; Petrash, G.G. (Eds.) Proceedings of the SPIE, Society of Photo Optical Bellingham, WA, 2004, pp. 272–286.

[99] Heit, G.; Braun, A.M., *Spatial resolution of oxygen measurements during VUV-photolysis of aqueous systems*, Journal of Information Recording, 22, 543–546, 1996.

[100] Heit, G.; Braun, A.M., *VUV-Photolysis of aqueous systems: spatial differentiation between volumes of primary and secondary reactions*, Water Science and Technology, 35, 25–30, 1997.

[101] Kőhidai, L., *Method for determination of chemoattraction in Tetrahymena pyriformis*, Current Microbiology, 30, 251-253, 1995.

[102] Sáfár, O.; Kőhidai, L.; Hegedűs, A., *Time-delayed model of the unbiased movement of Tetrahymena pyriformis*, Periodica Mathematica Hungarica, 63 (2), 215-225, 2011.

[103] Arany, E.; Láng, J.; Somogyvári, D.; Láng, O.; Alapi, T.; Ilisz, I.; Gajda-Schrantz, K.; Dombi, A.; Kőhidai, L.; Hernádi, K., *Vacuum ultraviolet photolysis of diclofenac and the effect of the treated aqueous solutions on the proliferation and migratory responses of Tetrahymena pyriformis*, Science of the Total Environment, 468–469, 996–1006, 2014.

[104] Sosnin, E.A.; Oppenländer, T.; Tarasenko, V.F., *Applications of capacitive and barrier discharge excilamps in photoscience*, Journal of Photochemistry and Photobiology, C: Photochemistry Reviews, 7, 14–163, 2006.

[105] Liptak, M.D.; Gross, K.C.; Seybold, P.G.; Feldgus, S.; Shields, G.C., *Absolute pKa determinations for substituted phenols*, Journal of the American Chemical Society, 124, 6421–6427, 2002.

[106] Garcia-Araya, J.F.; Beltran, F.J.; Aguinaco, A., *Diclofenac removal from water by ozone and photolytic TiO_2 catalysed processes*, Journal of Chemical Technology and Biotechnology, 85 (6), 798-804, 2010.

[107] Black, E.D.; Hayon, E., *Pulse radiolysis of phosphate anions $H_2PO_4^-$, HPO_4^{2-}, PO_4^{3-} and $P_2O_7^{4-}$ in aqueous solutions*, The Journal of Physical Chemistry, 74 (17), 3199−3203, 1970.

[108] Maruthamuthu, P.; Neta, P., *Phosphate radicals − spectra, acid-base equilibria and reactions with inorganic compounds*, Journal of Physical Chemistry, 82 (6), 710-713, 1978.

[109] Anbar, M.; Neta, P., *A compilation of specific bimolecular rate constants for the reactions of hydrated electrons, hydrogen atoms and hydroxyl radicals with inorganic and organic compounds in aqueous solutions*, International Journal of Applied Radiation and Isotopes, 18, 493–523, 1967.

[110] Sato, K.; Takimoto, K.; Tsuda, S., *Degradation of aqueous phenol solution by gamma-irradiation*, Environmental Science & Technology, 12 (9), 1043-1046, 1978.

[111] Horspool, W.M.; Lenci, F., *CRC Handbookof Organic Photochemistry and Photobiology, Second Edition*, CRC Press, USA, 2004.

[112] Zheng, B.G.; Zheng, Z.; Zhang, J.B.; Luo, X.Z.; Wang, J.Q.; Liu, Q.; Wang, L.H., *Degradation of the emerging contaminant ibuprofen in aqueous solution by gamma irradiation*, Desalination, 276 (1–3), 379–385, 2011.

[113] Madhavan, J.; Grieser, F.; Ashokkumar, M., *Combined advanced oxidation processes for the synergistic degradation of ibuprofen in aqueous environments*, Journal of Hazardous Materials, 178 (1-3), 202-208, 2010.

[114] Mendez-Arriaga, F.; Esplugas, S.; Gimenez, J., *Photocatalytic degradation of non-steroidal anti-inflammatory drugs with TiO_2 and simulated solar irradiation*, Water Research, 42 (3), 585-594, 2008.

[115] Mendez-Arriaga, F.; Esplugas, S.; Gimenez, J., *Degradation of the emerging contaminant ibuprofen in water by photo-Fenton*, Water Research, 44 (2), 589–595, 2010.

[116] Caviglioli, G.; Valeria, P.; Brunella, P.; Sergio, C.; Attilia, A.; Gaetano, B., *Identification of degradation products of ibuprofen arising from oxidative and thermal treatments*, Journal of Pharmaceutical and Biomedical Analysis, 30 (3), 499–509, 2002.

[117] Marco-Urrea, E.; Perez-Trujillo, M.; Vicent, T.; Caminal, G., *Ability of white-rot fungi to remove selected pharmaceuticals and identification of degradation products of ibuprofen by Trametes versicolor*, Chemosphere, 74 (6), 765-772, 2009.

[118] Whitten, K.W.; Davis, R.E.; Peck, M.L., *General Chemistry*, Saunders College Pub., 2000.

[119] Gonzalez, M.C.; Le Roux, G.C.; Rosso, J.A.; Braun, A.M., *Mineralization of CCl_4 by the UVC-photolysis of hydrogen peroxide in the presence of methanol*, Chemosphere, 69 (8), 1238-1244, 2007.

[120] Asmus, K.-D.; Möckel, H.; Henglein, A., *Pulse radiolytic study of the site of hydroxyl radical attack on aliphatic alcohols in aqueous solution*, Journal of Physical Chemistry, 77 (10), 1218-1221, 1972.

[121] Castell, J.V.; Gomez-L., M.J.; Miranda, M.A.; Morera, I.M., *Photolytic degradation of ibuprofen. Toxicity of the isolated photoproducts on fibroblasts and erythrocytes*, Photochemistry and Photobiology, 46 (6), 991–996, 1987.

[122] Vargas, F.; Rivas, C.; Miranda, M.A.; Bosca, F., *Photochemistry of the non-steroidal anti-inflammatory drugs, propionic acid-derived*, Pharmazie, 46 (11), 767–771, 1991.

[123] Skoumal, M.; Rodriguez, R.M.; Cabot, P.L.; Centellas, F.; Garrido, J.A.; Arias, C.; Brillas, E., *Electro-Fenton, UVA photoelectro-Fenton and solar photoelectro-Fenton degradation of the drug ibuprofen in acid aqueous medium using platinum and boron-doped diamond anodes*, Electrochimica Acta, 54 (7), 2077–2085, 2009.

[124] Michael, I.; Achilleos, A.; Lambropoulou, D.; Torrens, V.O.; Perez, S.; Petrovic, M.; Barcelo, D.; Fatta-Kassinos, D., *Proposed transformation pathway and evolution profile of diclofenac and ibuprofen transformation products during (sono)photocatalysis*, Applied Catalysis B-Environmental, 147, 1015-1027, 2014.

[125] Brückner, R., *Advanced Organic Chemistry: Reaction Mechanisms*, Elsevier, 2002.

[126] Illés, E., *Radiolízis és egyéb nagyhatékonyságú oxidációs eljárások alkalmazása nem-szteroid gyulladáscsökkentők bontására vizes oldatokban (Radiolysis and other advanced oxidation processes for degradation of non-steroidal anti-inflammatory drugs in dilute aqueous solutions)*, PhD Thesis, University of Szeged, Szeged, Hungary, 2014.

[127] Martinez, C.; Vilarino, S.; Fernandez, M.I.; Faria, J.; Canle, M.; Santaballa, J.A., *Mechanism of degradation of ketoprofen by heterogeneous photocatalysis in aqueous solution*, Applied Catalysis B-Environmental, 142, 633-646, 2013.

[128] Boscá, F.; Miranda, M.A., *Photosensitizing drugs containing the benzophenone chromophore*, Journal of Photochemistry and Photobiology, B: Biology, 43, 1–26, 1998.

[129] Musa, K.A.K.; Matxain, J.M.; Eriksson, L.A., *Mechanism of photoinduced decomposition of ketoprofen*, Journal of Medicinal Chemistry, 50 (8), 1735-1743, 2007.

[130] Kosjek, T.; Perko, S.; Heath, E.; Kralj, B.; Zigon, D., *Application of complementary mass spectrometric techniques to the identification of ketoprofen phototransformation products*, Journal of Mass Spectrometry, 46 (4), 391-401, 2011.

[131] Matamoros, V.; Duhec, A.; Albaiges, J.; Bayona, J.M., *Photodegradation of carbamazepine, ibuprofen, ketoprofen and 17 alpha-ethinylestradiol in fresh and seawater*, Water Air and Soil Pollution, 196 (1–4), 161–168, 2009.

[132] Mas, S.; Tauler, R.; de Juan, A., *Chromatographic and spectroscopic data fusion analysis for interpretation of photodegradation processes*, Journal of Chromatography A, 1218 (51), 9260-9268, 2011.

[133] Illés, E.; Szabó, E.; Takács, E.; Wojnárovits, L.; Dombi, A.; Gajda-Schrantz, K., *Ketoprofen removal by O_3 and O_3/UV processes: Kinetics, transformation products and ecotoxicity*, Science of the Total Environment, 472, 178-184, 2014.

[134] Boscá, F.; Miranda, M.A.; Carganico, G.; Mauleón, D., *Photochemical and photobiological properties of ketoprofen associated with the benzophenone chromophore*, Photochemistry and Photobiology, 60 (2), 96–101, 1994.

[135] Borsarelli, C.D.; Braslavsky, S.E.; Sortino, S.; Marconi, G.; Monti, S., *Photodecarboxylation of ketoprofen in aqueous solution. A time-resolved laser-induced optoacoustic study*, Photochemistry and Photobiology, 72 (2), 163-171, 2000.

[136] Monti, S.; Sortino, S.; DeGuidi, G.; Marconi, G., *Photochemistry of 2-(3-benzoylphenyl)propionic acid (ketoprofen) .1. A picosecond and nanosecond time resolved study in aqueous solution*, Journal of the Chemical Society-Faraday Transactions, 93 (13), 2269-2275, 1997.

[137] Miranda, M.A.; Morera, I.; Vargas, F.; Gomezlechon, M.J.; Castell, J.V., *In vitro assessment of the phototoxicity of anti-inflammatory 2-arylpropionic acids*, Toxicology in Vitro, 5 (5-6), 451-455, 1991.

[138] Boscá, F.; Miranda, M.A.; Vañó, L.; Vargas, F., *New photodegradation pathways for Naproxen, a phototoxic non-steroidal anti-inflammatory drug*, Journal of Photochemistry and Photobiology, A: Chemistry, 54 (1), 131–134, 1990.

[139] Jiménez, M.C.; Miranda, M.A.; Tormos, R., *Photochemistry of naproxen in the presence of beta-cyclodextrin*, Journal of Photochemistry and Photobiology, A: Chemistry, 104, 119–121, 1997.

[140] Calza, P.; Sakkas, V.A.; Medana, C.; Baiocchi, C.; Dimou, A.; Pelizzetti, E.; Albanis, T., *Photocatalytic degradation study of diclofenac over aqueous TiO_2 suspensions*, Applied Catalysis B-Environmental, 67 (3-4), 197-205, 2006.

[141] Landsdorp, D.; Vree, T.B.; Janssen, T.J.; Guelen, P.J.M., *Pharmacokinetics of rectal diclofenac and its hydroxy metabolites in man*, International Journal of Clinical Pharmacology and Therapeutics, 28 (7), 298-302, 1990.

[142] Perez-Estrada, L.A.; Malato, S.; Gernjak, W.; Aguera, A.; Thurman, E.M.; Ferrer, I.; Fernandez-Alba, A.R., *Photo-Fenton degradation of diclofenac: Identification of main intermediates and degradation pathway*, Environmental Science & Technology, 39 (21), 8300–8306, 2005.

[143] Vogna, D.; Marotta, R.; Napolitano, A.; Andreozzi, R.; d'Ischia, M., *Advanced oxidation of the pharmaceutical drug diclofenac with UV/H_2O_2 and ozone*, Water Research, 38 (2), 414-422, 2004.

[144] Sein, M.M.; Zedda, M.; Tuerk, J.; Schmidt, T.C.; Golloch, A.; von Sonntao, C., *Oxidation of diclofenac with ozone in aqueous solution*, Environmental Science & Technology, 42 (17), 6656-6662, 2008.

[145] Petrovic, M.; Barcelo, D., *LC-MS for identifying photodegradation products of pharmaceuticals in the environment*, Trac-Trends in Analytical Chemistry, 26 (6), 486-493, 2007.

[146] Martinez, C.; Canle, M.; Fernandez, M.I.; Santaballa, J.A.; Faria, J., *Aqueous degradation of diclofenac by heterogeneous photocatalysis using nanostructured materials*, Applied Catalysis B-Environmental, 107 (1-2), 110-118, 2011.

[147] Gonzalez-Rey, M.; Bebianno, M.J., *Does non-steroidal anti-inflammatory (NSAID) ibuprofen induce antioxidant stress and endocrine disruption in mussel*

Mytilus galloprovincialis?, Environmental Toxicology and Pharmacology, 33 (2), 361-371, 2012.

[148] Schmitt-Jansen, M.; Bartels, P.; Adler, N.; Altenburger, R., *Phytotoxicity assessment of diclofenac and its phototransformation products*, Analytical and Bioanalytical Chemistry, 387 (4), 1389-1396, 2007.

[149] Rizzo, L.; Meric, S.; Kassinos, D.; Guida, M.; Russo, F.; Belgiorno, V., *Degradation of diclofenac by TiO_2 photocatalysis: UV absorbance kinetics and process evaluation through a set of toxicity bioassays*, Water Research, 43, 979-988, 2009.

[150] Reinecke, A.J.; Maboeta, M.S.; Vermeulen, L.A.; Reinecke, S.A., *Assessment of Lead Nitrate and Mancozeb Toxicity in Earthworms Using the Avoidance Response*, Bulletin of Environmental Contamination and Toxicology, 68, 779-786, 2002.

Acknowledgments

The authors would like to express their gratitude to Prof. Dr. Klára Hernádi and to Prof. Dr. András Dombi for their scientific advices and moral support.

The suggestions and reviewing comments of Prof. Dr. Attila Horváth and Dr. Zsuzsanna László to improve the quality of the present work are highly valued.

Many thanks for the generosity of Dr. Ágota Tóth and Dr. Dezső Horváth, who helped in the interpretation and the kinetic modeling of the degradation curves.

The technical and scientific help as well as the patience of Dr. István Ilisz in the performance and interpretation of the chromatographic and MS measurements is highly appreciated.

The authors would like to express their gratitude to Dr. Júlia Láng, Dr. László Kőhidai and Dr. Orsolya Láng for performing the cell biological measurements.

The help of Katalin Kacsala, Sandra Cerrone, Zsuzsanna Kozmér, Georgina Rózsa, László Apáti and Dávid Somogyvári in the performance and evaluation of the photolytic experiments as well as that of Ágnes Juhászné in collecting the scientific articles is greatly acknowledged.

The authors would like to thank to their families for their humor, encouragement and tolerance as well as to their colleagues (especially for Dr. Zsolt Pap for the scientific discussions and for Dr. Erzsébet Illés for her enthusiasm and technical help).

Eszter Arany is grateful for the financial support and the scholarship of the German Academic Exchange Service (DAAD) at the Hochschule Furtwangen University and for the hospitality and scientific support of Prof. Dr. Thomas Oppenländer. The authors would like to thank Prof. Oppenländer for his critical comments concerning this work.

Tünde Alapi thanks for the support of the Magyary Zoltan postdoctoral fellowship. This research was supported by the European Union and the State of Hungary, co-financed by the European Social Fund in the framework of TÁMOP-4.2.4.A/ 2-11/1-2012-0001 'National Excellence Program'.

This document has been produced with the financial assistance of the European Union (Project HU-SRB/0901/121/116 OCEEFPTRWR Optimization of Cost Effective and Environmentally Friendly Procedures for Treatment of Regional Water Resources).

The financial support of the Swiss Contribution (SH7/2/20) is also greatly honoured.

Appendix

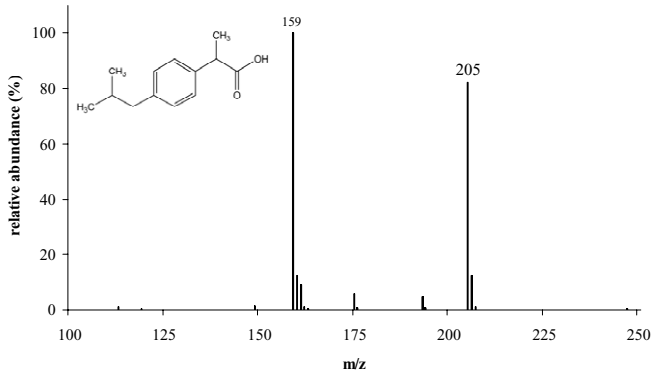

Fig. A1. The mass spectrum and chemical structure of IBU.

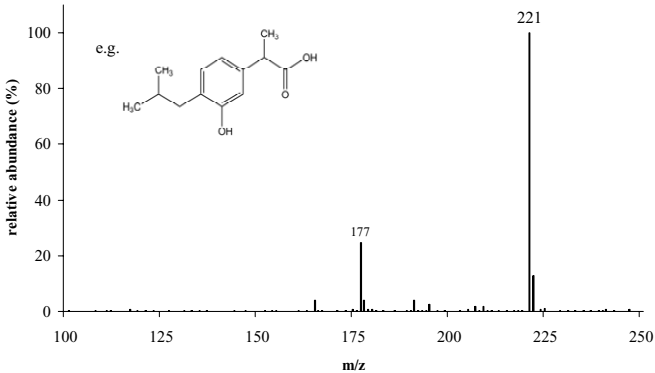

Fig. A2. The mass spectrum and a possible structure of A_{IBU}.

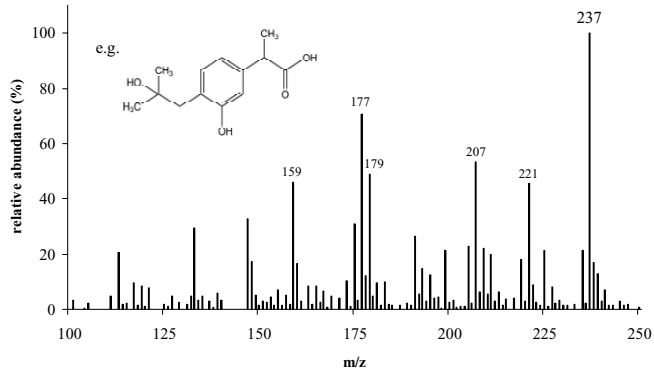

Fig. A3. The mass spectrum and a possible structure of B_{IBU}.

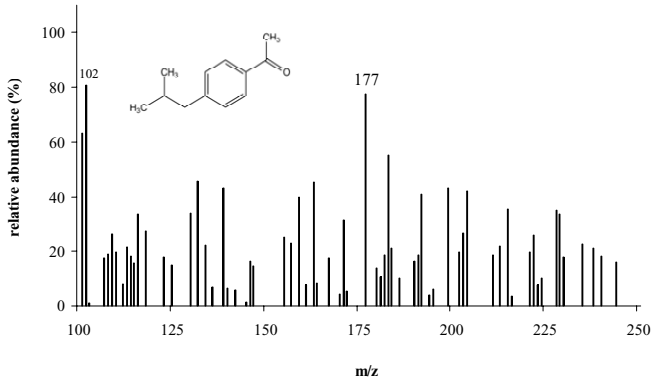

Fig. A4. The mass spectrum and a possible structure of C_{IBU}.

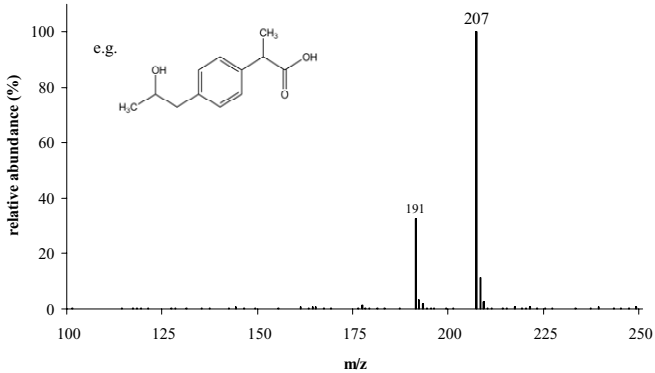

Fig. A5. The mass spectrum and a possible structure of D_{IBU}.

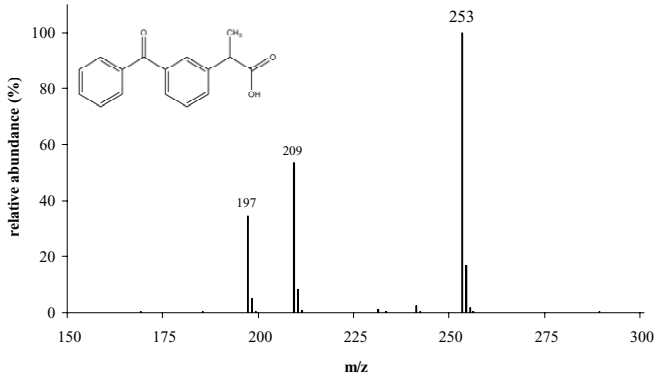

Fig. A6. The mass spectrum and chemical structure of KETO.

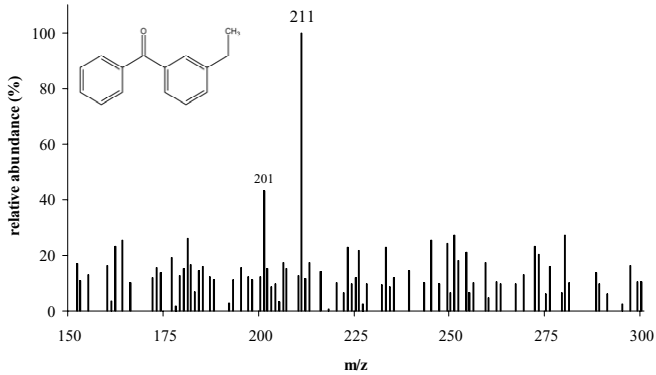

Fig. A7. The mass spectrum and a possible structure of A_{KETO}.

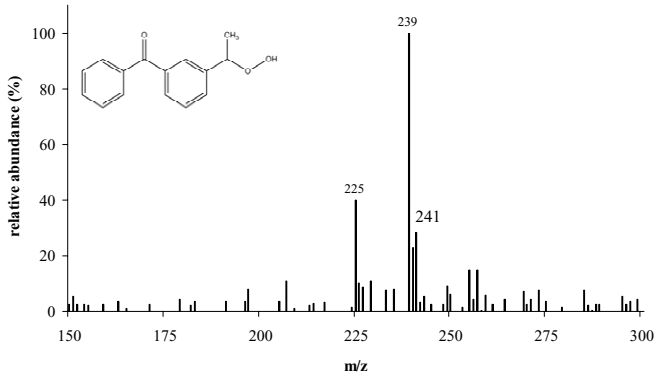

Fig. A8. The mass spectrum and a possible structure of B_{KETO}.

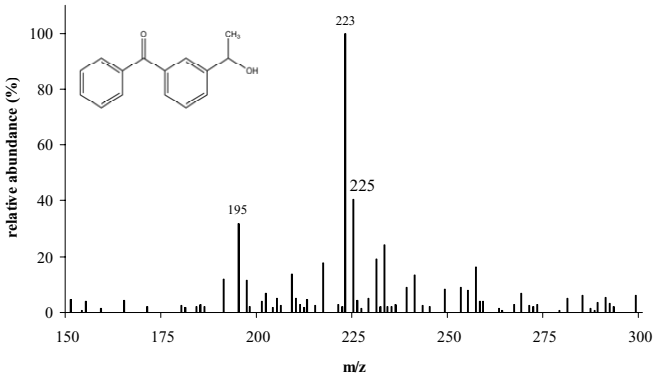

Fig. A9. The mass spectrum and a possible structure of C_{KETO}.

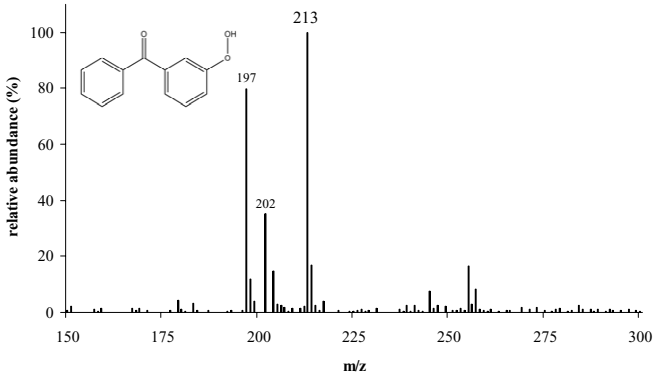

Fig. A10. The mass spectrum and a possible structure of D_{KETO}.

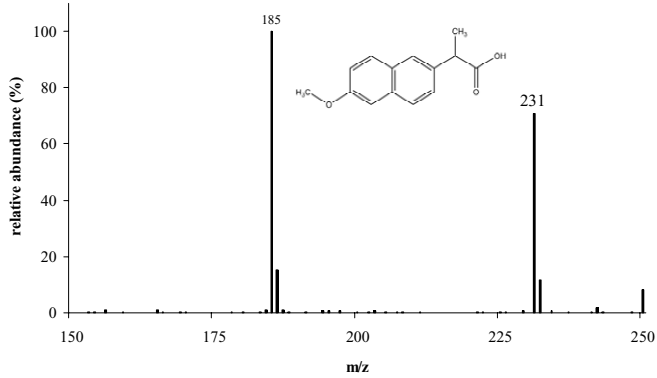

Fig. A11. The mass spectrum and chemical structure of NAP.

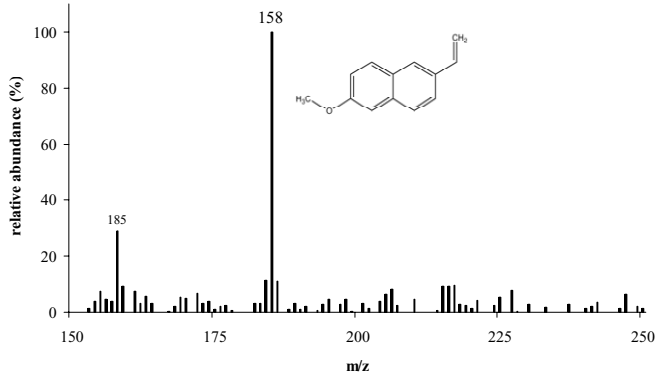

Fig. A12. The mass spectrum and a possible structure of A_{NAP}.

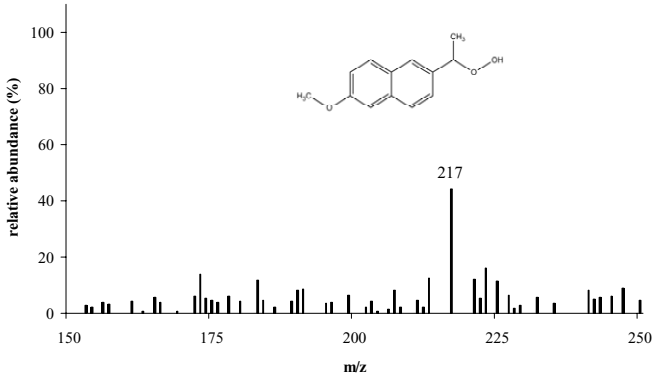

Fig. A13. The mass spectrum and a possible structure of B_{NAP}.

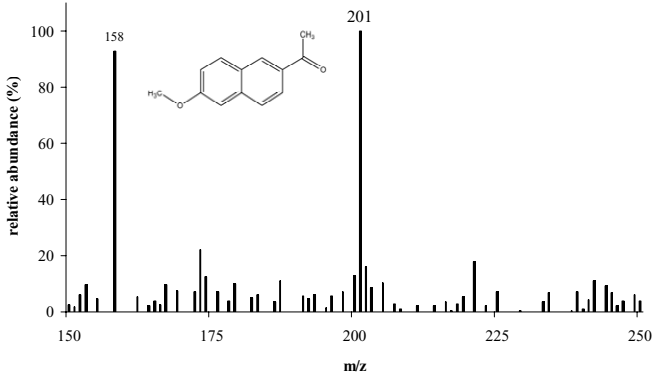

Fig. A14. The mass spectrum and a possible structure of C_{NAP}.

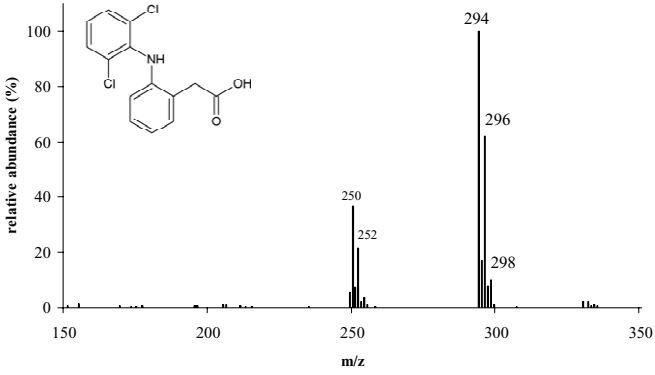

Fig. A15. The mass spectrum and chemical structure of DICL.[7]

[7] Reprinted from ibid. with permission from Elsevier.

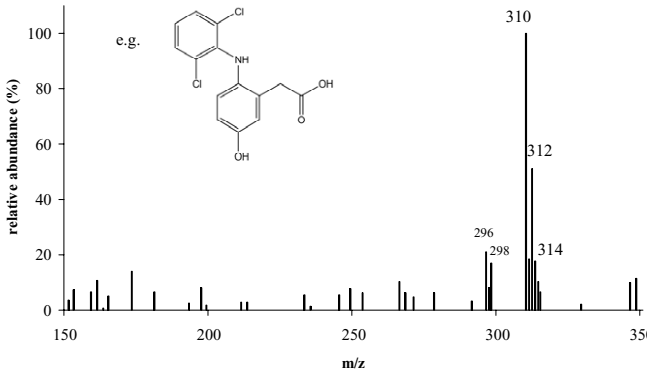

Fig. A16. The mass spectrum and a possible structure of A_{DICL}.[8]

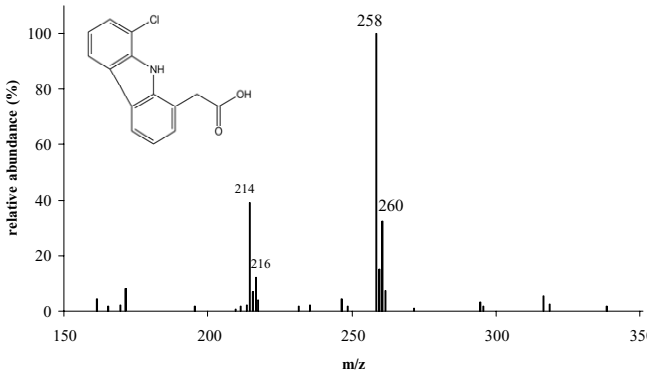

Fig. A17. The mass spectrum and a possible structure of B_{DICL}.[9]

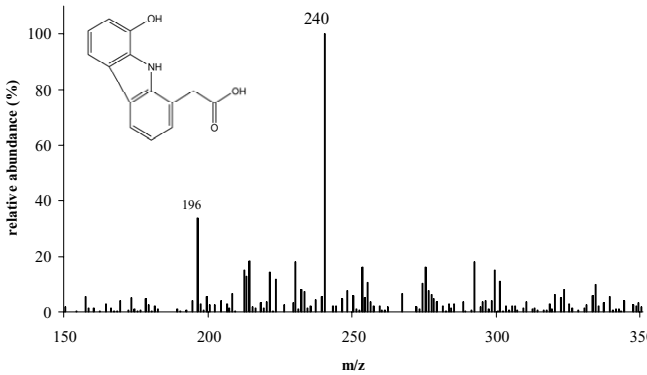

Fig. A18. The mass spectrum and a possible structure of C_{DICL}.[9]

[8] Reprinted from ibid. with permission from Elsevier.

Co-authors of the book

Tünde Alapi, PhD: 2002-2007: PhD study at the University of Szeged in the Environmental Chemistry doctoral program. From 2007 assistant lecturer at the University of Szeged, Department of Inorganic and Analytical Chemistry. The main topics of the research are the oxidative transformation of organic pollutants, VUV and UV photolysis, heterogeneous photocatalysis and ozonation.

Krisztina Schrantz, PhD: Chemistry studies, University of Novi Sad (1994). PhD in Chemistry, University of Szeged (2002). Environmental Engineer MSc, University of Pannonia (2009). Research interest in Advanced Oxidation Processes and Environmental Chemistry. Assistant Professor at the University of Szeged, Hungary.